Development of blood interactive co-assembling systems for regenerative medicine applications

Soraya Scarlette Padilla Lopategui

March, 2021

Submitted in partial fulfilment of the requirements of the Degree of Doctor of Philosophy

School of Engineering and Materials Science
Queen Mary, University of London

Declaration

I, Soraya Scarlette Padilla Lopategui, confirm that the research included within this thesis is my own work or that where it has been carried out in collaboration with, or supported by others, that this is duly acknowledged below and my contribution indicated. Previously published material is also acknowledged below.

I attest that I have exercised reasonable care to ensure that the work is original, and does not to the best of my knowledge break any UK law, infringe any third party's copyright or other Intellectual Property Right, or contain any confidential material.

I accept that the College has the right to use plagiarism detection software to check the electronic version of the thesis.

I confirm that this thesis has not been previously submitted for the award of a degree by this or any other university.

Signature: Soraya S. Padilla Lopategui

Date: 13-03-2022

Supervisory team

Primary supervisor: Dr. Thomas Iskratsch

Secondary supervisor: Dr. Julien Gautrot

External supervisor: Prof. Alvaro Mata

Ethics approval

The use of human blood for this project was reviewed and approved the NHS Research Ethics Committee, Ethics REC Reference Number: 19/LO/0814, for Queen Mary University.

Details of collaborations

Mr. Carlos Alberto Redondo Gomez (School of Engineering and Materials Science, Queen Mary)

• Organised the synthesis, purification and availability of peptide amphiphiles for initial testing for Chapter 4.

Publications

Carlos Redondo-Gómez, Soraya Padilla-Lopategui, Helena S. Azevedo, and Alvaro Mata. (2020). Host–Guest-Mediated Epitope Presentation on Self-Assembled Peptide Amphiphile Hydrogels. ACS Biomaterials Science & Engineering 6 (9), 4870-4880. DOI: 10.1021/acsbiomaterials.0c00549

Abstract

The human body has evolved to enable healing in most of our tissues with remarkable efficacy. This process relies on a rich and dynamic microenvironment, which coordinates a myriad of molecular and cellular processes that ultimately culminate in complete healing. Imagine being able to harness and controllably guide and amplify this regenerative environment to heal larger non-regenerating defects in tissues and organs.

This project proposes a new way to think about regenerative materials by going beyond bioinspiration to establish a "bio-cooperative material", where the patient's own blood is transformed into living personalised devices (i.e. implants, grafts, in vitro models) that reconstruct and enhance the natural regenerative process. Self-assembling peptides were used as "supramolecular organisers" to guide the assembly of blood components, using coagulation as an active step of the fabrication technique. The project was developed along 3 main stages focused on a) understanding underlying molecular mechanisms and establishing supramolecular design rules and fabrication processes, b) understating the interaction of the materials with living cells, and c) developing personalised scaffolds that exhibit and enhance the properties of the regenerative process.

A novel hydrogel was developed based on the co-assembly of peptide amphiphiles (PAs) with blood proteins. The peptide PA-K_3 was used as a model to understand the molecular mechanisms behind the hydrogels assembly with blood components. It was established that negatively charged proteins (e.g. albumin and fibrinogen)

interact with the positively charged peptide and trigger the gelation process and hydrogel formation.

A set of different PAs (PA-K_3Q, PA-Q_3K_3 and PA-K_3Q_3) were designed to interact with the blood enzyme Factor XIII by incorporating lysine and glutamine residues in the peptides sequences. From these sequences, two of the resulting hydrogels exhibited enhanced mechanical properties (PA-K_3Q) and good biocompatibility (PA-K_3Q and PA-Q_3K_3). The bio-functionality of the hydrogels was evaluated using different cell lines: fibroblasts (NIH-3T3), endothelial cells (HUVECs) and mesenchymal stem cells (hMSCs). Results showed that all cell types were able to attach and grow on the surface of the hydrogels, while hMSCs cells showed early signs of migration inside the gels.

Extrusion liquid in liquid 3D printing was explored as a biofabrication method for the creation of more complex scaffolds. PA-K_3 was used as a bioink and was extruded into a blood bath to create the scaffolds. Multi-layer constructs were created using this fabrication method. Further optimisation of this method in order to improve resolution and stability of the constructs will be required.

In summary, this thesis highlights the potential of combining self-assembling peptide amphiphiles with blood biomolecules in order to generate bioactive tissue constructs for regenerative medicine.

Acknowledgments

I would like to express my sincere gratitude towards the following people for their continuous support and contributions to this research project.

First and foremost, to my two supervisors. Professor Alvaro Mata for his guidance, support, and continuous input throughout the development of this doctoral project. Dr. Thomas Iskratsch, for his invaluable input and assistance in biological experimental planning and continuous guidance on the project. Their input and support during the development of my project were undoubtedly crucial for the successful outcome of this project.

Next I would like to thank Dr. Carlos Redondo for his assistance in the synthesis and purification of peptide amphiphiles, and for the many hours of discussions on the significance of new findings on this work.

To all the researchers from the Mata Bioengineering and Iskratsch groups, a big thank you for all the hours working together side by side in the laboratory and for their kind help setting up experiments and trainings.

My deepest gratitude to the National Council of Science and Technology from Mexico (CONACyT), the Institute of Technology I2T2, and Queen Mary University for the financial support provided to develop this project.

To my partner, who has been an incredible support and source of happiness throughout this journey. Thank you for encouraging me to keep going, and for giving me your time and patience.

Lastly, I want to thank my family, for all their love and support, endless encouragement and words of wisdom throughout these four years. Words cannot express my eternal gratitude for walking with me along this journey.

Covid-19 Impact Statement

This research work was carried out during the COVID-19 pandemic. The challenges faced regarding different aspects of the research are listed below:

Laboratory closures and social distancing rules

Laboratory work was suspended as Queen Mary University was closed for 4 months (March to June 2020) at the start of the pandemic.

After laboratories re-opened in June 2020, there were additional difficulties and delays in collecting data due to the restrictions in schedules (e.g. reduced time in the laboratories) and social distancing rules established in the building. This meant that each room could only have a maximum capacity of 1-4 people at the time depending on the room size, resulting in limited time to use equipment and set up experiments. For PhD students, the 24-hour access was restricted to 7am - 7pm on weekdays and 10am- 4pm on weekends. These measurements remained in place for the next academic year.

Working with human blood

Work with human blood samples was suspended due to it being a potential hazardous biological fluid until the virus was deemed safe by the corresponding authorities. In addition to this, our sample provider was NHS Blood and transplant bank. The shortage of staff and resources meant the work involved in sample processing for research was deprioritised in order to relocate resources to high priority areas of the health sector. Additional paperwork, new permits, and new

measures needed to be established to work with blood, which resulted in considerable delays to obtain blood samples, even after the samples were deemed safe. This had a significant impact on the research work planned for Chapters 5 and 6 as all experiments required the use of blood. As a result, experiments on protein release from blood-PA hydrogels and the identification of blood proteins could not be extended and further in depth characterisation of the samples was not done (Section 5.2.3 and 5.2.4).

In addition, the work for Chapter 6 on bioprinting suffered a significant impact in terms of the data collected. All experiments were preliminary results before the pandemic started. These were carried out in collaboration with Blizard Institute and Nottingham University printing facilities. Access to both institutes was revoked due to the new rules on social distancing and travelling restrictions, as well as prioritising the students from those institutes. The access to both sites was not re-established for the rest of the duration of the project. The School of Engineering did not have printing facilities; hence no additional work was carried out for this chapter.

Table of Contents

List of abbreviations

2D Two-dimensional

3D Three-dimensional

BSA Bovine serum albumin

CD Circular dichroism

DMEM Dulbecco's Modified Eagle medium

ECM Extracellular matrix

FBS Foetal bovine serum

FGEN Fibrinogen

HA Hyaluronic acid

HCl Hydrochloric acid

HEPES 4-(2-hydroxyethyl)-1-piperazineethanesulfonic acid

hMSCs Human mesenchymal stem cells

HSA Human serum albumin

HUVECs Human umbilical vein endothelial cells

HWB Human whole blood

IF Immunofluorescence

NaOH Sodium hydroxide

PA Peptide amphiphile

PBS Phosphate buffered saline

PDMS Polydimethylsiloxane

PEG Polyethylene glycol

PFA Paraformaldehyde

PCL Polycaprolactone

PLA Polylactide

PLG Poly(lactide-co-glycolide)

PGA - Polyglycolic acid, PCL - polycaprolactone

PRP Platelet rich plasma

P/S Penicillin-Streptomycin antibiotic

Rh Rhesus factor

SBF Simulated body fluid

SEM Scanning electron microscopy

SRM Superresolution microscopy

TEM Transmission electron microscopy

List of nomenclature

Symbol	Description	Units
G’	Storage modulus	Pa / kPa
G’’	Loss modulus	Pa / kPa
Z	Zeta potential	mV
MW	Molecular weight	kDa
pI	Isoelectric point	pH

List of Figures

List of Tables

Chapter 1.

Introduction

This chapter provides the motivation behind the project, the thesis statement and the outline on how this thesis has been organised.

1.1 Motivation

Regenerative medicine is a growing field with the goal to restore tissues and organs damaged by disease or injuries (Atala et al., 2019). However, the current impact of regenerative medicine has been limited (Wu et al., 2018; Madl et al, 2018). This is evidenced by only 18 cell and gene therapy products approved by the FDA, of which about half rely on cord blood cell (FDA, 2020), as well as limited clinical successes from conventional scaffold-based tissue engineering approaches (Williams et al., 2019). Consequently, there is a pressing need for new and more effective regenerative therapies (Terzic et al., 2015). This need is exacerbated when considering that currently, the majority of the world population does not have access to sophisticated treatments.

The last decade has seen a growing number of emerging regenerative technologies based on for example stem cells (Wu et al., 2018), organoids (Brassard et al., 2019), gene editing (Bailey et al., 2019), nanotechnology (Mitchell et al., 2016), and biofabrication (Pavlovich et al., 2016). A major challenge for all these approaches is the capacity to recreate the inherent complexity and functionality of the wound healing process, an evolving environment of dynamic molecular and cellular processes that ultimately lead to regeneration (Mao et al., 2015).

Bioinspired materials can generate sophisticated structures with remarkable control but remain far from recreating the complexity and functionality of biological systems (Zhang et al., 2016). Emerging technologies such as three dimensional printing offer exciting possibilities but, again, are limited by the materials available, which cannot fully recreate the dynamic molecular and cellular microenvironment needed to

achieve regeneration (Morgan et al., 2020). To overcome this challenge, there is growing interest in the use of different types of cell-based systems including stem cells, organoids, and genetically modified cells lines. However, these also face challenges associated to their control when released inside the body, ensuring of safety, and efficiency of the treatments.

The goal of this research is to go beyond bioinspiration to establish a “bio-cooperative material” that enables the use of blood to engineer scaffolds that exhibit the regenerative properties of the blood clot microenvironment. To develop this approach, research into the fundamental understanding of how blood and its coagulation can be tuned and controlled to transform the patient’s own blood into personalised implants is needed. For this, the use of self-assembling peptides, not as main material building-blocks, but rather as “supramolecular organisers” that selectively interact with and guide the assembly of blood components while enabling biofabrication processes will be explored.

This approach represents a conceptual and technological leap forward in biomaterials design by working with the intrinsic regenerative capacity of the host and turning blood into a tuneable, scalable, and renewable biomaterial. This project aims to enable the first steps to be taken towards the development of widely accessible and personalised regenerative implants with potential impact on the patient’s healing process.

1.2 Thesis statement

Based on the motivation, a thesis statement was formulated which serves as the overarching aim of this research work:

"This doctoral thesis focuses on the development of a new co-assembly based method that allows the use of peptide amphiphiles and biological fluids (blood) for the creation of personalised, reproducible and bioactive three dimensional scaffolds for tissue engineering applications".

1.3 Thesis outline

This work is based on an interdisciplinary research project between materials science, cell biology and biofabrication, and cell biology. This thesis is divided into eight chapters.

Chapter 1 aims to provide the motivation for the project, a thesis statement, and a brief outline of the thesis structure. **Chapter 2** focuses on a review of literature related to the wound healing process, the current state of the art of different materials created to interact with blood and help the wound healing process, and the use of new emergent technologies such as self- assembling hydrogels and three dimensional printing to enhance the wound healing process. **Chapter 2** also provides an overview of the thesis aim and objectives. **Chapter 3** explains in detail the experimental materials and methodologies used throughout this thesis.

The experimental work is divided into three chapters, each of them presenting

results and discussion sections. **Chapter 4** focuses on the development of a new method to create scaffolds based on the co-assembly of peptides with biomolecules present in blood. This chapter is divided into two main sections: the first part covers initial peptide amphiphile testing, characterisation of initial interactions between peptides and blood molecules, determination of key components needed for the co-assembly, and hydrogel behaviour. The second part covers the design of new peptide sequences inspired by blood components and their characterisation.

Chapter 5 is dedicated to the study of relevant biological interactions between peptide amphiphiles and blood components, as well as the biocompatibility of the co-assembled materials and their effect on cell behaviour.

Chapter 6 introduces bioprinting as a potential technology to improve the materials obtained by co-assembly. This chapter demonstrates the feasibility of combining the use of PAs as a bioink and liquid in liquid printing method, and highlights the ability to create reproducible scaffolds.

Lastly, **Chapter 7** summarises the research work, and provides a perspective on future directions, and a discussion on the significance of the work.

Chapter 2.

Literature review

This chapter is divided into 5 main sections. The first and second section reviews fundamental aspects of blood biology, tissue injury and wound healing, and blood as a source for creating materials. The third section focuses on the use of peptide amphiphiles for tissue engineering and regenerative medicine applications. The fourth section aims to explain how this project integrates these two concepts to create a new approach towards personalised biomaterials. The fifth section defines the aim and objectives of this thesis project by providing a brief description of the experimental plan to create hybrid biomaterials by using a biological fluid (blood) and peptide amphiphiles.

The majority of this chapter is in preparation for submission as a review article:

• Padilla Lopategui et al. (2022). Blood-based bioengineering: Harnessing the regenerative and engineering potential of blood. *(In preparation)*

2.1 Blood through history

Blood has been a source of mystery and fascination since the beginning of humankind. It has been the central piece of many rituals and religions where it has been perceived as a link to divinity, as well as a symbol of life and death (Munson et al., 2014).

In medieval times, it was also regarded as a symbol of pride and status. The royal bloodlines were born as a result of the conquering of lands. This power was then passed on to the descendants of the kings and rulers (birth right), thus establishing a system of classes and hierarchies that was determined by the bloodline. However, genetic diseases were also transmitted amongst bloodlines. Haemophilia, a blood disorder, was diagnosed in the British Royal family in the 19th century and was known as the "royal disease" (Bhadra et al., 2015).

Blood has also played a central role in arts, where it has been used as a metaphor to talk about a number of topics including inheritance, religion, power, sacrifice, disease, racism and violence (Davidson et al., 1997; Codreanu et al., 2015). Other literary pieces such as Dracula, have created fantasy worlds where blood plays a main role with different connotations.

The study of the mind has also been linked to blood. The four temperament theory, developed by the greek physician Hippocrates, talks about personality types that come from 4 humours in the body: blood, yellow bile, black bile and phlegm. Therefore, having more blood leads to a "sanguine" type which tends to be a very social and risk taker person (Merenda et al., 2010). Another theory originated in

Japan, suggested that the blood groups ABO determines personality traits (Furukawa, et al., 1929). Blood has also been studied for its potential link to mental illness (Rinieris et al., 1980).

Medicine has studied blood for a long time, from its role in the body to its potential uses. Some antique procedures using leeches were developed to get rid of “bad blood” while others such as transfusions were developed to replace “bad blood” for healthy blood (Giangrande et al., 2000). Interestingly, blood has always occupied a central part of human history and it has connected disciplines from different fields together.

2.1.1 Blood functions

2.1.1.1 Blood as a source of life

Blood is a complex and highly dynamic biofluid. It is comprised of a mixture of proteins, ions, gases and cells. Its components are involved in many different processes that constantly take place inside the body. Blood is responsible for carrying biomolecules to different tissues and organs involved in a variety of essential functions including tissue oxygenation, nutrient transport, and removal of waste products, amongst others. The main blood components are summarised in Table 2.1. (Tutwiler et al, 2016).

Component	Types	Function	Physiological concentrations
Cells	Red blood cells	Oxygen carriers.	4,000,000-6,000,000 cells/µl
	White Blood cells	Defence against pathogens.	4000-10,000 cells/µl
	Platelets	Blood clotting, wound sealing.	150,000 to 450,000 cells/µl
Proteins	Serum Albumin	Biomolecule carrier.	35-50mg/ml
	Globulins	Blood clotting and defence against pathogens.	20-25mg/ml
	Fibrinogen	Blood clotting, fibrin network formation.	2.0-4.5mg/ml
	Regulatory proteins	Immunomodulation, homeostasis.	N/A
	Clotting factors	Blood clotting.	N/A
Ions	Na^+	Maintain homeostasis in blood.	142.0 mM
	K^+	Allow flow of electrical signals through the body.	5.0 mM
	Mg^{2+}	Cell protection against damage.	1.0 mM
	Ca^{2+}		1.3 mM
	Cl^-		103.0 mM
	HCO_3^-		27.0 mM
	HPO_4^{2-}		1.0 mM
	SO_42^-		0.5 mM

Table 2.1. Main blood components, functions and physiological concentration in the human body.

2.1.1.2 Blood as a defence mechanism

The body's defence mechanisms critically depend on blood. It is involved in key processes like immune cell mobilisation and confinement of pathogens, when the body is fighting an infection. Upon injury, a cascade of signalling molecules is triggered and immune cells are activated and recruited to the wound site to help the detection and destruction of pathogens in a matter of seconds (Minasyan & Flachsbart, 2019).

Although this system is highly effective, the immune response can be affected by different factors including ageing, leading to inefficient detection and decreased response against pathogens, as well as a higher risk of developing other autoimmune or inflammatory diseases (Castelo-Branco et al., 2014).

2.1.1.3 Blood as a vector for disease transmission

Certain pathogens have the ability to remain in blood for long periods of time, or in some cases indefinitely, without causing an immediate disease to the host. In these instances, blood can become a vector for disease transmission of viruses or bacteria. These blood borne diseases are highly dangerous due to their remarkable ability to spread to different hosts through contamination with blood and other fluids (Gerberding, 1995).

2.1.1.4 Blood as a source of genetic information

Blood is common in the animal kingdom, but it is also unique. Although many different species have blood and a circulatory system, key differences have been found in terms of: a) the chemical composition (e.g. ionic content), b) the biological composition (e.g. cell types), and c) the physical properties (e.g. viscosity) of blood; variability is also observed within individuals of the same species. In addition, the genetic information stored in red blood cells leads to the expression of different antigens in the cell membrane, which gives rise to the existence of different blood groups. The most relevant blood group systems for humans are ABO and Rh (Rhesus factor), which are based on the presence or absence of specific antigens on the surface of erythrocytes. These unique combinations of antigen expression determine blood compatibility or lack of thereof between individuals of the same species (Farhud, et al., 2013; Avent & Reid, 2000).

2.1.1.5 Blood as a cure or treatment

Blood was historically used as a cure for certain ailments. Blood transfusion is one of the oldest techniques developed and currently most widely used in the clinic as a treatment for different conditions like anaemia or congenital blood disorders as well as some other circumstances like haemorrhage due to trauma/surgery (Sharma, et al., 2011). Medical advances have made it possible to preserve blood or isolate different plasma fractionations for therapeutic use, including coagulation factors, anticoagulants or protease inhibitors.

Current research has focused on the use of genetic modification for the treatment of blood diseases such as sickle cell disease and β-thalassemia (Kohn et al., 2019). Moreover, genetic modification of immune cells, such as Chimeric antigen receptor T cells (CAR T) therapy, is currently under development to make cells more efficient against detection and destruction of cancer cells (Maldini et al., 2018).

2.1.1.6 Blood as a protective mechanism after injury

One of the most exceptional properties of blood is the ability to transform from a liquid to a solid material when the body suffers injury. Blood clotting is essential to prevent a person from bleeding out and develop a life-threatening condition. This is an extraordinary example of self-assembling in nature by which a temporary scaffold is created with the purpose of giving the body enough time to repair and heal the damaged tissue (Rausch et al., 2021).

2.1.1.7 Blood as a diagnostic tool

Blood is a source of unparalleled biological information. Its richness in terms of cells, proteins and metabolites has been exploited for its use as a diagnostic tool for different pathologies including:

- Blood disorders (genetic analysis, blood cells count, enzymatic activity) (Bates & Bain, 2009)
- Metabolic disorders (quantitation of metabolites) (Bonilla et al., 2018)
- Mental health disorders (biomarkers) (Ashton et al., 2020)
- Cancer (liquid biopsy) (Buscail et al., 2019; Cohen et al., 2018)
- Infections (detection of pathogens) (Wilson et al., 2020)

2.1.1.8 Blood as a source for creating materials

Due to its dynamic nature, blood has been considered a powerful resource for the creation of different types of therapies as well as a primary source of materials to aid modern medicine.

a) Blood fractions

The separation of blood into different components has made it possible to obtain fractions with different properties and cellular content. Currently, transfusions of whole blood or fractions are the main clinically approved procedure for blood loss due to trauma injuries and surgery, or as a treatment for blood disorders. Plasma and platelet transfusions, are routinely used to aid patients with coagulation issues. (Sharma, 2011)

Major limitations of these products are the availability of donors, risk of disease transmission and rejection, and shelf life (Burnouf et al., 2009; Burnouf et al., 2013). The downside of these materials represents an opportunity for the innovation of improved products that could overcome these issues.

b) Sealants, adhesives and haemostatic agents

When bleeding is excessive and traditional methods such as sutures are not adequate or effective, bleeding control agents have proven to be a helpful tool to repair damage and avoid life threating conditions. They can be classified mainly in 2 categories: tissue adhesives and sealants (Mehdizadeh et al., 2003; Zhu et al., 2018). These materials have been created by isolating useful blood components (e.g. fibrin, albumin, thrombin) and combining them with different polymers or crosslinking agents to create functional materials.

From a clinical perspective, there are key factors that must be considered for the routine use of these materials including: safety, efficacy, cost and approval by regulatory organisations (Spotnitz et al., 2012). On the other hand, from a materials perspective, mechanical properties and biocompatibility of these materials are key aspects that need to be addressed.

2.2 Biological, physical and mechanical properties of blood from a materials perspective

Blood is a heterogeneous fluid composed of numerous types of biomolecules and cells (Table 2.1). This heterogeneity is responsible for the different properties

discussed before. It can be easily separated via centrifugation into different fractions to obtain the following: (Basu & Kulkarni, 2014; Mescher et al., 2018)

- ***Haematocrit:*** Constitutes around 44% of whole blood. It is comprised of red blood cells and its main function is oxygen transport. This fraction is routinely used in the clinic for blood transfusions.
- ***Buffy coat:*** Constitutes around 1% of whole blood. It is comprised platelets and white blood cells and its main function is blood clotting and the immune response. This fraction is used for DNA extraction and detection of certain pathogens.
- ***Plasma:*** Constitutes around 55% of whole blood. It is comprised of water, salts, proteins, lipids, hormones and gases. The main function of plasma is to transport cells and nutrients/waste products. It is also routinely used to help patient's blood clotting ability after injury.

Further processing of blood by creating protocols with multiple centrifugations steps and additional reagents has been developed in order to obtain non-traditional blood fractions with different compositions. Some of the most relevant fractions are:

- ***Serum:*** Serum is a blood fraction composed of all the proteins, electrolytes and antibodies present in blood, with the exception of the ones involved in the blood clotting process. Recently, hyperacute serum (HAS) has been developed, this fluid is isolated from activated platelet-rich fibrin, and does not contain any cellular components or blood clotting factors. It has been widely used for research on the effect on cell health and growth (Jeyakumar, et al., 2017; Kardos et al., 2019; Simon et al., 2018).

- ***Platelet poor plasma:*** Plasma with very low number of platelets. It has been used for platelet aggregation studies (Cattaneo et al., 2007)
- ***Platelet rich plasma:*** Concentrated mixture of platelets, inflammatory molecules, and growth factors (Kawase et al., 2015). It has been created with the purpose of promoting wound healing but research has not proved its effectivity (Everts et al., 2006; Alves et al., 2018). This biofluid has also been more recently used for dermatology and cosmetic purposes (Man et al., 2001)

From a materials perspective, we can dissect the different components of blood and see how the interaction between them or lack thereof can cause blood or derived fractions to acquire unique properties. **Table 2.2** summarises the physical and mechanical properties of blood's main components.

The shape and stiffness of cells play a key role in the fluidic behaviour of blood but also, on the mechanical properties of blood clots. In the case of single cells, these properties can affect how cells organise and flow in the veins. Red blood cells are more likely to remain in the middle section of blood vessels whereas platelets and white blood cells are usually found on the periphery. This spatial organisation is important for the cells' response to physiological changes or stimulus. Moreover, perturbations on cells' morphology and mechanical properties have been associated with impaired function and pathological conditions (Qiu et al., 2019).

After injury, cells and proteins are activated and recruited to form a blood clot to prevent blood loss and seal the wound. The stiffness of a blood clot is around 3.2 kPa (Mercado et al., 2018) whereas a plasma clot strength can vary from 70-600 Pa (Jen et al., 1982). The resulting material has different stiffness and adhesive properties

than the starting building blocks which has been directly associated to the cellular and protein content of the starting fluids (whole blood or plasma). Research has been able to manipulate the content of these fluids in order to create materials with different mechanical properties.

Blood components	Type	Stiffness (Pa)	Adhesion force	Reference
Individual cells	***Red blood cells***	150 Pa 5kPa 7.57 ± 3.25 kPa 26 ± 7 kPa		Fay et al., 2016. Lekka et al., 2005. Barns et al., 2017. Tomaiuolo et al., 2014; Dulinska et al., 2006.
	White blood cells			
	- Lymphocytes	2,900 Pa 1.15 ± 0.12 kPa		Zheng et al., 2014. Kubankova et al., 2021.
	- Granulocytes	500 Pa		Fay et al., 2016.
	- Neutrophils	0.96 kPa		Kubankova et al., 2021.
	- Eosinophils	0.94 kPa		Kubankova et al., 2021.
	- Monocytes	580 Pa 1.0 kPa		Bufi et al., 2015. Kubankova et al., 2021.
	- Macrophages	930 Pa		Bufi et al., 2015.
	Platelets	10 kPa	70 nN (5 kPa)	Lam et al., 2010.
Individual proteins	Fibrin fibre	1.7 ± 1.3 to 4.5 ± 3.5 Mpa		Collet et al., 2005.
	Pure Fibrinogen clot (15mg/ml)	45 kPa	4.5 kPa	Alston et al., 2007.
Bulk (Cells and proteins)	Blood clot	3.21 ± 1.97 kPa		Mercado et al.,2018.
	Platelet rich clot (from PRP)	600 Pa		Jen et al., 1982.
	Platelet free clot (from PPP)	70 Pa		Jen et al., 1982.
	Plasma clot	10 kPa	1 kPa	Alston et al., 2007.

Table 2.2. Mechanical properties of blood components. Blood has different properties that can change through time depending on the type of cells, proteins and other biomolecules present in the blood fraction studied. This table aims to highlight the differences between the mechanical properties of single cells or biomolecules and their combinations.

The blood clot is another interesting example of how this particular biofluid can interact and adapt to its surrounding environment in response to an external

stimulus. The creation of a naturally occurring temporal scaffold is a key requirement for the wound healing process in different tissues. One of the most representative examples of this process is bone healing after fracture, where the blood clot plays a key role in the initial upregulation of angiogenic and osteogenic factors (Schell et al.,2017). Several studies show how the removal of this blood clot has a negative outcome on the bone healing process (Grundnes et al., 1993).

The examples above highlight the importance of the type of molecules and their interactions for the construction of materials with emergent properties, which is a key aspect of materials design (Okesola, & Mata, 2018).

2.3 Tissue injury and the wound healing process

After tissue injury, several molecular mechanisms are instantly activated in an attempt to re-establish the body's equilibrium and repair the damage inflicted to the organism. Depending on different factors, there are a couple of possible outcomes: regeneration, normal repair, excessive healing, deficient healing (Figure 2.1) (Diegelmann et al., 2004).

Regeneration and exact replacement of the damaged tissue is not possible in humans, however, this process has been studied in detail in other organisms such as the salamander. *Repair* of the damaged tissue implies that the homeostasis has been restored and the tissue has healed in an appropriate manner, nonetheless this implies that part of its initial functionality level might have been compromised or lost during repair.

In some other instances, injury can be followed by an aberrant wound healing process where the body undergoes *excessive healing* and development of fibrosis, which is a chronic degenerative condition characterised by over proliferation of cells, ultimately leading to loss of function in the damaged organs (e.g. kidney, lung, liver). Lastly, *deficient healing* can also occur after damage, which is characterised by a chronic inflammatory state and non-healing wounds (Figure 2.1).

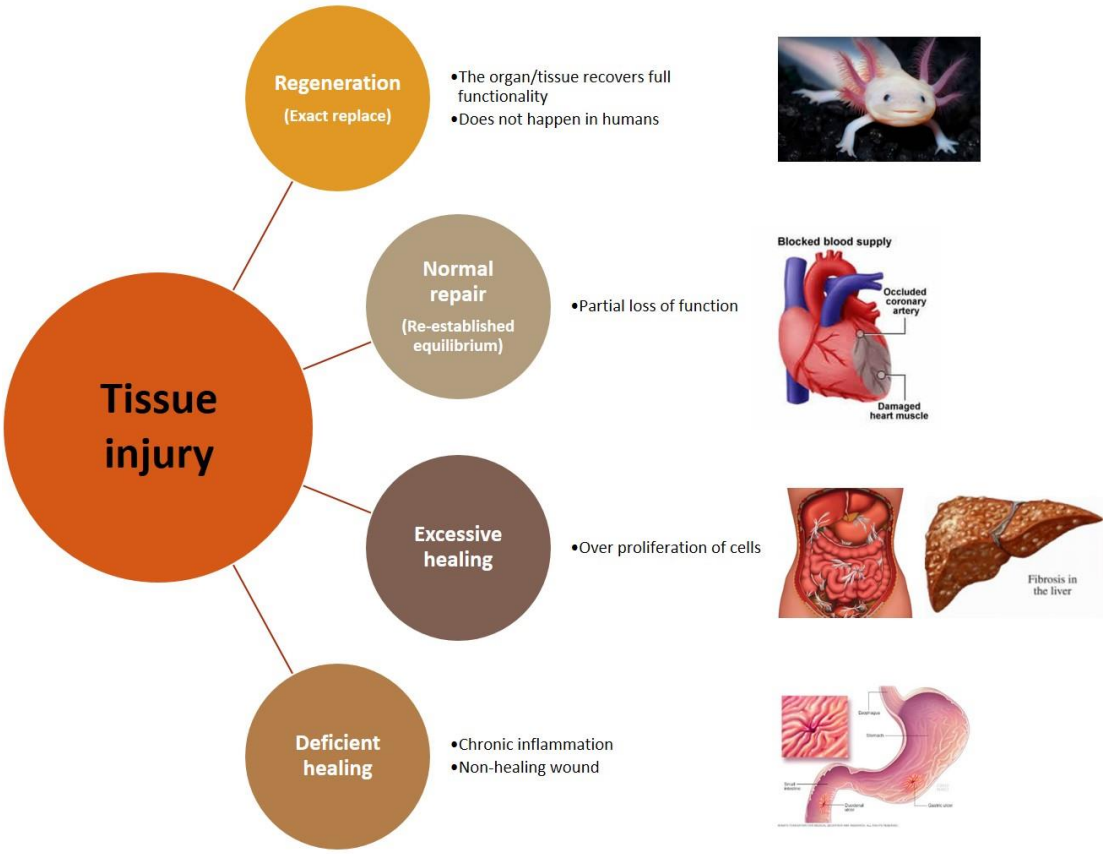

Figure 2.1. Healing mechanisms after tissue injury. When the body undergoes damage, the blood clotting process is triggered with subsequent activation of wound healing mechanisms. There are four possible responses that can be activated after injury: *regeneration* refers to the exact replace of the damaged tissue whereas during *normal repair*, homeostasis is achieved and the tissue heals with partial loss of function. However, *excessive healing* or *deficient healing* can occur when aberrant pathways are activated, which could lead to the development of secondary disorders.

2.3.1 Wound healing process

The wound healing process has key stages that allow recovery after injury, all of which may be hampered causing complications of different magnitudes (Figure 2.2). This process is characterised by four overlapping phases (Broughton et al., 2006). The first step towards tissue healing is *Haemostasis*, the body's mechanism to stop bleeding. During this stage, platelets arrive to the damaged site and secrete clotting and growth factors as well as cytokines, essential for the coagulation of blood. This process is activated instantly after injury, ultimately resulting in clot formation that closes the wound site, thus preventing excessive blood loss. However, different bleeding disorders like Haemophilia and Thrombocytopenia can hamper this process and could ultimately lead to death (Jeffrey et al., 2014).

An *inflammatory state* is also active during injury; its main purpose is to remove any foreign material from the injury site as well as the damaged tissue itself. This phase is executed by neutrophils and macrophages that clean the wound and secrete inflammatory molecules needed for activation of additional signalling pathways, some of which intervene in cell recruitment to the wound site. Even when inflammation is needed for healing, it is important to point out that, during normal repair, this is a transitory state. On the contrary, in pathological conditions, inflammation becomes a chronic stage that leads to the development of non-healing wounds, like ulcers.

After activation of signalling pathways, fibroblasts are the first cells that start proliferating and depositing ECM in the wound site, this phase is known as

proliferative stage. Lastly, the *remodelling phase* takes place, where ECM is cross-linked and adapted to repair tissue. A dysregulation of the proliferation process can trigger a fibrotic condition, characterised by over proliferation of fibroblasts and excess of ECM deposition with reduced or no remodelling (Diegelmann et al., 2004).

Depending on the extent of the damage, the healing process can take place in different time frames. However, it is important to point out that after tissues have healed, some functionality can be lost and other complications such as post-surgical adhesions or chronic pain might still be present in patients, affecting their quality of life.

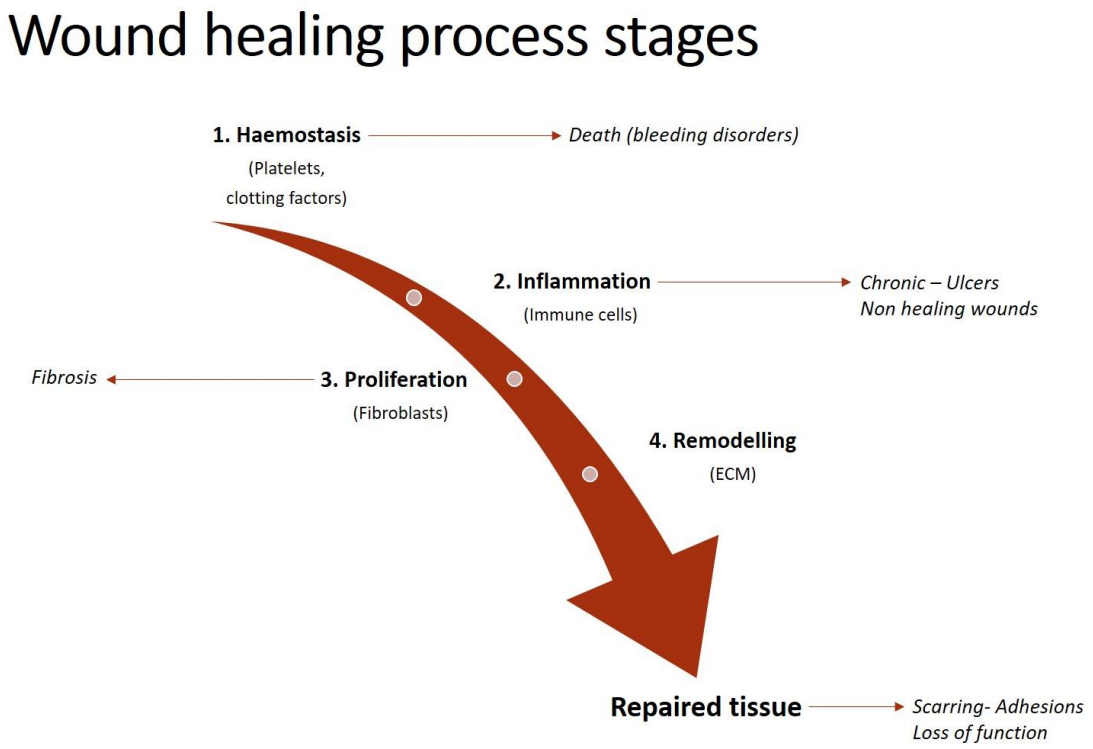

Figure 2.2. Wound healing stages. The process of wound healing after tissue injury is characterised by different stages that overlap each other. First, blood clotting is activated to achieve haemostasis and prevent bleeding (1). Second, an inflammatory process (2) takes place at the site of the injury where immune cells are involved in its regulation. Third, the

proliferation phase (3), which involves the recruitment of cells like fibroblasts to close the wound and repair the damaged tissue. And fourth, the remodelling phase (4), where the ECM is shaped to repair the tissue. Hampering of any of these stages by pathological conditions leads to unsuccessful tissue repair.

2.3.2 Haemostasis and blood clotting

Blood is a dynamic, renewable, and living tissue that plays a key role in tissue regeneration. Upon injury, blood coagulates through a tightly controlled process where multiple molecular and cellular components progressively interact to create the resulting hematoma.

The process begins through a cascade of enzymatic activation events that take place through intrinsic (i.e. from inside the vascular system) and extrinsic (i.e. from outside the vascular system) pathways.

A cascade of events then leads to the formation of thrombin, which cleaves fibrinopeptides from the plasma protein fibrinogen to create fibrin monomers, which in turn, through specific and tightly controlled reactions, polymerize into the fibrin polymer. This polymer then is crosslinked by clotting Factor XIIIa through glutamine (Q) and lysine (K) residues on the fibrin molecules (Chernysh et al., 2012). This process transforms blood from a functional fluid to a living, yet firm and stable, solid which plays a key role in the regeneration of the corresponding tissue. Figure 2.3 summarises the main steps of the clotting cascade and the molecular pathways of activation.

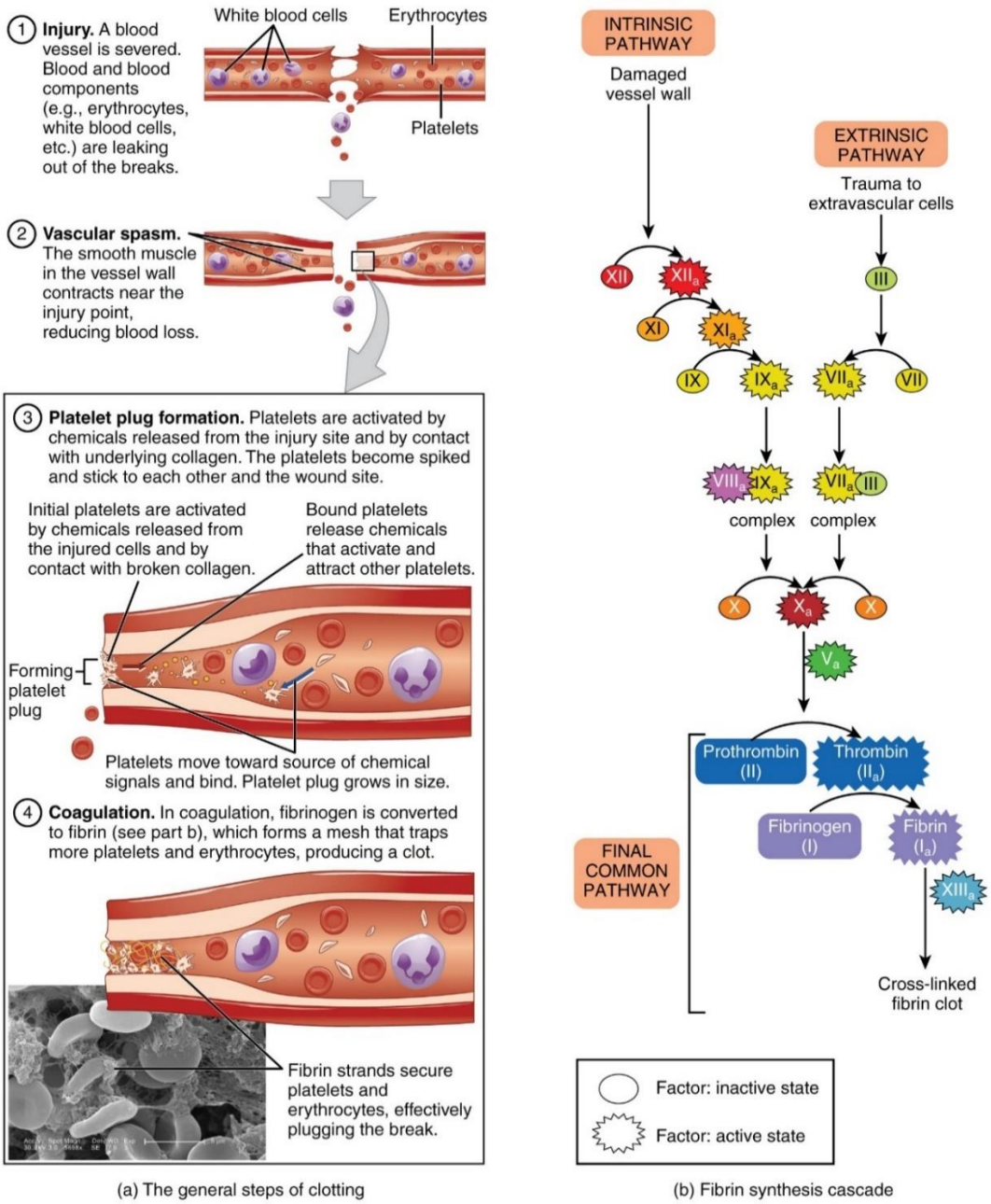

Figure 2.3. Blood clotting cascade. After injury (1), the process of haemostasis is characterised by the following steps: vascular spasm (2), the smooth muscle tissues contract to prevent blood loss; platelet plug formation (3), characterised by platelet activation and recruitment to the wound site; and coagulation (4), where fibrinogen is polymerised into a fibrin mesh that produces and stabilises the blood clot. These events are regulated by the coagulation cascade where clotting factors are sequentially activated via different pathways: intrinsic pathway (triggered by internal damage), extrinsic pathway (triggered by external damage), both of which share the final steps of blood clotting with the final common pathway of fibrin synthesis and blood clot formation. (Image reproduced from Anatomy & Physiology OpenStax College, 2013).

2.4 Tissue engineering and the use of biomaterials

In some instances, when the body suffers large traumatic injuries or has chronic diseases, the mechanisms of wound healing are not sufficient to repair the damage and the traditional methods of medicine fall short. This can affect the quality of life of the patients severely and on the least favourable of the outcomes, lead to death.

In the past decades, tissue engineering has emerged as a new approach for the need to create new and improved materials and therapies to help improve patients' care and develop alternatives to enhance tissue healing and regeneration. This is a multidisciplinary field that combines cell and molecular biology with biomaterials science with the goal to produce new functional tissues that can be used to maintain, repair or replace damaged organs (Langer & Vacanti, 1993).

This discipline combines the use of cells, scaffolds and signalling molecules to direct the process of tissue organisation ex vivo or in vivo (although not all three components are always present). Biomaterials play a key role in the development of scaffolds that serve as a guide to direct cell behaviour and organisation (Place et al., 2009). Research in natural and synthetic materials has been conducted to create the *"ideal biomaterial"* which should have at least the following characteristics: biocompatibility, biodegradability, bioactivity, integration to native tissue (mechanical properties), and non-immunogenic (Kim et al., 2000; Place et al., 2009; Patel et al., 2012). The properties of these materials should be optimised according to their final applications.

Materials used for tissue engineering scaffolds can be generally classified as follows (Vats et al., 2003):

a) *Natural materials.* These include polysaccharides and proteins found in nature. The main advantages of using natural materials is their biodegradability, low toxicity and low inflammatory response. They have been used a lone or as a combination with other natural or synthetic materials to tune their mechanical properties. Examples of these materials include alginates, collagen and chitosan.
b) *Synthetic materials.* These type of materials can be manufactured at large scales and their properties can be modified easily. Some examples are synthetic polymers (e.g. PLA - Polylactic acid, PGA - Polyglycolic acid, PCL - polycaprolactone) and their co-polymers, ceramics, and bioactive glasses.

Regardless of the type of biomaterials used, the need for smart materials that respond and adapt to the biological environment is a critical feature for the success of the tissue engineering approach.

2.4.1 Self-assembling materials. Peptide amphiphiles.

Supramolecular polymers are materials in which the monomers are linked together by non-covalent bonds such as hydrogen bonds and hydrophobic interactions (Azevedo et al., 2018). Self- assembling peptide amphiphiles (PAs) are a class of supramolecular polymers. One of their main characteristics is that they possess the

ability to spontaneously organise into well-defined nanofibres that can form three-dimensional networks (El-sherbiny & Yacoub, 2013).

The interest in these hydrogel systems for regenerative medicine and tissue engineering has grown due to their biomimetic properties, which enable them to form 3D networks resembling the extracellular matrix and also, to enhance cell signalling. The architecture and bio-functions achieved with the use of these materials makes them suitable for creating artificial scaffolds for tissue regeneration. Their versatility of design has proven to be a significant advantage for directing cell behaviour and regeneration of tissues such as brain, skin, bone, heart, nerve, tooth and cartilage (Cavalli et al., 2010; Inostroza-Brito et al., 2015; Mata et al., 2009; Tejeda-Montes et al., 2014; Zhang et al., 2010; Koutsopoulos et al., 2016).

Two main strategies have been contemplated for the use of these materials in tissue regeneration: scaffold based (growth factor or drug) delivery systems and cell seeded scaffolds. The first approach consists of binding bioactive molecules to the hydrogels to enhance cell attachment and proliferation ultimately leading to tissue organisation and functionality. By controlling matrix degradation with pre-programmed triggering mechanisms involving environmental changes such as pH, temperature or enzymatic cleavage, it is possible to release drugs or growth factors “on demand” mimicking the real response in the body (Lee et al., 2011). These stimuli-responsive hydrogels present clear advantages over other synthetic or animal-derived materials including the reduction of the drug doses or growth factor, the controlled release over a longer period of time and the reduction of off-target side effects (Culver et al., 2016; Koutsopoulos et al., 2016).

The second strategy is based on the addition of a cell suspension to the liquid peptide solution prior to its gelation. By using this method, the microenvironment created allows easier encapsulation of the cells and has proved, in certain instances, to extend cell survival rates compared with other polymeric materials (Beniash et al., 2005; Cheng et al., 2016; Matson et al., 2011).

The spatio-temporal control of growth factors and other morphogens is crucial for tissue formation (Lee et al., 2010; Mata et al., 2017). The ability to design "smart materials" that can respond to stimuli in real time mimicking, for example, the body's response to injury, is one of the reasons hydrogels have been catalogued as a promising solution to adapt to the highly variable changes that occur during the healing process.

Especially, PAs are ideally suited for in vivo tissue engineering. After injecting a liquid solution into the patient, the gelation process can be then activated through a pH change, ionic concentration change or light induction to form a gel inside the body, thus reducing the invasiveness of the procedure and allowing localised therapy (Zhang et al., 2010; Koutsopoulos et al., 2017).

Moreover, researchers have shown that it is possible to create peptide/protein hybrid systems that enable morphogenesis into stable tubular structures, which could be used to create more complex bioactive scaffolds that, can support and guide cell growth (Inostroza-Brito et al., 2015).

According to several studies (Beniash et al., 2005; Cheng et al., 2013; Kretlow et al., 2007; Cui et al., 2010; Seelbach et al., 2015), some of the main advantages of using this material as a scaffold are:

- Enhanced adhesion and directional guidance of cells.
- Cell proliferation and motility are not arrested by cell entrapment.
- Control over cell differentiation (depending on bio-functionalisation).
- Improved cell survival.
- Lower immunogenicity (depending on the design).
- Controlled biodegradation.
- Non-toxic degradation products (amino acids) that could be used in metabolic routes.

The properties of the hydrogels depend on many different variables like peptide composition, nanofiber structure, intermolecular forces between nanofibers, crosslinking agents, amongst others. Each of these properties can be modified by different methods in order to achieve the ideal biomaterial for tissue regeneration.

By designing materials at a molecular level, the incorporation of key amino acid sequences with known biological activity and secondary structure formation (e.g. nanofibres) has resulted in the ability to mimic highly complex biological environments that can interact with their surroundings and stimulate the process of tissue regeneration (Mata et al., 2017).

2.4.1.1 PAs chemical and physical properties

PAs are molecules that behave like surfactants due to their strong amphiphilic nature. These molecules have two key segments in their design: hydrophobic and peptidic sequence, containing four essential domains (Figure 2.4) (Cui et al., 2010; Azevedo et al., 2018).

The *hydrophobic segment* is comprised of an *alkyl chain*, which directs the first interactions between PAs due to the generation of hydrophobic interactions leading to aggregation. This allows the molecules to assemble, exposing the peptidic sequence on the exterior of the structures.

The *peptidic segment* is formed by 3 domains: β-sheet forming sequence, charged sequence and bioactive sequence. The β-sheet forming sequence is composed of hydrophobic aminoacids (i.e. valine, alanine) that potentiate intermolecular hydrogen bonding interactions due to their propensity to form β-sheet regions.

The *charged sequence* enhances PA solubility and helps purification of these molecules. This region also confers the ability to trigger PA assembly by changing the pH or ionic concentration (salts).

Lastly, the bioactive sequence is based on short motifs found in nature that have an effect in cell adhesion, proliferation or differentiation (i.e. RDG, IKVAV) and are incorporated to the materials to enhance biological responses (Cui et al., 2010; Edwards-Gayle & Hamley, 2017).

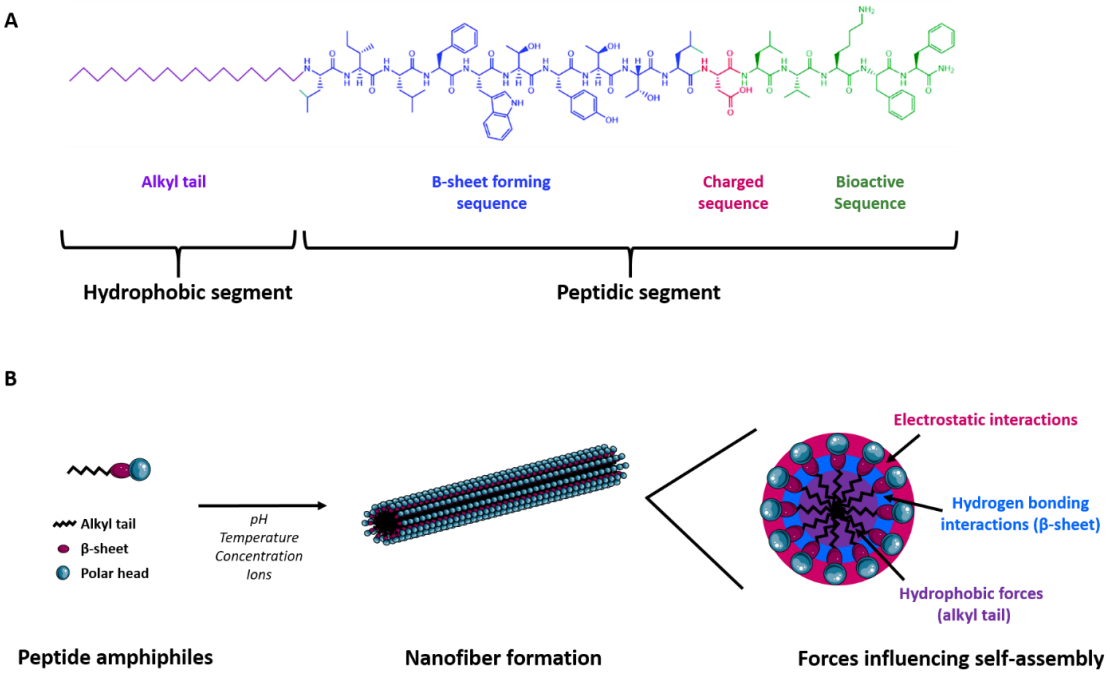

Figure 2.4. Chemical and physical properties of peptide amphiphiles. A) Peptide amphiphiles chemical structure is comprised of 2 regions: the hydrophobic and the peptidic segment. Each of these regions have essential domains that enable the self-assembling process. (This image was adapted from Edwards-Gayle & Hamley, 2017) B) Peptide amphiphiles self-assembly mechanism into nanofibers can be triggered by different factors (e.g. pH, temperature, ions) and is directed by different intra and intermolecular forces that allow and stabilise hydrogel formation.

2.4.1.2 Self-assembling mechanisms

Spontaneous self-assembly of PAs is the result of an interplay between attractive and repulsive forces within the peptides, leading to the formation of inter and intramolecular bonding (Figure 2.4). Three types of forces play a major role in the assembling of these complex structures.

Hydrophobic interactions originated by the alkyl chain are responsible for the stability of the supramolecular structures. Weaker hydrophobicity will lead to micelle

formation whereas a strong hydrophobic core will lead to nanofiber formation (Fu et al., 2014). Similarly, the β-sheet sequence of PAs creates hydrogen bonds which also contribute to the formation and stability of the structures (Paramonov et al., 2006; Tekin et al., 2015; Lee et al., 2012). A thoughtful molecular design and aminoacid selection is needed since some residues will be more prone to prevent or alter the hydrophobic and hydrogen bonding interactions, thus altering the internal order of the molecules and disturbing their assemble and architecture (Jiang et al., 2007).

Electrostatic interactions also play a key role in the assembly mechanisms. Charged residues in the surface of the PAs help the solubility of the materials (Fu et al., 2013). Other forces that contribute to the stabilisation of these materials include van der Waals and π-π stacking forces (Lee et al., 2011; Guler et al., 2006).

2.4.1.3 Control of gelation properties

The control of nanostructure formation and gelation of PAs can be tuned by manipulating the molecular forces that contribute to the assembling process. This can be achieved through the modification and optimisation of the molecular design, environment and introduction of co-assembling molecules (Cui et al, 2010).

In terms of the molecular design, it has been shown that the length of the alkyl chain plays a key role in the formation of structures and its nature (micelles, ribbons or nanofibers). Also the β-sheet strength depends on the length of the peptide sequence and nature of the amino acid residues.

The environment changes can also contribute to activate the gelation process. Depending on design, different systems have been created to respond to pH, temperature and salt concentrations, thus triggering reversible or non-reversible assembling processes.

The combination of peptide amphiphiles with other type of biomolecules such as proteins, synthetic proteins (such as elastin like proteins), carbohydrates, and lipids has begun to be explored more recently (Inostroza-Brito et al., 2015; Inostroza-Brito et al., 2017; Hedegaard et al., 2018). Recent studies have shown that by combining these molecules, emergent properties can be achieved that do not relate to those of the initial building blocks (Okesola et al., 2018).

2.4.1.4 Characterisation methods

As previously described, peptide amphiphiles based materials assemble in a modular and dynamic fashion. Therefore, their characterisation proposes a challenge as they present different mechanical properties and behaviour depending on the scale of the assembling process. To characterise these highly versatile systems, a set of studies is performed at different stages of the self-assembling process to identify emergent properties at the nano, micro and macro scale. A summary of the different characterisation techniques utilised to determine PAs properties is shown in Figure 2.5.

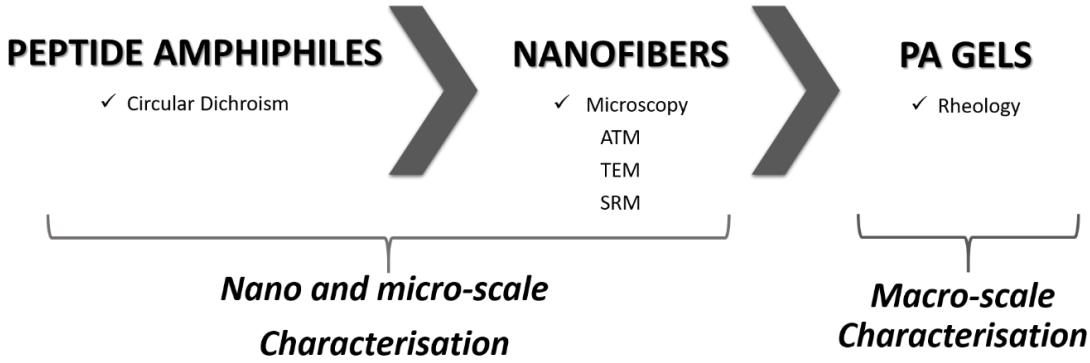

Figure 2.5. Techniques utilised for the characterisation of self-assembling peptide amphiphile gels. There are different characterisation techniques for PAs depending on the stages of the self-assembling process. First, on the nano and micro-scale, peptide amphiphiles secondary structure can be analysed using techniques like circular dichroism. After triggering gelation, microscopy techniques like AFM, TEM, and SRM are useful to study nanofibres formation and their properties. On the macro-scale, mechanical properties of the resulting hydrogel can be measured using techniques like rheology.

2.4.1.4.1 Characterisation of PA molecules

After PA synthesis, the first step towards characterising a new material is to determine if the molecules have been correctly synthesised and the product has the structure previously desired. Circular dichroism spectroscopy is a method used for the evaluation of the secondary structure, folding ad binding capabilities of peptides or proteins in solution (Greenfield et al., 2006). This form of spectrometry is based on the different absorption of right (ER) and left handed (EL) circularly polarised light by optically active biomolecules due to their dextrorotary and levorotary components (Greenfield et al., 2006; Beychok et al., 1996). A distinctive CD spectral signature is obtained which is dependent on the secondary structure of the biomolecule analysed (i.e. alpha-helix, beta-sheets) (Khalily et al., 2015; Pérez et al., 2014; Velichko et al., 2008; Jiang et al., 2007).

2.4.1.4.2 Characterisation of PA Nanofibers

In order to characterise these biomaterials at the nanoscale, microscopy techniques such as Atomic Force Microscopy (AFM) and Transmission Electron Microscopy (TEM) can be utilised to determine the diameter and length of the self-assembled nanofibers.

Super-resolution microscopy (SRM) has recently been proposed as another tool to characterise supramolecular materials due to its nanometric resolution. These materials are known to assemble in multiple scales and are composed of different building blocks, therefore the spatiotemporal localisation of each molecule at specific scales could be improved by using SRM and fluorescently tagged peptides that allow their real time tracking (da Silva, et al., 2016). SRM nanoscopy has the capacity to resolve these multiscale structural features with nanometric accuracy. In addition, the multicolour and quantitative nature of SRM has been shown to allow the visualisation and counting of different molecules which is important for the study the properties of these dynamic materials (Pujals et al., 2019). Moreover, this type of nanoscopy could also be used to track the assembly and disassembly of these materials in situ due to its minimal invasiveness (Azevedo et al., 2018).

2.4.1.4.3 Characterisation of PA hydrogels

The assembly of PAs into nanofiber networks allows them to encapsulate water which results in hydrogel formation. The transition from liquid state to gels is a

characteristic feature of these systems which gives them new properties that allow them to withstand external shear stress. (Stendahl et al., 2006).

Generally, hydrogels present a viscoelastic behaviour, meaning they exhibit both viscous and elastic properties when undergoing deformation. The term viscoelasticity can be defined as the process of molecular rearrangement in materials. When stress (force) is applied to a polymeric material, parts of the polymeric chains can change their conformation resulting in the deformation of the material. In this case, the molecular rearrangement that occurs is needed in order to withstand the applied force (viscous behaviour). When the force ceases, the material is expected to fully recover and return to its original form (elastic behaviour), also known as self-healing ability. (Niece et al., 2009)

A typical mechanical spectrum of hydrogels is shown in Figure 2.6. The storage modulus (G') measures the stored energy and represents the elastic portion of the material. It is often associated with the Young Modulus, therefore represents the stiffness of the material. On the other hand, the loss modulus (G'') measures the energy dissipated as heat and represents the viscous portion of the material. An important characteristic of gel formation is that G' > G'', which means PA nanofiber gels have a predominantly elastic rather than viscous behaviour.

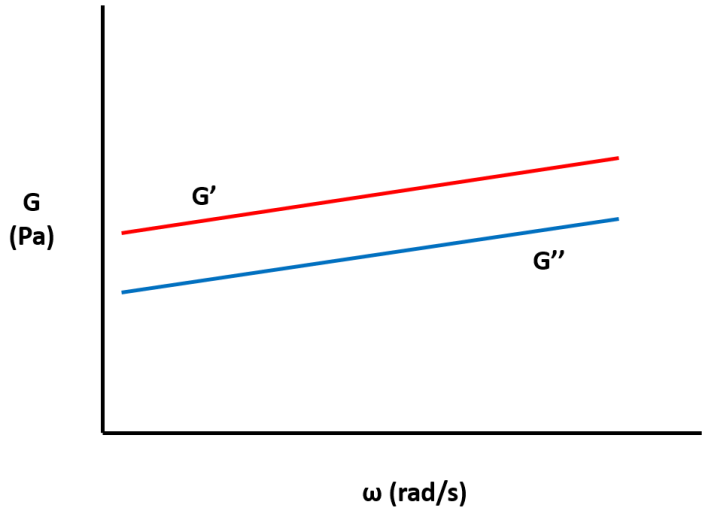

Figure 2.6. Representation of a typical mechanical spectrum of PA gels. Rheology is routinely used to study the hydrogels' viscoelastic behaviour. The average G' (Storage Modulus) and G'' (Loss Modulus) are plotted versus Frequency (ω). The obtained spectrum is characteristic of hydrogel formation.

Another important parameter to take into account is G' and G'' sensitivity to frequency changes (ω). If there is minimal or no change of both of these moduli when frequency increases, this is regarded as a clear indicator of materials with high degrees of intermolecular crosslinking. (Stedahl et al., 2006)

A particular feature of PA hydrogels is that they strengthen over time. In order to track the changes in their mechanical properties and their gelation times, rheology studies can be utilised to monitor their behaviour (Niece et al, 2008). Another interesting characteristic is that they display a predominantly elastic rather than viscous behaviour which is a clear indicator of their gel state, separating them from viscous liquids (Toksoz et al., 2011). Although PA gels present a well-known behaviour, their moduli can be highly variable depending on their molecular structure

and the use of crosslinking agents (Stendahl et al., 2006; Khalily et al., 2015; Ding et al., 2013).

In summary, the techniques mentioned above are complementary to each other and represent important tools to evaluate different phases of peptide amphiphiles based materials. Thus, it is highly recommended to use multiple tools for the better understanding of the mechanics of these systems.

2.4.1.5 Optimisation of systems

The properties of PA gels depend on a number of variables including amino acid composition and order of the sequence, secondary structure, nanofiber formation and types, inter and intra molecular forces between fibres, and crosslinking agents, amongst others. By changing any of these parameters, it is possible to tune these properties and modify existing sequences to achieve smart materials that react to different stimuli. Table 2.3 summarises studies to optimise PA-based hydrogels.

The stiffness of materials has been studied for some time now. According to different studies, stiffness plays a decisive role in cell adhesion and shape, signalling, proliferation and differentiation (Sur et al., 2013; Engler et al., 2006). Matching the Storage Moduli (G') of the materials with the one of the native ECM of different tissues gives us the possibility to integrate mechanical cues into these materials which could have a great impact in terms of integration of the material and bioactivity, ultimately leading to a successful outcome. For example, collagenous bone has an approximate stiffness of 100KPa, whereas muscle tissue is around 10KPa.

On the other hand, neurons need softer substrates (100–500 Pa) to grow and differentiate, while the differentiation process to glial cells requires higher stiffness of the substrate (1,000-10,000 Pa) (Her et al., 2013; Engler et al., 2006; Saha et al., 2008).

Hydrogels usually have low mechanical stability with a Storage Moduli range of 100–5000 Pa (Ding et al., 2013; Khalily, et al., 2015). However, it is possible to design and optimise PA gels to have a wider range of stiffness between 10^2-10^5 Pa (Stendahl, et al., 2006; Khalily et al., 2015; Ding et al., 2013) without compromising their ability of self-assembling. Modifications and tailoring of these versatile materials opens the possibility to use them in different regenerative medicine related applications.

	Modification	Function	Outcome	Reference
Stiffness				
- *Molecular design*	β-sheet region formed by Alanine and Glycine residues.	Reduces stiffness on the material.	Soft hydrogels: 7.3 ± 0.9 kPa.	Sur et al., 2013.
	β-sheet region formed by Alanine and Valine residues.	Increases stiffness of the material.	Stiff hydrogels: 22.9 ± 5 kPa.	
	Systematic variation of Alanine and Valine residues.	Increase of valine residues is effective to increase stiffness, whereas alanine residues tend to reduce it.		Pashuck et al., 2009.
- *Crosslinking agents*	Metal ions.	Hydrogels prepared with higher-valence ions are generally stiffer than those with lower-valence ions.	Hydrogels stiffness of ~10^5 Pa.	Stendahl et al., 2006.
	Imine covalent bonding.	Enhances mechanical stability, higher stiffness.	Hydrogels stiffness of >10^5 Pa.	Khalily et al., 2015.
	Photo-crosslinking.	Enhances mechanical stability through a di-tyrosine linkage.	Hydrogels stiffness of ~10^5 Pa.	Ding et al., 2013.
Topography				
- *Nanofibre alignment*	Parallel alignment of nanofibres.	Improves electrical activity and synapse formation of neurons.	Good biofunctionality. Neurons were capable of generating spontaneous action potential and forming synaptic connections.	Berns et al., 2015.
		Differential neural progenitor cell response.	Differentiated neurons on aligned IKVAV-PA scaffolds had a greater neurite growth than on unaligned scaffolds. Neurite length was shown to be ~3 times longer in aligned IKVAV PA scaffolds.	
		Enhances cell migration.	Cell migration within the scaffold was guided by the alignment of the nanofibres. Also, cell motility was higher on aligned IKVAV-PA scaffolds than on the unaligned PA gel.	
Gelation time				
	Use of more hydrophilic and bulky amino acids.	Effectively slows down gelation.	Varying the composition of 3 different PA gels resulted in substantial changes in gelation times. PA_1 gel point <5 minutes, Pa_2 ~15 minutes and PA_3 ~1 hour.	Niece et al., 2008.
	Use of more hydrophobic amino acids.	Accelerate gelation kinetics.		
	Combination of peptide amphiphiles with different sequences.	Enhanced control on gelation properties.	Functionalised PA-molecules with poor gelation and mechanical properties were combined with a stronger gelating, non-biologically active PA molecule. Enhanced gelation properties and stiffness of the hydrogels were observed.	Anderson et al., 2009.

Table 2.3. Summary of different approaches used to optimise the properties of self-assembling PA nanofibers.

The optimisation of stiffness can be achieved through a several strategies. The two main approaches are: modification of the molecular design and use of crosslinking agents. The first strategy relies on the design of PA sequences utilising residues that allow the maximum number of hydrogen and disulphide bonds as well as hydrophobic interactions. The second approach is based on the use of different crosslinking agents to create intra or intermolecular covalent and ionic bonds in the materials, resulting in a major increase of their stiffness (Pashuck et al., 2010; Niece et al., 2008; Anderson et al., 2009; Stendahl et al., 2006; Khalily et al.,2015; Ding et al., 2013).

Surface topography is a key component to help direct the organisation of the micro-architecture of tissues (i.e. nerves). Nanofiber alignment has been achieved by different methods and has proven to potentiate cell organisation into more complex structures and tissues.

Although self-assembling PAs seem like a promising tool, they still face several challenges such as stiffness optimisation, adequate bio-functionalisation, cell compatibility and migration inside gels, amongst others.

As previously mentioned, the combination of PAs with several other biomolecules is currently being explored as an alternative to improve the mechanical properties and biocompatibility of these materials. Building up on the idea of designing biomimetic materials, several combinations including PAs and biomolecules have been developed. For example, by combining hyaluronic acid and PAs, it is possible to form multi-layer organised membranes (Mendoza-Meinhardt et al., 2018). Moreover, a

new bio-ink using keratin and PAs has also been developed which allows to 3D print PA gels and has proven to be biocompatible in cell culture (Hedegaard et al., 2018). This new approach still relies on the assembling mechanisms mentioned earlier. The new materials formed by co-assembly have proven to have interesting emergent properties.

2.5 Blood-interacting biomaterials

The first body fluid to come in contact with medical materials or devices is blood, which activates a series of pathways inside the body. Protein absorption is the first response of the body to foreign materials, followed by platelet adhesion and coagulation (blood clot formation), and in some instances thrombosis (Xu et al., 2014).

A blood clot is an interesting example of naturally formed scaffolds. After injury, several components in blood activate and start the coagulation process, which finalises in the creation of a temporary scaffold that helps close the wound and gives the body enough time to repair the damaged tissues. This scaffold has some of the ideal properties that we aim to have in synthetic scaffolds: it is bioactive, personalised, biocompatible, biodegradable and has the right mechanical properties to help the regenerative process (Kim et al., 2000; Place et al., 2009; Patel et al., 2012).

However, the exploitation of a blood clot as a naturally sourced biomaterial has not been feasible primarily due to difficulties processing blood, directing its coagulation,

and controlling the properties of the resulting clot. Instead, the focus has been on dissecting key components of blood for the generation of biomaterials and scaffolds that take advantage of specific properties, including platelet-rich plasma (PRP), serum, albumin and fibrin.

The materials currently used in the clinic remain far from recreating the much-needed complex, active, and living regenerative environment provided by the blood clot. To effectively translate this regenerative potential into complex clinical situations requiring the use of grafts or exogenous materials with specific geometries, physical properties, and composition; it is essential to develop methodologies that enable the processing of blood and formation of the hematoma in a controlled and reproducible manner.

2.5.1 Current state of the art for clinically used blood interacting materials

For the past decades, a number of products have been developed to actively or passively contribute to help close and seal wounds after injury (Figure 2.7). They can be classified mainly in 3 categories: tissue adhesives, haemostatic agents and sealants (Table 2.4) (Mehdizadeh et al., 2003; Zhu et al., 2018):

- **Tissue adhesives or bio-glues.** Developed to help close wounds by bringing the edges of damaged tissues together and help wound healing. Their mechanism of action is to create covalent bonds with tissues which

results in adhesion between the material and the wound edges and controls bleeding.

- **Haemostatic materials.** Used to help and enhance blood clotting (directly or indirectly) and are routinely used during surgeries or in trauma injuries.
- **Sealants.** Used to stop air or fluid leakage. They are composed by different components that react when mixed together and form a solid material that seals the wound area (i.e. hydrogels).

Type of material	Examples	Advantages	Limitations
Tissue adhesives	• Cyanoacrylates (Dermabond, Indermil, Histoacryl) • Bovine albumin and glutaraldehyde (Bioglue, Cryolife)	• Quick and painless method. • Strong, rapidly acting adhesive properties • Ease of use • Low dehiscence rates	• Only external use • Release of heat • Prevention of wound healing • Not to be used in high-tension areas • Hypersensitivity • Local tissue necrosis
Sealants	• Fibrin sealants (Tisseel, Evicel) • PEG (Coseal, Duraseal)	• Effective, irrespective of patient's coagulation status. • Ease of use	• Infection or poor wound healing • Rejection (pooled donors) • Swelling • Leaks
Haemostatic materials	• Porcine gelatin (Gelfoam) • Bovine collagen (Avitine, Helistat, Helitene, Integra). • Oxidised cellulose	• Mechanical haemostats are only appropriate for • patients with an intact coagulation system • Improve control of residual • Oozing	• Foreign body reaction • Swelling • Prevention of healing • Allergies • Preparation times • Disease transmission

Table 2.4. Current blood derived materials for wound healing applications. This table aims to highlight the advantages and disadvantages of the most commonly used materials on the clinic **(**Mehdizadeh et al., 2003; Zhu et al., 2018).

So far, the development of these materials has focussed on sealing the defect. Current tissue adhesives such as fibrin glue or cyanoacrylates present a myriad of advantages. For example, their ease of use and rapid haemostasis and prevention of

blood loss in large injuries. From a materials perspective, the main limitation of current tissue adhesives is the mechanical strength and biocompatibility (Taboada et al., 2020).

From the biological aspect, one of the main complications of having large size defects in traumatic injuries is that the materials designed as well as the current surgeries performed are aimed to seal the defect as quickly as possible to prevent blood loss in order to increase the survival odds of the patients. However, post-surgical outcomes include the excess of tissue scaring and loss of function of the affected site, leading to overall discomfort of the patient and in the worst cases, lower quality of life.

From a clinical perspective, there are key factors that must be considered for the routine use of these materials including: safety, efficacy, cost and approval by regulatory organisations (Spotnitz et al., 2012). From a materials perspective, mechanical properties and biocompatibility of these materials are key aspects that need to be addressed.

Another approach developed is the creation of blood interacting devices, which has focused mainly on designing blood compatible materials that avoid blood interaction and prevent blood clotting (Figure 2.7). Their applications are mainly in the bio-fabrication of stents and other biomedical devices. These materials need to be coated in order to prevent interaction with blood components and reduce the risk of thrombosis (Reviakine et al., 2018; Sperling et al., 2009)

Human blood and the endothelium naturally possess anticoagulant properties, however, when this body fluid gets in contact with biomaterials, this often activates the natural defence mechanisms of the body, that include inflammation and coagulation. These events might lead to undesired complications such as thrombosis and strokes if not controlled strictly. Control and management of these undesired responses has been so far based on the use of anticoagulants to lower the risk of thrombosis. However, the use of these pharmaceutical therapies might partially solve the previous issue only by generating a new one: risk of internal bleeding. Therefore, the use of medical devices and biomaterials is limited by these factors (Sperling et al., 2009).

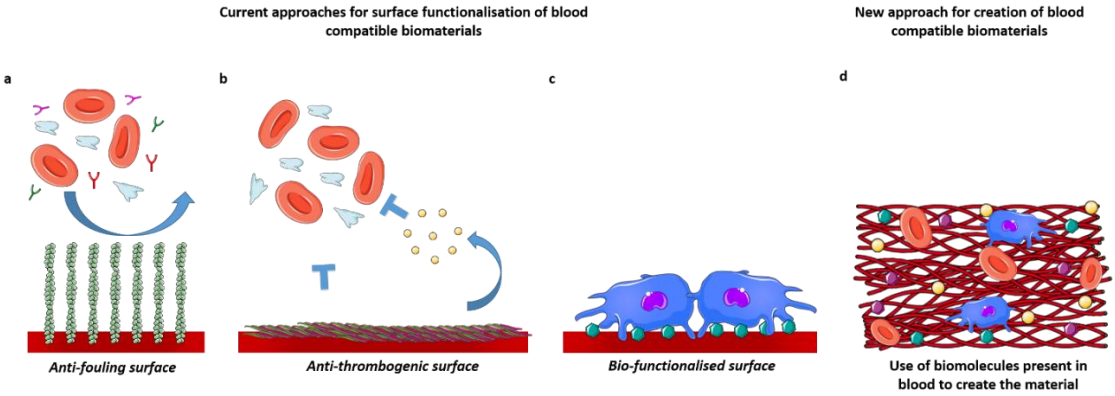

Figure 2.7. Current approaches for the creation of blood compatible materials. a) Anti-fouling surfaces aim to minimise interactions between the materials and blood components. b) Anti-thrombogenic surfaces rely on the use of anti-thrombogenic or anti-coagulant substances attached or released from the materials' surface to prevent blood clotting or thrombosis. c) Bio-functionalised surfaces are used to promote rapid endothelialisation. d) The new approach to create blood compatible materials aims to use biomolecules already present in blood to be used as building blocks that enable the material formation. (Image adapted from Ippel et al., 2018)

2.5.2 Current state of the art in blood-derived hybrid materials

2.5.2.1 Hydrogels

For the past decades, different strategies have been developed in order to help tissue healing. For example, the use of hydrogels has been broadly explored as an alternative to create scaffolds that support and guide cell growth and proliferation.

In an attempt to improve the bioactive properties of current hydrogel materials (e.g. agarose, gelatin, chitosan, alginate, cellulose, hyaluronic acid), research has been focused on the combination of such proteins or polymers with blood fractions such as fibrin, platelet rich plasma, plasma or plasma lysates, in an attempt to exploit their richness in growth factors, known to be involved in tissue regeneration.

Fibrin is the most extensively studied blood fraction for hydrogel development due to its exceptional mechanical properties, bioactivity, availability and ease of use (Rausch et al., 2021). Different systems have been created by taking advantage of these properties (Figure 2.8).

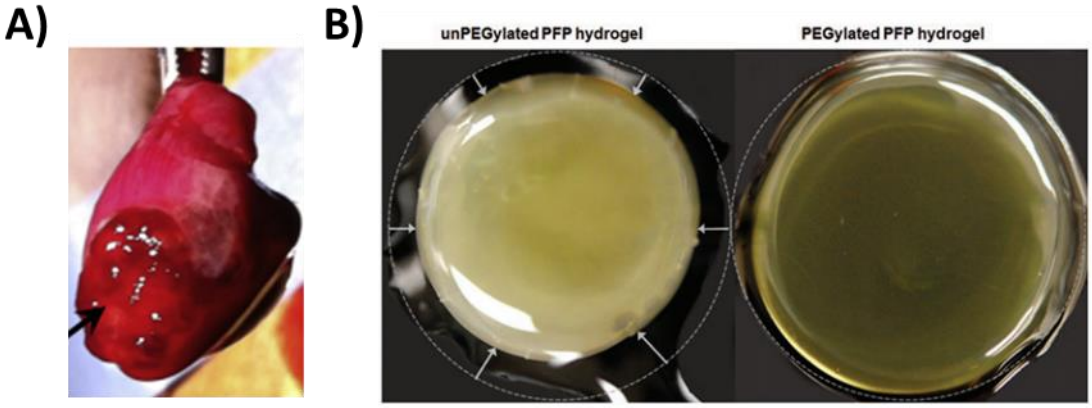

Figure 2.8. Hydrogel development with blood components. An example of a) HA-blood lysate adhesive hydrogel developed to act as a cardiac patch demonstrated the ability of this material to adhere to the heart and cover a defect after myocardial infarction and improved cardiac function. (Reproduced from Chang et al., 2012), b) PEGylated Platelet-Free Plasma based hydrogel combined with adipose derived stem cells showed potential regenerative effects in full-thickness skin wounds (Reproduced from Natesan et al., 2018).

One of the main limitations of these materials from a clinical perspective is the ease of preparation and shelf-life. Current methods to prepare and store these bioactive hydrogels are not suitable for off the shelf use in patients. In addition, some of these technologies still rely on the use of animal derived components such as gelatin, which increases ethical and health concerns. Table 2.5 summarises the current research on hydrogels development from blood components.

Hydrogels Material	Application	Components	Reference
Platelet-Rich Plasma Impregnated in Biodegradable Gelatin Hydrogel	Enhanced angiogenesis and vascularisation for critical ischemia	Platelet rich plasma (PRP) and porcine gelatin.	Kurita et al., 2011.
Hyaluronic acid-human blood hydrogels	Stem cell transplantation for cardiac regeneration	Lysed whole blood and hyaluronic acid (HA).	Chang et al., 2012.
Platelet-rich plasma loaded hydrogel scaffold	Chondrogenic differentiation for cartilage regeneration	Gelatin-poly(ethylene glycol)-tyramine (GPT) and Platelet-rich plasma (PRP)	Lee et al., 2012.
Photocrosslinkable PRP hydrogel glue (HNPRP)	Cartilage regeneration	Photoresponsive hyaluronic acid that generates aldehyde groups upon light irradiation and subsequently react with amino groups, into autologous PRP.	Liu et al., 2017.
Autologous platelet-rich plasma hydrogel compound	Myocardial restoration model for ventricular repair	Extracel-HP™ hydrogel, autologous PRP, ibuprofen, allopurinol and ascorbic acid.	Vu & Pal et al., 2017.
Injectable Hyaluronic Acid Hydrogels Enriched with Platelet Lysate	Cryostable Off-the-Shelf System for Cell-Based Therapies	Hyaluronic Acid Hydrogels and Platelet Lysate.	Neves et al., 2017.
Platelet-rich plasma loaded degradable PEG hydrogels	Potential therapeutic drug delivery depot of multicomponent mixtures like PRP	Hydrolytically degradable polyethylene glycol (PEG) hydrogel and Platelet-rich plasma (PRP).	Jain et al., 2017.
PEGylated platelet free plasma hydrogel	Vascularization and targeted cell delivery for volumetric muscle loss	Composite hydrogel: PFP hydrogel (Modified polyethylene glycol, Platelet free plasma, thrombin) m-ECM scaffold (muscle derived ECM scaffold).	Aurora et al., 2018.
PEGylated Platelet-Free Blood Plasma hydrogels	Treatment of full-thickness skin injuries	Polyethylene glycol (PEG)-modified platelet-free plasma combined with human adipose-derived stem cells, gelled with calcium chloride or thrombin.	Natesan et al., 2018.
Magnetic fibrin-agarose hydrogel	Cartilage tissue engineering	MagP-OH® magnetic nanoparticles (NanoMyp®), type VII-agarose (Sigma Aldrich), human plasma, $CaCl_2$.	Bonhome-Espinosa et al., 2020.

Table 2.5. Summary of the current state of the art on hydrogels development using blood components.

2.5.2.2 Three dimensional printing and hydrogel based bio-inks

Three dimensional printing (3D) printing is a biofabrication technology that allows precise positioning of biomaterials and biologicals (e.g. living cells or proteins) to create 3D-scaffolds that resemble the complex architecture of tissues. This

technology presents a number of advantages over other approaches such as control of the micro and macro structure, reproducibility, and high precision (Hedegaard et al.,2020).

However, the development of new bioinks is in need of further refinement and hydrogels have been explored for their potential use as bioinks (Li et al., 2020). Specific components of blood (e.g. proteins and enzymes) have been isolated and incorporated to bioinks in the hope to take advantage of their biological properties. Table 2.6 summarises the current state of the art on bioinks development from blood components.

Bioinks Material	Application	Components	Reference
Fibrin-based bioink	3D printing of neural tissues.	Bioink: Fibrin, alginate, neural aggregates from hiPSCs Crosslinker: Genipin.	Abelseth et al., 2018.
Human platelet lysate-based nanocomposite bioink	Possible future application: xeno-free 3D tissue models or tissue and organ surrogates for clinical applications.	Bioink: Nanocomposite bioink: Platelet lysate and cellulose nanocrystals Crosslinker: Thrombin from human plasma and $CaCl_2$.	Mendes et al., 2019.
Fibrin-based bioink	Bioprinting of glioblastoma tumor model for drug screening.	Bioink: Fibrin, alginate, genipin, GBM cells. Crosslinker: Chitosan, $CaCl_2$ and thrombin.	Lee et al., 2019.
Visible Light-Cross-Linkable, Fibrin–Gelatin-Based Bioprinted Construct	Drug cytotoxicity screening or heart diseases in vitro.	Bioink: Furfuryl–gelatin, fibrinogen, rose Bengal and cardiomyocytes. Dualstep cross-linking process: light crosslinking with 400 nm wavelength visible light and chemical crosslinking with $CaCl_2$ and thrombin.	Kumar et al., 2019.
Plasma-Based Bioink	Bone regeneration.	Human plasma, 3 w/v% alginate and 9 w/v% methylcellulose with calcium phosphate cement.	Ahlfeld et al, 2020.

Table 2.6. Summary of the current state of the art on bioinks development using blood components.

In this category, fibrin is again one of the most studied molecules from blood. Some of the challenges of 3D printing with fibrin are: a) the need of suitable crosslinkers, b) the improvement of mechanical properties as a bioink, and c) its rapid degradation (Veiga et al., 2021). In response to these disadvantages, polymers and cross linkers have been incorporated in order to improve the resolution and fidelity shape of the printed scaffolds by creating composite systems (Figure 2.9).

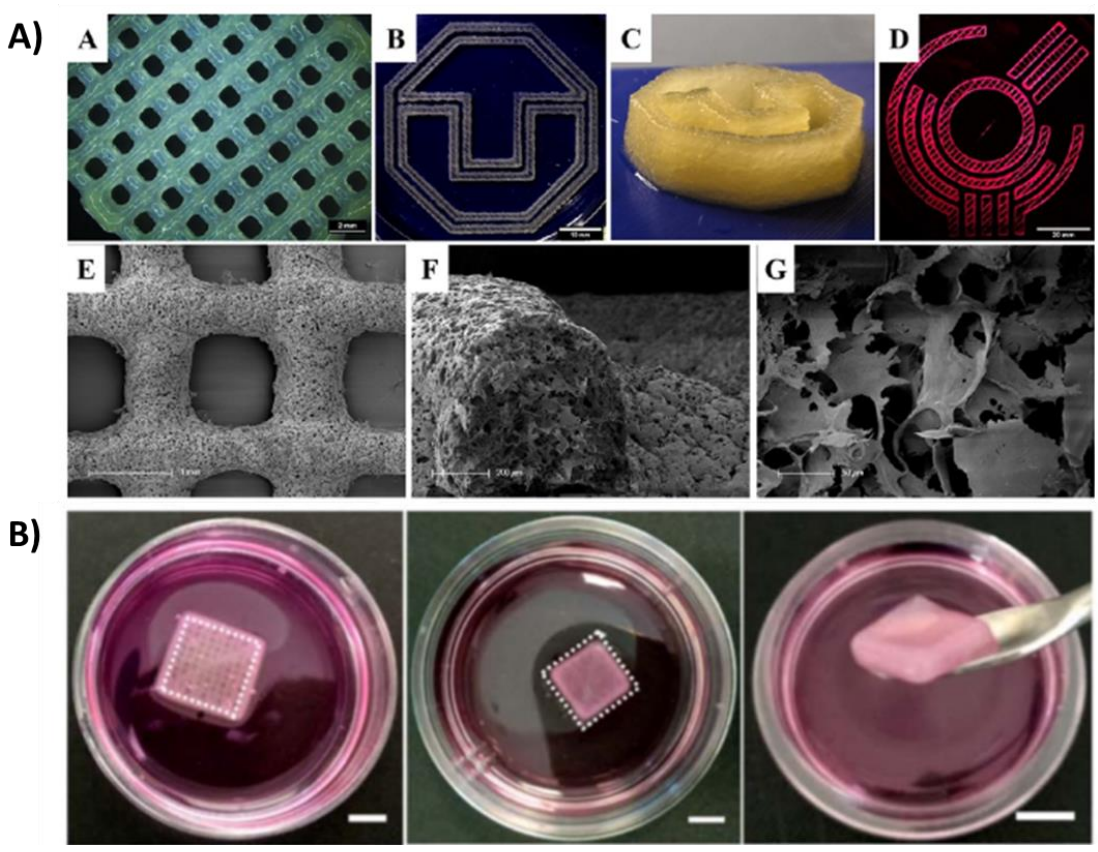

Figure 2.9. Recent advances in bioprinting with blood components. A) An example of a nanocomposite ink bio-functionalised with platelet lysate showed superior properties for biofabrication of three dimensional constructs and enhanced survival of mesenchymal stromal cells (Reproduced from Ahlfeld et al., 2020), *B*) A composite ink based on platelet lysate reinforced by cellulose nanocrystals improved mechanical properties and shape fidelity of the constructs (Reproduced from Mendes et al., 2019).

2.5.2.3 The use of biomolecules present in blood as building blocks to create personalised scaffolds

The use of peptide amphiphiles provides the opportunity to design systems that incorporate blood components as building blocks rather than to block their possible interactions with materials. These materials provide the opportunity to assemble interactive systems that create ECM-like nanostructures that promote cell migration inside the material and tissue regeneration instead of the current approaches, which focus mainly on the construction of a physical barrier to prevent blood loss.

One of the advantages of this designing method is that it allows the entrapment of biomolecules of interest so they can be available for the cells to use as biological cues. This can have a great impact for the enhancement of the wound healing process.

Our research focused on studying the dynamics of assembly of these systems in order to be able to control the assembly process, thus opening up the possibility of placing certain biomolecules at different gradients and spatiotemporally located in different manners. The benefits of using this technology rely on their unmatched properties such as co-assembly of the materials and biological fluids that are available in the patient's body, controlled biodegradability and the possibility of enhancing tissue regeneration and reduce scaring leading to the recovery of function (Figure 2.10).

Another important feature to take into account when mimicking tissues and organs is their three dimensional structure. As we know, the first attempts to regenerate tissues have been studied in 2D culture which have provided a detailed

understanding about the basic functions of cells. However, it has been shown that the 3D environment has key effects on cell behaviour and functionality as well as on the capacity to form biological structures that resemble their in vivo counterparts (Jell et al., 2009).

Therefore, we aimed to construct personalised scaffolds using the patients' own blood, which eliminates the hazards associated to the use of animal-based materials (prion related diseases, viruses) or human donors (blood transmitted diseases HEP C, HIV), and could also help reduce the risk of immunogenicity, inflammation and rejection.

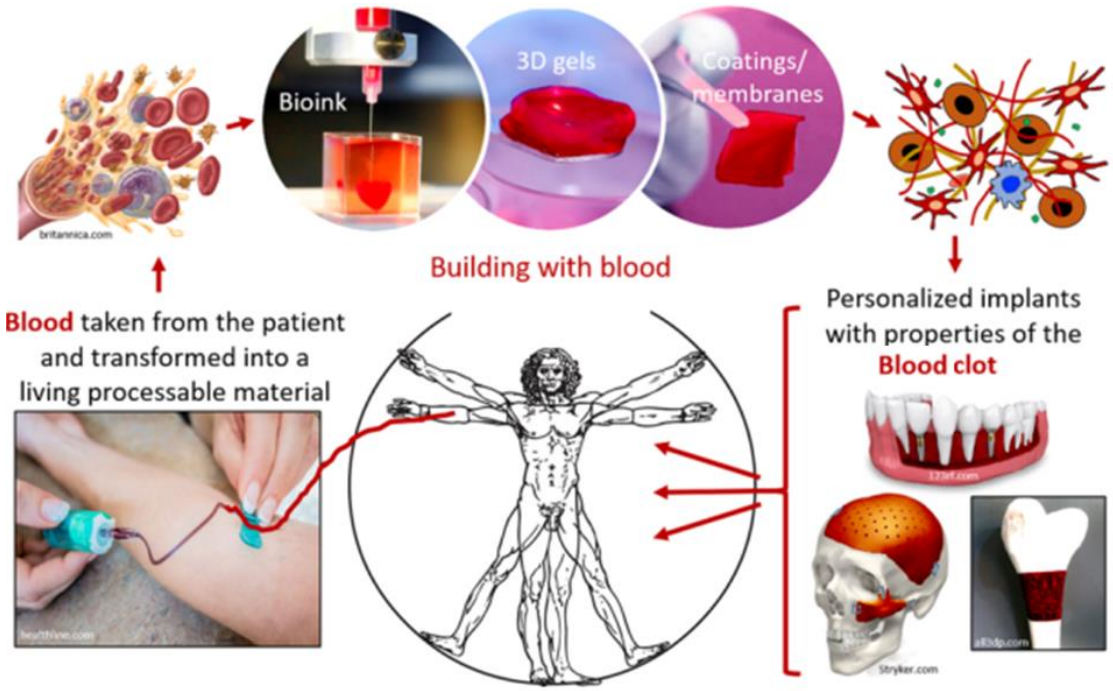

Figure 2.10. Summary of this research in engineering and building with blood. (Bioink image reproduced from Prof. Tal Dvir's Lab)

2.6 Aims, hypothesis and objectives

This section defines the aim, central hypothesis, and objectives of this thesis project by providing a brief description of how a biological fluid (blood) and peptide amphiphiles are merged to create a new type of personalised biomaterial.

2.6.1 Aim

The aim of this project is to produce a new generation of biomaterials that use biomolecules present in the body and self-assembling materials as building blocks to co-assemble into biomimetic hydrogels. The study of PA interactions with biomolecules (i.e. proteins) and the detailed characterisation of the dynamics of these systems will allow the creation of highly interactive personalised scaffolds for regenerative medicine applications. This project will focus on the study of interactions between blood components and peptide amphiphiles to create functional biomaterials.

2.6.2 Central hypothesis

We hypothesise that peptide amphiphiles assembly into hydrogels can be triggered by using components present in patients' blood in order to construct personalised scaffolds that serve as a platform to enhance tissue regeneration.

2.6.3 Objectives

Objective 1

Assess the potential of peptide amphiphiles to interact with components present in human blood or fractions (serum/plasma) to create hydrogels. Focus on the versatility of design of peptide amphiphiles. Determine key components involved in the co-assembly between peptide amphiphiles and blood components.

Objective 2

Tailor and design a set of new self-assembling peptides to enhance interactions with blood components based on results obtained from Objective 1. Characterise the new peptide amphiphile sequences. Evaluate the performance of the new self-assembling peptides for hydrogel formation and mechanical properties.

Objective 3

Evaluate the biocompatibility of the new peptide amphiphiles and their potential to be used for tissue engineering and regenerative medicine applications.

Objective 4

Develop a new 3D-printing system by using peptide amphiphiles as bio-inks for 3D printing of scaffolds. Determine the potential of the 3D-printed scaffolds to serve as a platform for tissue regeneration.

Chapter 3.

Materials and Methodology

This chapter gives a detailed description of the materials, experimental design, characterisation protocols and used to develop this research project.

3.1 Materials

3.1.1 Peptide amphiphiles

Materials were purchased from Biomatik Company. These peptides were purified by HPLC. Purity values above 95% were reported for every material.

3.1.2 Blood samples

The use of human blood and derived fractions for this research project was reviewed and approved the NHS Research Ethics Committee, Ethics REC Reference Number: 19/LO/0814, for Queen Mary University. Blood samples from healthy donors were purchased from the NHS Blood and Transplant Bank. Blood samples were fractioned into serum, plasma and platelet rich plasma.

3.1.3 Human reagents

Human fibrinogen, human albumin and human thrombin were purchased from Sigma-Aldrich (UK). Human Factor XIII was bought from Enzyme Research Laboratories. Mouse anti-Human Serum Albumin (HSA), Rabbit anti-fibrinogen and Sea Block Serum-Free blocking buffer were purchased from ABCAM. Goat anti-mouse IgG (H+L) Alexa Fluor 488 and Goat anti-rabbit IgG (H+L) Alexa Fluor 568 were purchased from Thermo Fisher.

3.1.2 Buffers

HEPES buffer was the main buffer used to dissolve PAs. This buffer was prepared at 10 mM concentration of 4-(2-hydroxyethyl)-1-piperazineethanesulfonic acid (HEPES) in ddH2O with 0.9 % NaCl. The pH was adjusted to 7.4 using 1 M NaOH and 1M HCl. The buffer was filtered using a 0.02 microns pore size syringe filter to sterilise it.

Saline solution was used to dissolve PAs for studies in Section 4.1.3.4 and 4.1.4.1.2. For preparing this buffer, 0.9% NaCl was added to ddH2O. pH was not adjusted. The buffer was filtered using a 0.02 microns pore size syringe filter to sterilise it.

Ringer's lactate solution was used to dissolve PAs for studies in Section 4.1.3.4 and 4.1.4.1.2. The buffer was filtered using a 0.02 microns pore size syringe filter to sterilise it.

Simulated body fluid (SBF) was used to determine the impact of the ionic concentration in blood on PAs gelation in Section 4.1.2. This buffer has concentrations of dissociated ions equal to those of blood plasma. It was stored for up to 4 weeks at 5°C and freshly prepared every 4 weeks due to its short shelf-life. The recipe for preparing this buffer (i-SBF) was based on the work by Oyane et al., 2002 (Table 3.1).

	Concentration/mM					
	Blood Plasma					
Ion	Total	Dissociated	c-SBF	r-SBF	i-SBF	m-SBF
Na^+	142.0	142.0	142.0	142.0	142.0	142.0
K^+	5.0	5.0	5.0	5.0	5.0	5.0
Mg^{2+}	1.5	1.0	1.5	1.5	1.0	1.5
Ca^{2+}	2.5	1.3	2.5	2.5	1.6	2.5
Cl^-	103.0	103.0	147.8	103.0	103.0	103.0
HCO_3^-	27.0	27.0	4.2	27.0	27.0	10.0
HPO_4^{2-}	1.0	1.0	1.0	1.0	1.0	1.0
SO_4^{2-}	0.5	0.5	0.5	0.5	0.5	0.5

Table 3.1. Nominal Ion concentration of the SBFs in comparison with those of Human Blood Plasma in total and dissociated amounts. i-SBF was selected as the buffer used for these experiments. Table reproduced from Oyane et al., 2002.

For the preparation of 100 ml of the buffer, a beaker with 50 ml of water was put into a magnetic stirring plate and heated at 37° with constant agitation. The reagents were dissolved in the water in the sequence listed in Table 3.2. The amounts

presented on Table 3.2 were scaled down to prepare 100ml of the solution. The buffer was filtered using a 0.02 microns pore size syringe filter to sterilise it.

Reagents[a]	Purity/%	Amount			
		c-SBF[d]	r-SBF[e]	i-SBF[e]	m-SBF[e]
NaCl	>99.5	8.036 g	5.403 g	5.585 g	5.403 g
$NaHCO_3$	>99.5	0.352 g	0.740 g	0.965 g	0.504 g
Na_2CO_3	>99.5	—	2.046 g	1.765 g	0.426 g
KCl	>99.5	0.225 g	0.225 g	0.225 g	0.225 g
$K_2HPO_4 \cdot 3H_2O$	>99.0	0.230 g	0.230 g	0.230 g	0.230 g
$MgCl_2 \cdot 6H_2O$	>98.0	0.311 g	0.311 g	0.217 g	0.311 g
1.0 M—HCl	—	40 mL	—	—	—
0.2 M—NaOH	—	—	—	—	100 mL[g]
HEPES[b]	>99.9	—	11.928 g[f]	11.928 g[f]	17.892 g[g]
$CaCl_2$	>95.0	0.293 g	0.293 g	0.191 g	0.293 g
Na_2SO_4	>99.0	0.072 g	0.072 g	0.072 g	0.072 g
TRIS[c]	>99.9	6.063 g	—	—	—
1.0 M—HCl	—	≒ 0.2 mL	—	—	—
1.0 M—NaOH	—	—	≒ 0.8 mL	≒ 0.8 mL	≒ 15 mL

[a]Listed in sequence of dissolution; [b]HEPES = 2-(4-(2-hydroxyethyl)-1-piperazinyl)ethanesulfonic acid; [c]TRIS = tris(hydroxylmethyl)aminomethane; [d]buffered at pH 7.40 at 36.5°C with TRIS and 1.0 M—HCl aqueous solution; [e]buffered at pH 7.40 at 36.5°C with HEPES and 1.0 M—NaOH aqueous solution; [f]HEPES previously was dissolved in 100 mL of ultra-pure water; [g]HEPES previously was dissolved in 100 mL of 0.2*M*—NaOH aqueous solution.

Table 3.2. Reagents, their impurities and amounts for preparing 1000 ml of the SBFs. The amounts of each reagent were scaled down to prepare 100ml of i-SBF. Table reproduced from Oyane et al., 2002.

Phosphate buffered saline (PBS) buffer solution was used for the washing steps different protocols. This was purchased as a ready to use 1X PBS stock solution from Sigma.

3.2 Methodology

3.2.1 Peptide amphiphile resuspension

Peptide amphiphiles powders were re-suspended at ac concentration of 10mg/ml in HEPES buffer (10 mM with 0.9 % NaCl), and pH was adjusted to pH5, unless stated otherwise.

3.2.2 Blood fractioning protocols

Blood collected from the donors was processed to obtain different fractions that were used to test materials interaction according to the following protocols:

a) *Whole blood.* Blood samples were collected from donors utilising a 21G needle into sterile 15ml falcon tubes with Sodium Citrate (3.2%). Blood was re-calcified with 2mM $CaCl_2$ before using for experiments.

b) *Platelet rich plasma (PRP).* Blood samples were collected from donors utilising a 21G needle into sterile 15ml falcon tubes with Sodium Citrate (3.2%). The samples were maintained in slow agitation (mixer) at room temperature before further processing. To obtain PRP, samples were centrifuged at 175g for 15 minutes. The supernatant was collected (PRP) and re-calcified with 2mM $CaCl_2$ before using for experiments.

c) *Serum*. Blood samples were collected from donors utilising a 21G needle into sterile serum vacutainer tubes (yellow cap). After collecting the blood into the tubes, the components were mixed by gently inverting the tubes 2-3 times. The samples were left to settle in vertical position for 30 minutes after the blood sample was obtained. After, the samples were centrifuged at 1000g for 10 minutes. The supernatant above the transparent gel layer was collected (serum) and used for analysis.

3.2.3 Hydrogel formation

3.2.3.1 Hydrogel formation with blood or fractions

Two different settings were used for the initial screening of PAs and blood interaction (Figure 3.1).

a) ***Model 1.*** Peptide amphiphile solution inside blood (or fraction). A small volume of five microliters of peptide amphiphile solution (10mg/ml) was injected inside a drop of 15ul of whole blood or fraction (Plasma/PRP/serum).

b) ***Model 2.*** Blood (or fraction) inside peptide amphiphile solution. Five microliters of whole blood or fraction (Plasma/PRP/Serum) were injected inside a drop of 15ul of peptide amphiphile solution (10mg/ml).

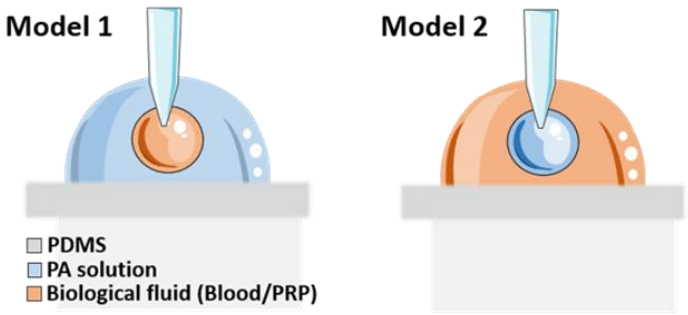

Figure 3.1. Diagram illustrating the two different models used for the creation of hydrogels. In model 1, a peptide amphiphile solution was injected inside the biofluid to create the hydrogel. For model 2, the biofluid was injected into a peptide solution.

Hydrogels were incubated at room temperature for 24 hours prior to analysis.

Controls. Bovine serum albumin (BSA) 35mg/ml or Human serum albumin (HSA) 35mg/ml and simulated body fluid (SBF) were used as controls. SBF was prepared according to a previously reported protocol (Oyane et al., 2002).

3.2.3.2 Hydrogel formation in vitro

Model 1 was selected for the initial screening of PAs and blood components interaction in vitro, samples were prepared as follows:

Peptide amphiphile solution inside Albumin (HSA). Five microliters of 1% peptide amphiphile solution (10mg/ml) were injected inside a drop of 15ul of Albumin (35mg/ml). Hydrogels were incubated at room temperature overnight. Following hydrogel formation, the PA gels were transferred to 96 well plates and incubated in 120ul of human fibrinogen (2mg/ml) at 37°C overnight. After, Human Thrombin (Factor XIIa) was added at a concentration of 2.5U/ml and incubated at 37°C for 8 hours. Next, hydrogels were washed with PBS 1X three times (5 minutes between each wash). Finally, Human Factor XIIIa enzyme was added to the samples at a concentration of 10ul/ml and incubated at 37°C overnight, to act as a crosslinking agent.

3.3 Peptides characterisation

3.3.1 Circular dichroism

Peptides and proteins secondary structure were assessed by using circular dichroism. Measurements were carried out at 25°C using a 0.1 cm path length and 300 µL volume quartz cuvette (Chirascan, Applied Photophysics, UK).

For secondary structure evaluation of peptide amphiphiles, the PAs were dissolved in HEPES 10 mM saline buffer (155mM NaCl, pH 7.4) at a final concentration of 0.01mg/ml. For determination of interactions of mixtures of PAs and proteins, the biomolecules were dissolved in HEPES 10 mM saline buffer (0.9% NaCl, pH 7.4) at a final concentration of 0.25mg/ml and mixed on a1:1 ratio (volume: volume). Far UV spectra were recorded from 190 to 270 nm a wavelength step of 0.5nm. Each spectrum presented in the results is the average of three consecutive readings. ($n \geq 3$). The data obtained was normalised to the baseline (blank control: HEPES buffer) and the averaged spectrum was smoothed to reduce noise without causing spectrum distortion using the Chirascan trace manipulation software.

3.3.2 Diffusion assays

Fluorescently tagged proteins were used for this assay. These tagged proteins were purchased from Thermo: Albumin from Bovine Serum (BSA), Texas Red™ conjugate (A23017) and Fibrinogen from Human Plasma, Alexa Fluor™ 488 Conjugate (F13191). These proteins were used at the concentrations found in blood. Bovine albumin (red)

was dissolved in HEPES buffer at a concentration of 35mg/ml whereas fibrinogen (green) was used at a concentration of 2 mg/ml.

An ibidi microchannel slide with 2 outlets and a channel total volume of 30 µl was used for the test. First, the slide was placed and focused under the microscope to avoid movement during the test. Then, 15 µl of PA solution was injected into one of the outlets and next, 15 µl of the protein solution was injected onto the other outlet (Figure 3.2). Samples were then observed under the microscope in bright field and fluorescent modes, and diffusion distance was tracked over a period of 24 hours.

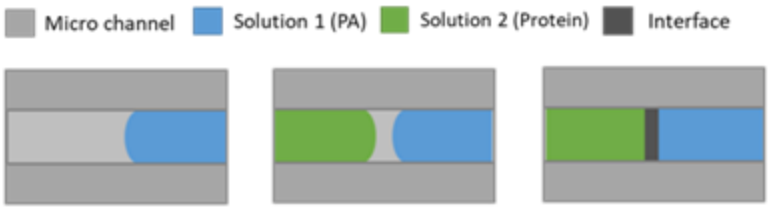

Figure 3.2. Diagram of experimental set up for diffusion experiments. Microchannel slides with two outlets were used for this test. Solution 1 (PA) was injected on one side of the microchannel and Solution 2 (fluorescent protein) was injected on the other outlet.

3.3.3 Zeta potential

PAs were dissolved in MilliQ water at a concentration of 0.1mg/ml and pH was adjusted by addition of HCl 1M or NaOH 1M. Solutions were then transferred to polycarbonate folded capillary cells where zeta potential measurements were acquired in triplicate at 25°C using a Zetasizer (Nano-ZS ZEN 3600, Malvern Instruments, UK).

3.4 Hydrogels characterisation

3.4.1 Rheology

Samples for rheology measurements were created using higher volumes of the solutions in order to create larger size hydrogels. For this, thirty microliters of PA solutions were injected into 90 microliters of the biological fluid or protein solution.

Rheological characterisation of the hydrogels was performed using a DHR3 Rheometer (TA Instruments, USA) with an 8 mm diameter parallel plates geometry. The G' (storage modulus) and G" (loss modulus) of the hydrogels were monitored by using amplitude and frequency sweep tests. Measures were taken at 25 °C and at a constant frequency of 1 Hz in the 0.01%– 10% strain during the amplitude sweep, while the oscillation frequency experiments were carried out at a 0.1% fixed strain along a 0.1 – 100 Hz range.

3.4.2 Scanning electron microscopy (SEM)

SEM was used to examine micro and nanostructure of PA hydrogels ($n \geq 3$). Samples were fixed with 4% paraformaldehyde overnight at 5°C. The cross-linked samples were then dehydrated by immersion in ethanol solutions in serial concentrations (20, 50, 70, 80, 90, 95, and 100%) for 5 minutes and repeated twice each solution. The samples were then dried using a critical point dryer (K850, Quorum Technologies, UK) using carbon dioxide (CO_2). As a final step, the dried samples were carefully placed on SEM specimen stubs (12.5 mm diameter) using adhesive conductive carbon discs

(Agar Scientific, UK) and gold coated for 45 seconds. Samples were then imaging using the Fei Inspect F50 (FEI Company, the Netherlands).

For imaging the interior of the samples, the samples were cut open to reveal the inside of the hydrogel before proceeding to the gold coating and imaging steps. At least three samples were imaged per condition (n ≥ 3).

3.4.3 Confocal and epifluorescence microscopy

Fluorescence microscopy was used as a qualitative method to detect protein location and distribution in hydrogels (n ≥ 3). Briefly, hydrogels were fixed in 4% paraformaldehyde (4% PFA in PBS 1X) overnight. Then, they were washed with PBS 1X and left on agitation for 5 minutes, this step was repeated 3 times. Then, Sea Block Serum Free blocking buffer was added and incubated for 2 hours at room temperature. Next, primary antibodies (diluted in blocking buffer) were added at a specific concentration: Anti-Fibrinogen (1:100) and Anti-HSA (2.5ul/ml) and incubated overnight at 4°C. Hydrogels were washed with PBS 1X three times and put on agitation (20 minutes/wash) followed by incubation with secondary antibodies (5ul/ml) for 2 hours at room temperature. Hydrogels were then washed 3 times with PBS 1X (20 minutes/wash with agitation). Finally, hydrogels were transferred to ibidi 8-chamber microscopy slides with glass bottom and filled with 200µl of PBS 1X, prior to microscopic analysis (n ≥ 3).

3.5 Biological characterisation

3.5.1 Zeta potential for blood clotting measurements

PAs were dissolved in MilliQ water at a concentration of 0.1 mg/ml and pH was adjusted as previously reported. The proteins albumin and fibrinogen were dissolved in MilliQ water at a concentration of 0.1mg/ml with adjustment to pH 7.4. Human plasma samples were diluted from 1:100 to 1:300 in MilliQ water. Solutions were then transferred to polycarbonate folded capillary cells and measured individually or as a mixture of 1:1 (volume: volume). Zeta potential measurements were acquired in triplicate at 25°C using a Zetasizer (Nano-ZS ZEN 3600, Malvern Instruments, UK).

3.5.2 Haemolysis test

For the determination of the haemolytic potential of the PAs, an assay measuring the concentration of haemoglobin in plasma was set up using the Haemoglobin Assay kit from Sigma Aldrich (MAK115). First, 225 µl of whole blood were placed into 2 ml Eppendorf tubes. Next, 75 µl of each PA solution were injected into the different blood samples. Samples were incubated for 1 hour at room temperature.

To obtain the plasma, samples were centrifuged at 2,000 x g for 15 minutes. The plasma fraction was then collected and transferred into clean Eppendorf tubes.

For preparing the controls, 50 µl of water (Blank) and 50 µl of the Calibrator solution provided by the kit were added into different wells of a clear bottom 96-well plate. Then, 200 µl of water was added into the Blank and Calibrator wells for a total volume

of 250 µl. The diluted calibrator is equivalent to 100 mg/dL haemoglobin. For the samples, 50 µl of each plasma sample was added into wells. Then, 200 µl of the Reagent were added to the sample wells and the plate was tapped lightly to mix the components. The plate was then incubated for 5 minutes at room temperature. Measurement of the absorbance at 400 nm (A_{400}) was carried out using the Optima (BMG Laboratory) plate reader. The haemoglobin concentration of the samples was calculated as follows:

$$Haemoglobin\ concentration = \frac{(A_{400}\,Sample) - (A_{400}\,Blank)}{(A_{400}\,Calibrator) - (A_{400}\,Blank)}\ x\ 100\ mg/dL$$

Where:

A_{400} sample = Absorbance of sample at 400nm
A_{400} blank = Absorbance of water blank at 400nm
A_{400} calibrator = Absorbance of the calibrator at 400nm
100 mg/dL = Concentration of the diluted calibrator

3.5.3 Degradation studies

Samples for degradation studies were created using large size hydrogels. Thirty microliters of PA solutions were injected into 90 microliters of blood. Samples were incubated for 24 hours and washed 3 times with PBS 1X to get rid of any blood remaining that did not assemble into the hydrogel. Samples were then transferred to 5 ml clean vials and incubated with 1 ml of HEPES buffer. The supernatant was collected at different time points and HEPES buffer was refreshed each time. The supernatants were immediately frozen at -20°C and stored for further analysis.

To calculate the degradation rate of hydrogels, the samples were transferred to coverslips and their weight was measured at different time points. The mass loss percentage was calculated as follows:

$$\text{Mass Loss } (\%) = \frac{W_o - W_t}{W_o} \, x \, 100$$

Where:
W_0 = Initial hydrogel weight (g)
W_t = Final hydrogel weight (g)

3.5.4 Protein release studies

The frozen supernatant collected from degradation studies was thawed and the total protein concentration was measured using the Bradford assay following the manufacturer's protocol. For this, protein standards were prepared ranging from 0.1–1.4 mg/ml using a BSA standard in HEPES buffer. Five µl of the protein standards were added to separate wells in a 96-well plate. For the blank wells, 5 µl of buffer were added. Then, 5 µl of the samples were added to different wells in triplicate. Next, 250 µl of the Bradford Reagent were added to all wells and mixed on a shaker for ~30 seconds. Samples were incubated at room temperature for 45 minutes. Then the absorbance was measured at 595 nm. To determine protein concentration, the net absorbance vs. the protein concentration of each standard were plotted. Protein concentration of the unknown samples was determined by comparing the Net A_{595} values against the standard curve.

3.5.5 Protein identification studies

Samples for the protein identification studies were obtained by collecting the supernatant of large size hydrogels. Thirty microliters of PA solutions were injected into 90 microliters of blood. Samples were incubated for 24 hours and washed 3 times with PBS 1X to remove of any blood remaining that did not assemble into the hydrogel. Samples were then transferred to 5 ml clean vials and incubated with 1 ml of HEPES buffer. The supernatant was collected at different time points and HEPES buffer was refreshed each time. The supernatants were immediately frozen at -20°C and stored for further analysis.

After 7 days, the supernatants of each sample at different time points were thawed and pooled together and used for analysis. A whole blood sample was used as a control.

A human cytokine antibody microarray from Abcam with 42 protein targets was used to identify proteins of interest released from the hydrogels into the supernatants (ab133997). The protocol supplied by the manufacturer was followed. Briefly, the membranes were incubated with 2 mL 1X Blocking Buffer at room temperature for 30 min.

Next, the blocking buffer was removed and 1 ml of the samples was added into each well and incubate overnight at 4°C. Samples were removed and the membranes were washed with 20 ml of 1X Wash Buffer I per membrane at room temperature with gentle rocking for 45 min. After, two more washes with 2 ml of 1X Wash Buffer I were

done (5 minutes per wash). Next, two sequential washes with 2 ml of 1X Wash Buffer II were carried out (5 minutes per wash).

After, 1 ml of 1X Biotin-Conjugated Anti-Cytokines was added into each well and incubate overnight at 4°C. Then, the steps of washing with 1X Wash Buffer I and 1X Wash Buffer II were repeated. Next, 2 ml of 1X HRP-Conjugated Streptavidin into each well and incubate for 2 hours at room temperature. Membranes were then washed with Wash Buffer I and 2 as previously explained.

Last, chemiluminescence was measured with the chemiluminescent blot documentation system ChemiDoc Touch. Semi-quantitation of the proteins was done by normalising the signal to the internal positive control of the test using the Image Lab software for the analysis.

3.6 Cell culture techniques

3.6.1 Sterilisation of PAs

Before all cell culture experiments, lyophilised peptide and protein solids were treated with UV light for 20 min before dissolving in sterile 10 mM HEPES buffer at concentration 10 mg/ml.

3.6.2 Cells and culture conditions

NIH-3T3 fibroblasts were cultured with DMEM-Glutamax medium supplemented with 10% Foetal Bovine Serum (FBS) and 1% of antibiotics penicillin and streptomycin (P/S). Fibroblasts were used at passages $10 \leq P \geq 15$.

Human umbilical vein endothelial cells (HUVECs) were purchased from Promocell (pooled donors, C-12203) and cultured using EGM-2 Endothelial Cell Growth Medium (CC-3162) purchased from Lonza.

Human mesenchymal stem cells (hMSCs) (C-12974 hMSC-BM-c) were cultured in DMEM-Glutamax supplemented with 10 % FBS and 1 P/S. HUVECs and hMSCs were used at passages $2 \leq P \geq 7$.

All cell cultures were maintained in a humidified incubator with 5% CO_2 at 37 °C.

3.6.3 Cell seeding

For cell seeding experiments, a cell density of 10,000 cells per well of 96-well plates was used. Cell seeding experiments were performed in biological replicates with at least four hydrogel samples ($n \geq 4$ per condition, per time point).

3.6.4 Cell viability assays

Cell viability was measured using two different techniques: Live/Dead assay and Alamar Blue assay.

3.6.4.1 Live/Dead assay

This assay is based on the identification of live and dead cells using fluorescence stains. The Live/Dead assay kit was purchased from Thermo Fisher Scientific, UK. The staining solution was prepared using 2 µL ethidium homodimer-1 (2 mM) and 1µL calcein-AM (4 mM) in 1 mL of cell culture medium. 100 µL of the staining solution was

added per sample. Samples were imaged after 15 minutes using a confocal microscope (excitation wavelengths 544/594 nm for dead cells and 488 nm for live cells).

3.6.4.2 Alamar Blue assay

The Alamar Blue assay was used to measure metabolic activity as an indirect indication of proliferation. The Alamar Blue reagent was purchased from Invitrogen (DAL1100). This assay is based on the chemical compound rezasurin. As cells being tested grow, innate metabolic activity results in a chemical reduction of this compound. This causes the indicator to change from oxidized (non-fluorescent, blue) form to reduced (fluorescent, red) form. These changes can be measured by absorbance or fluorescence methods. The reagent was used at a concentration of 10 µL in 90 mL cell culture medium as instructed by the manufacturer. To measure the samples, the cell culture medium was removed and 100 µL of alamarBlue solution was added and incubated for 3 hours. After incubation, absorbance readings were measured at 570nm and 600 nm using Optima (BMG Laboratory) plate reader. The absorbance was converted to Percentage of Reduction (%) by using the following formula:

$$\%\, Reduction = \frac{(\varepsilon_{OX})\lambda_2 A\lambda_1 - (\varepsilon_{OX})\lambda_1 A\lambda_2}{(\varepsilon_{RED})\lambda_1 A'\lambda_2 - (\varepsilon_{RED})\lambda_2 A'\lambda_1} \; x\,100$$

Where:

C_{RED} = concentration of reduced form alamarBlue
C_{OX} = oxidized form of alamarBlue
ε_{OX} = molar extinction coefficient of alamarBlue oxidized form
ε_{RED} = molar extinction coefficient of alamarBlue reduced form
A = absorbance of test wells
A' = absorbance of negative control well. The negative control well should contain media and alamarBlue, but no cells.
λ1 = 570nm
λ2 = 600nm

To calculate this, Table 3.3 below shows the Molar Extinction Coefficients for alamarBlue at 570 and 600nm.

Wavelength (λ)	ε_{RED}	ε_{OX}
570nm	155,677	80,586
600nm	14,652	117,216

Table 3.3. Molar Extinction Coefficients for alamarBlue.

3.6.5 Immunofluorescence staining

3.6.5.1 Platelets and fibrin network

Hydrogel samples were fixed in 4 % PFA in 1x PBS solution for 2 hours, permeabilised in 0.2 % Triton X-100 in 1x PBS solution for 2 hours and blocked in a 2 % bovine serum albumin (BSA) in 1x PBS solution overnight at RT. Next, primary antibodies (diluted in blocking buffer) were added at a specific concentration: the fibrin marker Anti-Fibrinogen (1:100) and the platelet marker Anti-Selectin (1:100) were incubated overnight at 4°C. Hydrogels were washed with PBS 1X three times and put on agitation (5 minutes per wash, with agitation) followed by incubation with secondary

antibodies (1:500) for 2 hours at room temperature. Hydrogels were then washed 3 times with PBS 1X (5 minutes per wash, with agitation). Finally, hydrogels were transferred to ibidi 8-chamber microscopy slides with glass bottom and filled with 200µl of PBS 1X, prior to microscopic analysis (n ≥ 3).

3.6.5.2 Immunofluorescence staining of hydrogels with cells

After incubating the hydrogels with the different cell lines, samples were processed at Day 1, Day 4 and Day 7. Hydrogel samples were fixed in 4 % PFA in 1x PBS solution for 2 hours, permeabilised in 0.2 % Triton X-100 in 1x PBS solution for 2 hours and blocked in a 2 % bovine serum albumin (BSA) in 1x PBS solution overnight at RT.

DAPI (nuclei) and Rhodamine phalloidin (F-actin) were diluted 1:500 and 1:250 respectively in 1x PBS and incubated for 2 hours at RT. Samples were washed with 1x PBS between each step. Images were acquired using Leica TCS SP2 and Zeiss LSM710 confocal microscopes acquiring z-stacks ranging from 5-20 µm depending on the sample size.

3.7 3D-printing pilot study

Pilot experiments to determine the printing ability of the materials into biological fluids were carried out as follows. Droplets 5ul/each of PA solution (1mg/ml) were injected into wells containing 500ul of Blood/PRP (24-well plates) with a space of 1 minute between each drop. Then, they were incubated at room temperature overnight.

To determine the ability to attach to each other, the same initial set up as above was utilised and attachment ability was tested over different periods of incubation times (5 min, 15 min, 30 min, 1 hr, 3hr, 6hr and 24 hr).

3.7.1 Extrusion 3D-printing

Computer assisted design (CAD) software was used to create the 1-layer, 2-layer and 4-layer models and tested in a RegenHu 3D-printer.

For the one-layer experiments, a single filament was printed and incubated for 15 minutes before removing the blood for examination. Briefly, a peptide amphiphile solution (PA-K_3) at a concentration of 1mg/ml was injected into wells containing 1 ml of Blood (24-well plates). Samples were fixed with 4% PFA for one hour and washed with PBS 1X three times with 5-minute incubation between washes.

For the two-layer experiments, samples were printed and incubated for 15 minutes or 1 hour before removing the blood for examination. Samples were fixed with 4% PFA overnight and washed with PBS 1X three times with 5-minute incubation between washes.

For the four-layer experiments, samples were printed and incubated for one hour before removing the blood for examination. Samples were fixed with 4% PFA overnight and washed with PBS 1X three times with a 5-minute incubation between washes.

Scaffolds were prepared for SEM imaging following the protocol previously explained in Section 3.3.2.2.

3.8 Statistical analysis

All experiments were repeated at least three times with at least three replicates ($n \geq 3$). For qualitative results obtained from microscopy techniques (SEM, Confocal and Epifluorescence microscopy), at least 3 samples per condition were analysed and representative images were reported.

For rheology studies and future quantitative experiments, numerical data was reported as mean and standard deviation (SD). Statistical analysis was performed with GraphPad Prism software. A suitable model for statistical analysis was selected depending on the experiments performed and statistical significance was accepted when $p < 0.05$.

Chapter 4.

A co-assembly based multi-component hydrogel using a biological fluid

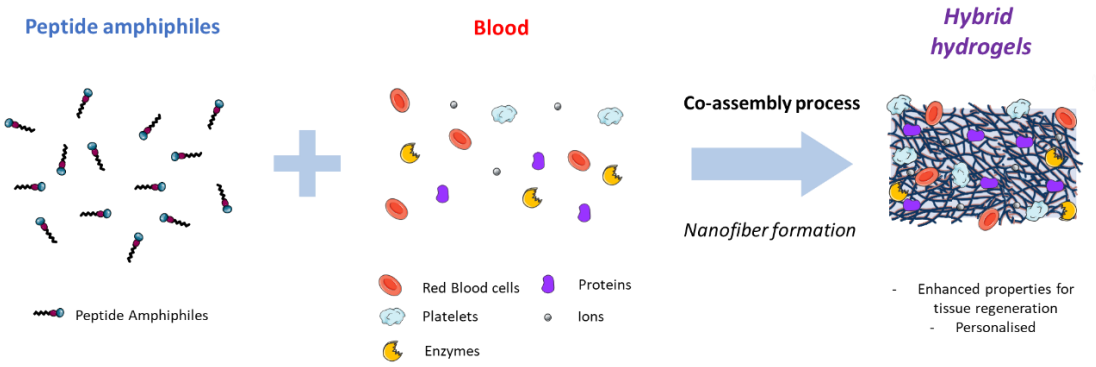

This chapter describes the development of a new type of hydrogel based on the co-assembly of peptide amphiphiles and blood components. The chapter is divided into 3 sections. The first section focuses on the initial screening of different peptide amphiphiles to determine their interactions with blood, followed by the identification of key components of blood required for the assembly. The second section presents a detailed characterisation on the co-assembly process. The third section covers the design an evaluation of new sequences.

The majority of this chapter is in preparation for submission as a research article:

Padilla Lopategui, et al. (2022). Design and development of blood interactive co-assembling systems for tissue engineering applications *(In preparation)*

4.1 Multi component co-assembly

In living organisms, complex and dynamic interactions between different molecules are necessary to carry out essential functions and to adapt to the constantly changing environment. Multicomponent self-assembly has been developed as a way to mimic these natural processes and relies on the interaction of different building blocks that can assemble into complex structures that resemble native tissues and provide some function (Okesola et al., 2018).

Peptide-protein based materials have increasingly become of interest for tissue engineering applications as they provide a platform to study specific molecular interactions as well as the material's emerging properties.

The studies presented in this chapter were used to address the first thesis objective (Refer to Section 2.6.3): 1) to assess the potential of peptide amphiphiles to interact with blood and blood fractions and to determine key components involved in these potential interactions, and 2) to tailor and design a set of new self-assembling peptides to enhance interactions with blood components. The experiments conducted were divided in 3 main stages. First, a set of peptide amphiphiles with different properties were selected and tested. Second, the co-assembly interactions were studied in terms of chemical, biological and mechanical properties. Third, new PA sequences were designed and characterised to determine their suitability for tissue engineering applications.

4.1.1 Components of the co-assembly

4.1.1.1 Peptide amphiphiles

The peptide amphiphile sequences used in this research are based on the first PA structure reported by Stupp's group (Hartgerink et al., 2001). PA molecules are constituted by three characteristic segments: a) charged hydrophilic segment, b) β-sheet forming segment, and c) hydrophobic (alkyl tail) segment. These individual PA molecules tend to self-assemble into nanofibres in aqueous solution due to their amphiphilic nature which drives their aggregation into micelles in order to shield the hydrophobic segment of the peptide (Mendes et al., 2013). Other interactions occur simultaneously, including hydrogen bonding between the amino acids from the β-sheet segment and electrostatic repulsion between the amino acids from the charged segment, which drive the assembly into cylindrical micelles (or nanofibres). This molecular arrangement ensures that the head group (containing bioactive epitopes) is exposed in the surface of the nanofibre and is therefore available to interact with its surrounding environment (Hendricks et al., 2017).

Increasing interest on the study of the interaction of PAs with proteins and other biomolecules for the creation of hydrogels has grown due to different factors. On one hand, the PAs enable the formation of nanofibrous networks and can contain bioactive sequences to help direct cell behaviour (Shi et al., 2018). On the other hand, the addition of biomolecules can enhance the strength of the hydrogels (Radvar & Azevedo, 2019; Yu et al., 2017) and provide other biological queues by mimicking the native cell environment, as well as enhancing cell-matrix interactions (Derkus et al.

2020). Altogether, it has been reported that the co-assembly of PAs with different molecules can contribute to the creation of tuneable hybrid hydrogels with enhanced properties.

For the initial screening, peptide amphiphiles (PAs) with different charges previously developed by the Mata group (Inostroza-Brito et al., 2015; Okesola et al., 2021; Hedegaard et al., 2018; Redondo, 2020) were used to test initial interactions with blood or blood fractions. Table 4.1 shows the peptides tested and their properties. Based on previous studies, the co-assembly is expected to be triggered by bringing the two solutions into contact, driven primarily by electrostatic and hydrophobic interactions (Hedegaard et al., 2020).

Peptide Amphiphile name	Sequence	Molecular Weight (KDa) ł	pI ł	pH*	Concentration**
PA-K_2	$C_{15}H_{31}$CONH-VVVAAAKK-$CONH_2$	1.02	10.0	5	10mg/ml
PA-K_3	$C_{15}H_{31}$CONH-VVVAAAKKK-$CONH_2$	1.15	10.3	5	10mg/ml
PA-K_4	$C_{15}H_{31}$CONH-VVVAAAKKKK-$CONH_2$	1.27	10.5	5	10mg/ml
PA-K_3G_3	$C_{15}H_{31}$CONH-VVVAAAKKKGGG-$CONH_2$	1.37	10.9	5	10mg/ml
PA-H_3	$C_{15}H_{31}$CONH-VVVAAAHHH-$CONH_2$	1.17	8.1	4	10mg/ml
PA-H_2K	$C_{15}H_{31}$CONH-VVVAAAHHK-$CONH_2$	1.17	9.1	4.5	10mg/ml
PA-E_3	$C_{15}H_{31}$CONH-VVVAAAEEE-$CONH_2$	1.15	3.7	8	10mg/ml
PA-E_3Y	$C_{15}H_{31}$CONH-VVVAAAEEEY-$CONH_2$	1.31	3.0	8	10mg/ml

Table 4.1. Molecular information of the materials utilised in the study. Peptide amphiphiles sequence, molecular weight (KDa) and pI. ł These are theoretical values from previous research on the peptides. * pH selected for experiments according to previous research on the materials. ** Concentration selected for experiments according to previous research.

The first set of PAs (PA-K_2, PA-K_3, PA-K_4) are well established sequences known to interact with negatively charged biomolecules (Inostroza-Brito et al., 2015). The head groups contain lysine residues which gives them a net positive charge. These sequences were used as controls. The PA-K_3G_3 peptide was added for its potential benefits in terms of biocompatibility (Redondo, 2020).

The second set of PAs (PA-H_3 and PA-H_2K) are positively charged peptides with histidine residues that have been studied for their ability to co-assemble with negatively charged biomolecules and known to be biocompatible (Hedegaard et al., 2018; Ajovalasit et al., 2021; Okesola et al., 2021).

The third set of PAs (PA-E_3 and PA-E_3Y) are negatively charged peptides that contain glutamic acid residues in their head group and known to interact with positively charged molecules. In addition, PA-E_3 sequence is known to have high biocompatibility with different types of cells (Zhang et al., 2010).

4.1.1.2 Bio-fluids

Blood is a biological fluid with a complex composition which is constantly changing depending on the microenvironment input. The Human Blood Atlas project has identified over 400 proteins actively secreted by cells into blood as well as the genetic profile and the transcriptomic of 18 different cell types present in blood (The Blood Atlas, 2019).

Blood can be separated into different fractions with unique composition and properties. For the initial testing, whole blood and blood fractions were used as follows:

a) Whole blood: Contains ions, proteins and cells (RBCs, WBCs, platelets).
b) Platelet rich plasma (PRP): Contains a higher concentration of ions, proteins and platelets than whole blood. The cellular part is removed.
c) Plasma: Contains ions and proteins.
d) Serum: Contains ions.

These fractions were separated by routinely used centrifugation methods (Refer to Chapter 3) and tested to determine their potential to assemble with peptide amphiphiles.

4.1.1.3 Controls

Due to the complexity of blood, a set of additional controls were selected due to their abundance and importance in blood. Having these controls is critical in order to build up an understanding of underlying mechanisms of the interactions between blood and PAs. For this reason, two proteins were selected:

a) Albumin: Represents around 55% of proteins in blood.
b) Fibrinogen: Represents around 7% of proteins in blood.
c) Simulated body fluid (SBF), contains the ionic component of blood. This was used to determine potential interactions of PAs with different ions, which are known to be able trigger PAs self-assembly via electrostatic interactions.

4.1.2 Initial screening to determine interactions between PAs and human blood or fractions

Two models previously described in the methodology section were used to evaluate initial interactions between blood (or blood fractions) and peptide amphiphiles. Briefly, for Model 1, a peptide amphiphile solution was injected inside the biofluid. For model 2, the biofluid was injected into a peptide solution (Figure 4.1 A). Peptides were incubated for 24 hours prior to manual inspection and washing.

The interaction of two sets of peptide amphiphile of positive and negative charges was evaluated with different blood fractions to determine their potential to create hydrogels.

PAs and blood components interactions were first evaluated qualitatively by macroscopic observation of hydrogel formation (Figure 4.1 B) and categorised manually according to their strength after washing (Table 4.2). The classification of stiffness was done according to a qualitative criterion as follows: a) Strong: hydrogels do not suffer deformation when moved or washed, b) Medium: hydrogels suffer mild deformation when moved or washed, c) Weak, hydrogels are brittle and break when moved or washed, d) Aggregate, a visible white precipitate is observed but no hydrogel is recovered, e) No gel formation observed.

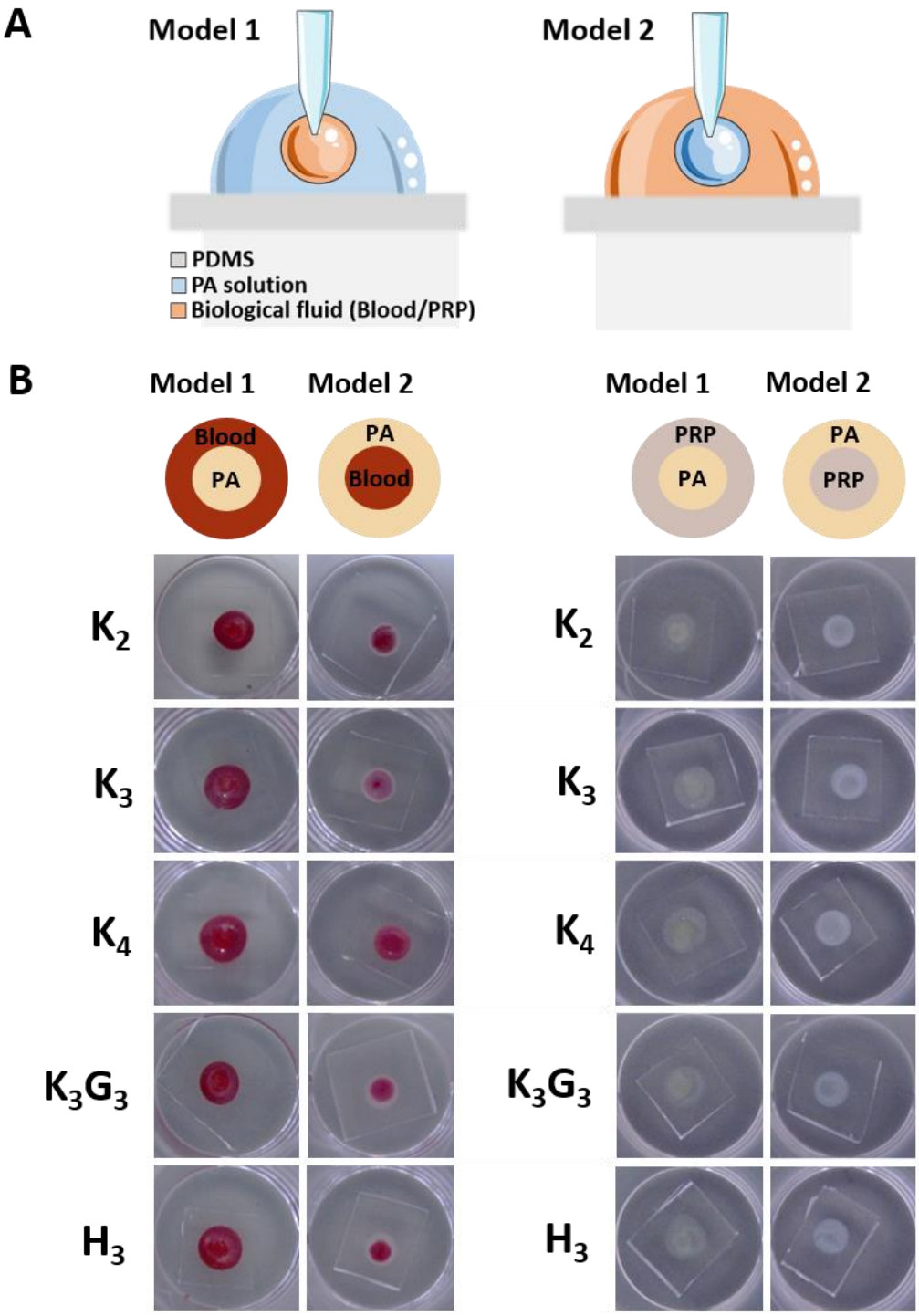

Figure 4.1. Preliminary screening of biological fluids interaction with PAs for hydrogels formation. A) Two different models were used to test initial interactions and diffusion patterns. B) Macroscopic observation of gel formation with different PAs.

Table 4.2 summarises the results of the preliminary evaluation of the peptide amphiphiles interactions with whole blood of human donors and fractions (PRP and Serum).

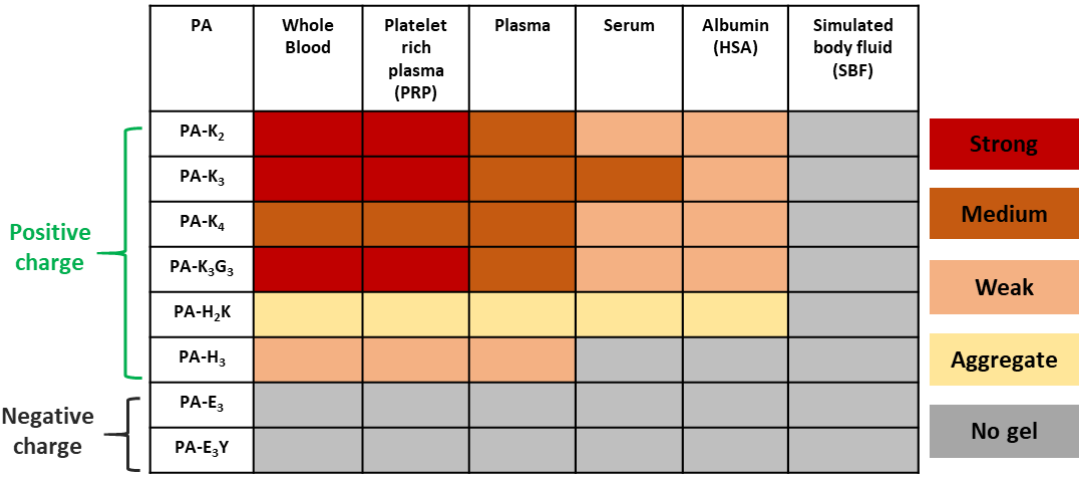

Table 4.2. Summary of results and gel strength. This table summarises the qualitative characterisation of hydrogels strength using different types of PAs that were assembled with different blood fractions. Results showed that hydrogels created with positively charged peptides presented higher strength. Controls utilised for these experiments include human serum albumin (HSA) and simulated body fluid (SBF). Results representative of $n \geq 4$.

4.1.2.1 Blood and Platelet Rich Plasma

Whole blood and platelet rich plasma were obtained from human donors and tested with the set of PAs. Preliminary results indicated that positively charged PAs were able to co-assemble with components present in whole blood and PRP whereas negatively charged PAs did not form hydrogels under the conditions tested (Table 4.2, Figure 4.1 B).

Peptides containing two or more lysine residues (PA-K_2, PA-K_3, PA-K_4, PA-K_3G_3) formed the strongest gels overall whereas peptides containing histidine residues formed weak gels or aggregates. These observations suggest lysine might be creating

stronger interactions with the biomolecules present in the bio-fluids. As a next step, other blood fractions were obtained to determine the impact of certain components in the assembly of the hydrogels.

4.1.2.2 Blood Plasma

Human blood plasma constitutes about 55% of the total blood volume. This bio-fluid contains the whole protein and ionic fraction of blood, including blood clotting factors but does not have the cellular component.

A similar trend than the one observed with Blood and PRP hydrogels was observed. When using plasma, peptides containing lysine residues (PA-K_2, PA-K_3, PA-K_4, PA-K_3G_3) were able to form hydrogels. The overall strength of these gels was lower compared to the other fractions. We hypothesise that components present in blood and the concentrated platelet rich plasma contribute to the observed change in stiffness.

4.1.2.3 Blood Serum

Human blood serum was obtained from whole blood samples via centrifugation. This biological fluid contains the ionic and protein concentration present in blood minus the blood cells (red and white blood cells, platelets), clotting factors and proteins involved in the coagulation cascade (fibrinogen). It also contains other components commonly present in blood including hormones and antibodies, and in some cases,

exogenous substances such as drugs or living cells like microorganisms, which have a high variability between donors and are dependent on the donors' health status.

Results indicated that PAs mixed with serum assembled the weakest gels when interacting with positively charged PAs containing two or more lysine residues. Despite hydrogel formation, there was a further decrease in the overall hydrogel strength compared with blood, PRP and plasma hydrogels (Table 4.2).

Although this set of experiments indicate that the cellular component, clotting factors and coagulating proteins might not play a key role in hydrogel formation, we hypothesise they could be contributing to the overall strength of the gels.

4.1.2.4 Albumin

Altogether, previous results suggested that positively charged PAs main interaction could be with negatively charged components present in blood. To test this hypothesis, we next evaluated hydrogel formation with a negatively charged protein.

Serum albumin represents 55% of blood proteins and has a concentration of 35-50 mg/ml in blood. Human serum albumin was used as a control to assess the effect of a negatively charged protein of 66.5KDa on the systems assembling process.

Positively charged peptides (PA-K_2, PA-K_3, PA-K_4, PA-K_3G_3) were able to form hydrogels when in contact with HSA solution. However, negatively charged peptides did not form hydrogels. This suggests that albumin alone could be a key component

in the activation of the gelation process and one of the molecules involved in the co-assembly.

4.1.2.5 Simulated body fluid

The co-assembling of our hydrogels and its strength can be tuned in vitro by varying the concentration of certain ions such as Ca^{+2} (for negatively charged PAs) and Phosphate (for positively charged PAs).

Simulated body fluid (SBF) is composed by all the ions present in the blood minus the protein and cell component. A SBF solution containing the ionic component of blood was used to determine the effect of the ions have in hydrogel formation. SBF was prepared with the exact ion concentration present in blood and plasma.

Peptide amphiphiles were not able to form hydrogels after a 24-hour incubation period regardless of their charge. These results agree with previous work from the Mata group, since the ionic concentrations present in blood are 20-50 times less than the concentrations previously used to assemble the systems in vitro.

Therefore, preliminary results seem to indicate that the ionic component of these biological fluids might be acting as a biological buffer and playing a minor role in hydrogel formation but does not have a major contribution in the assembly of these systems.

4.1.2.6 Selection of peptide amphiphile: PA-K_3

PA-K_3 was selected as the peptide model for further research as it showed good initial mechanical properties to form stable hydrogels with different blood fractions and proteins.

This peptide has been widely studied and characterised, making it a good candidate to validate further studies. In addition, the three lysine residues of the head group confer this PA high solubility, its high net positive charge gives its stability and low aggregation in solution. Moreover, it has shown the ability to form electrostatic interactions and it has proven to promote co-assembly with negatively charged proteins present in blood, which account for the majority of the total blood proteins.

In addition, positively charged PAs need to have a strong β-sheet interaction to support cell viability given that weak bonding forces in PAs can lead to interactions with the cell membrane and cause cytotoxicity (Hendricks et al., 2017). PA-K_3 has been reported to have a characteristic β-sheet structure (Behanna et al., 2005).

4.1.3 Molecular mechanisms insights of PA-K_3 - Blood hydrogels.

The co-assembly of PAs with biomolecules has been explored in order to overcome limitations of current self-assembling hydrogels in terms of strength and bioactivity. The combination of peptide amphiphiles with proteins, carbohydrates, and lipids has shown the potential of this technique to improve or modify the materials' properties (Inostroza-brito et al., 2015; Inostroza-brito et al., 2017; Hedegaard et al., 2018).

The use of blood, a complex mixture of proteins, salts and different cell types, provides the opportunity to explore PAs capabilities to bind and interact with multiple components at once and harness different properties for the creation of hydrogels. The main protein components of interest are listed in Table 4.3.

Blood protein	Concentration in blood	Abundance in blood (%)	Function
Albumin	35-50 mg/ml	55%	Create and maintain oncotic pressure, transport of insoluble molecules
Globulins	20-25 mg/ml	38%	Immune system
Fibrinogen	2-4.5 mg/ml	7%	Blood coagulation
Regulatory proteins	N/A	<1%	Regulation of gene expression
Clotting factors	N/A	<1%	Conversion of fibrinogen into fibrin

Table 4.3. Blood components and their function in the body. This table summarises the abundance of key proteins in blood in terms of concentration, and their main functions.

4.1.3.1 Microstructure analysis of PA-K_3 - Blood and PRP hydrogels.

After initial macroscopic observation (Section 4.1.2), PA-K_3 gels co-assembled with blood or PRP were analysed with Scanning Electron Microscopy (Figure 4.2) to evaluate nanofiber formation and potential biological interactions of the materials with the bio fluids.

Model 1 was used to study the effect of the interaction of the PA materials with blood and PRP on their surface and bulk properties. Cell attachment and network formation is observed in PA – Blood gels surface, an indication of the activation of the blood clotting process (Figure 4.2 a-b). The bulk of the materials showed nanofibre network formation (Figure 4.2 c-d).

A similar reaction to PAs was observed in PA – PRP gels which seem to have triggered platelet activation and fibrin deposition, thus resulting in the formation of a very dense fibrin network compared to the network in blood gels on the materials surface (Figure 4.2 e-f). The bulk of these hydrogels also presented nanofibre formation (Figure 4.2 g-h). PRP is a concentrated fluid with higher amounts of platelets, growth factors, blood clotting factors, and proteins, thus it is hypothesised that the clotting response is stronger and has an enhanced effect on network formation.

Model 2 was used for studying the encapsulation of the biological fluids inside PA materials. The inverse effect was observed in these samples, where PA-network formation is observed on the outer regions of the hydrogels (Figure 4.2 i-j), whereas there is encapsulation of cells that have attached together on the inside of the materials (Figure 4.2 k-l, red arrows). In the case of PA – PRP hydrogels the same effect is observed, where there is PA network formation on the external part of the hydrogels (Figure 4.2 m-n) and platelet attachment and some fibrin network begins to form inside the gels (Figure 4.2 o-p, red arrows).

SEM microscopy analysis of Blood and PRP samples showed differences in the density of the two different networks on the core and surface of the hydrogels, with fibres of different sizes and overall structure. The difference in the quantity of fibrin deposition and network formation observed can be explained by the different volumes used to create the samples. Importantly, the PA nanofiber network formation was observed regardless of the model or biological fluid utilised to create the hydrogels.

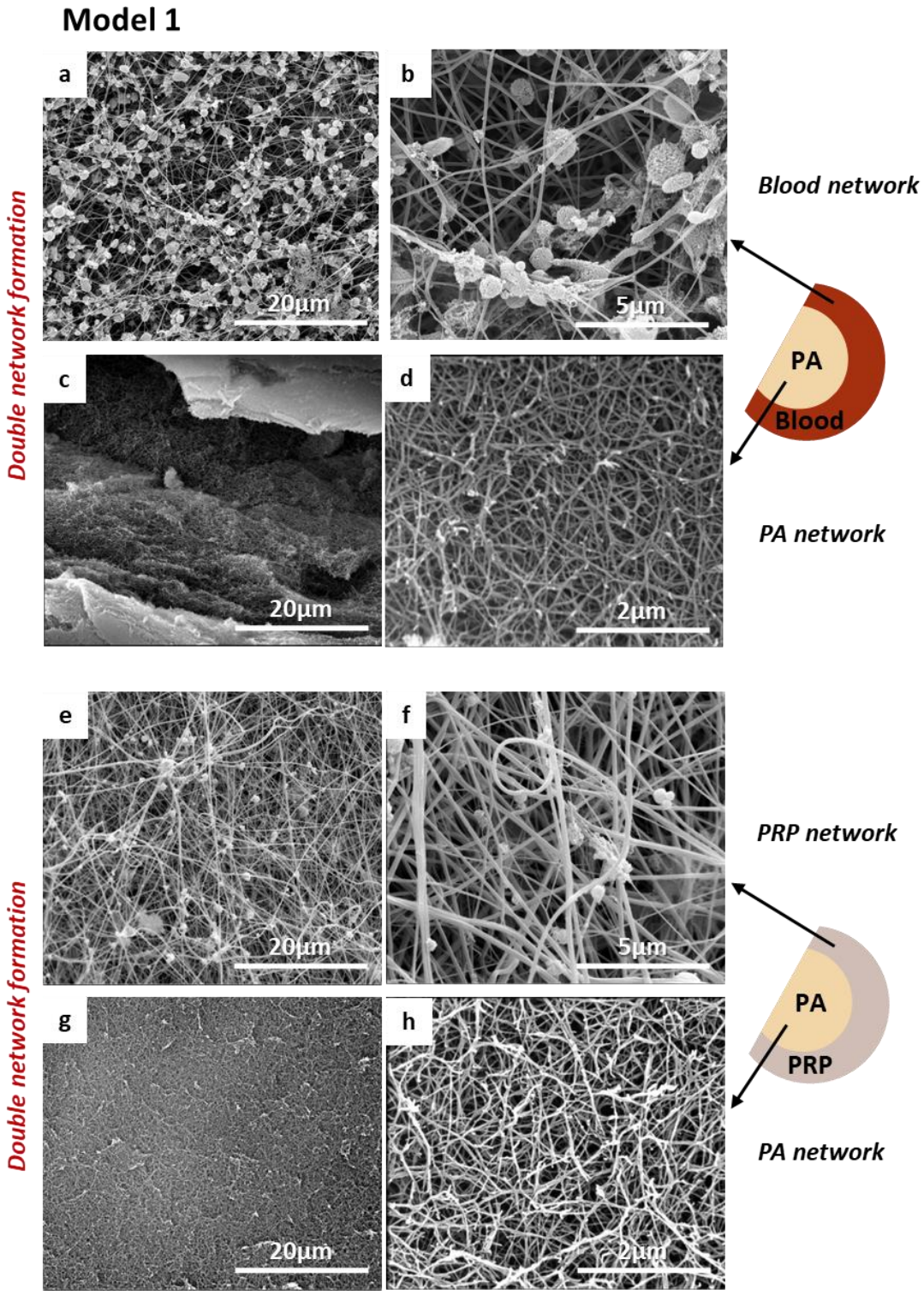

Figure 4.2. SEM images of blood/PRP and positively charged PAs hydrogels. Model 1 shows surface interaction of the PA materials with blood and PRP (a-b, e-f) whereas Model 2 shows the encapsulation of the biological fluids inside PA materials (k-l, o-p). Nanofiber network formation was observed regardless of the model utilised for testing (d, h, j, n). Images representative of n=3.

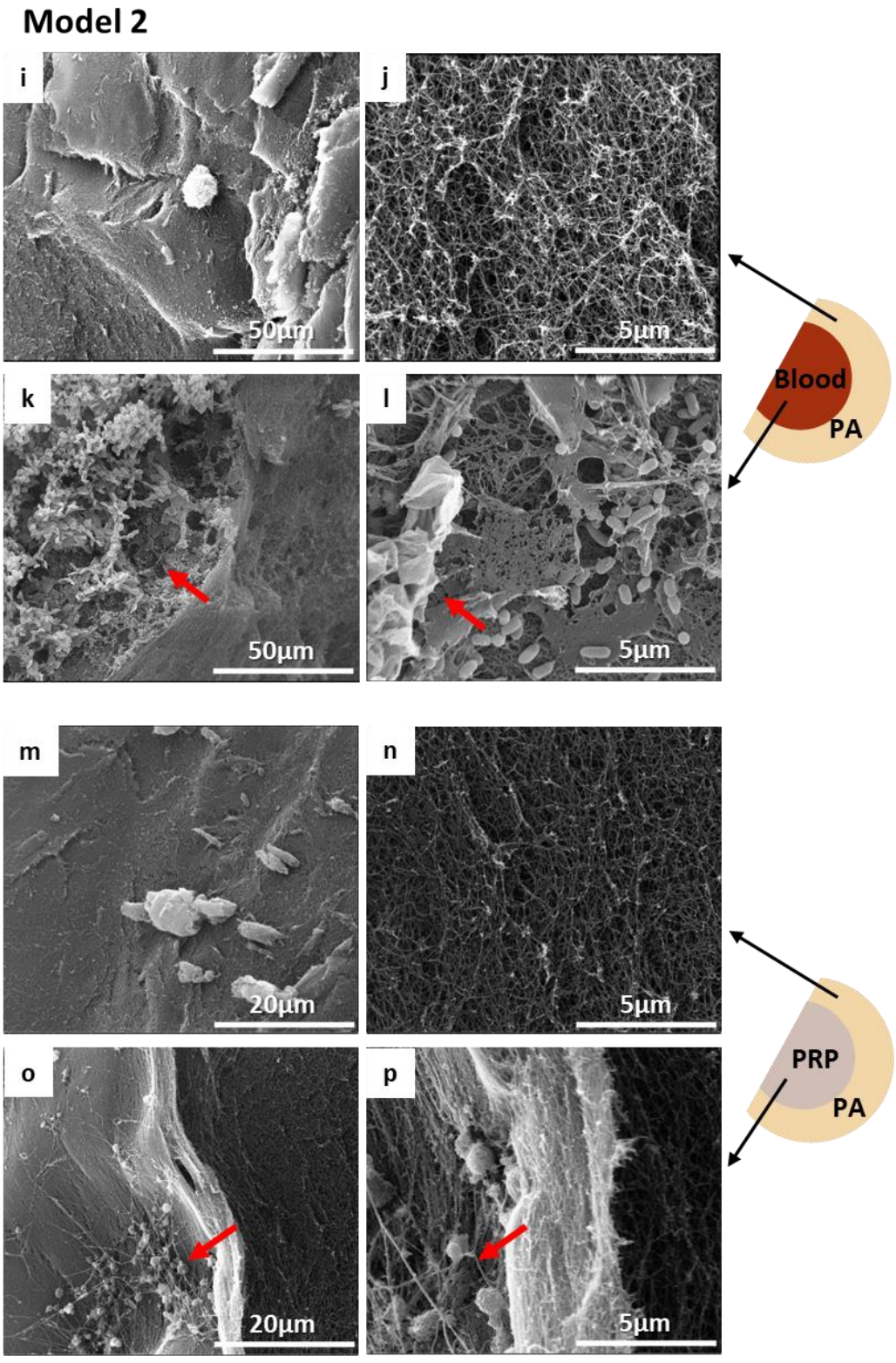

Figure 4.2. SEM images of blood/PRP and positively charged PAs hydrogels. Model 1 shows surface interaction of the PA materials with blood and PRP (a-b, e-f) whereas Model 2 shows the encapsulation of the biological fluids inside PA materials (k-l, o-p). Nanofiber network formation was observed regardless of the model utilised for testing (d, h, j, n). Cell attachment and a fibrin network can be observed (red arrows). Images representative of n=3.

Double network hydrogels have been previously characterised and it has been extensively documented that by having two different networks interacting, the gel strength increases in different orders of magnitude that depend on the materials combination and crosslinking methods (Wang et al., 2018). We hypothesise that the fibrin network formed by activated platelets is strengthening the overall stability of the gels by acting as a second network layer.

4.1.3.2 Comparison of the effect of biological fluids, blood proteins and enzymes on the hydrogels

The co-assembly of small molecules (PAs) with bio-macromolecules offers the possibility of creating materials with increasing levels of complexity including chemical gradients, control over the nano and micro structure and hierarchical organisation (Azevedo et al., 2018; Hedegaard et al., 2018). The building blocks of these multi-component hydrogels are key for the emergent properties of the materials and their study is imperative to determine their contribution to these new biomaterials.

4.1.3.2.1 Hydrogels bulk and surface microstructure

Blood and derived products (plasma, platelet rich plasma) were used to trigger the formation of PA-K_3 hydrogels and examine their structural features. The bulk and surface microstructure was analysed by SEM microscopy (Figure 4.3 A). PA nanofibers structure do not seem to be affected by the different biological fluids used in this study. However, the outer layer of the hydrogels has different characteristics depending on the blood fraction used. The density and diameter of the fibrin fibres

is different when using blood, plasma or PRP. In addition, blood gels show higher density of cells on the material's surface.

By using different blood proteins and enzymes we tried to identify key molecules of the blood that interact with our biomaterials in order to create the double network seen when using biological fluids (Figure 4.3 B). We observed that the PA nanofibers structure remain constant regardless of the blood proteins or enzymes utilised to assemble the gels.

Results showed that surface topography and microstructure changes depending on the proteins used. Albumin does not seem to have an impact on surface microstructure, however fibrinogen creates a surface without visible pores (at this magnification) when interacting with PA alone.

The addition of thrombin (enzyme 1) and Factor XIII (enzyme 2) showed that the fibrinogen protein starts to polymerise into a fibrin network that resembles the one observed in Plasma or PRP hydrogel samples, which mimics the natural blood clotting process.

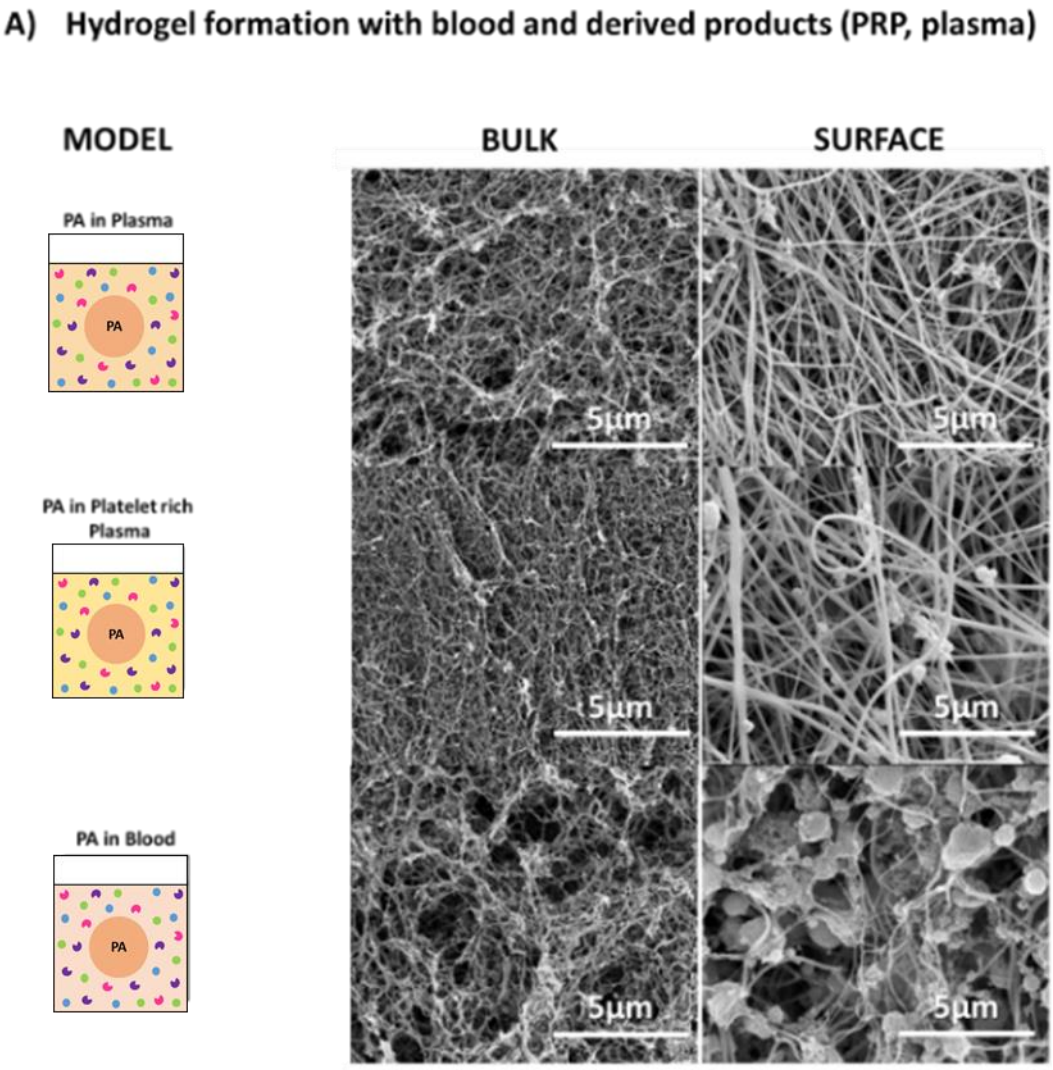

Figure 4.3. Evaluation of materials interaction with blood and derived products. A) Hydrogel formation with whole blood and fractions (Platelet rich plasma, plasma). SEM analysis of bulk and surface nano and microstructural changes. B) Hydrogel formation with blood proteins (HSA, FGEN) and enzymes (thrombin, FXIII). Bulk and surface changes are dependent of the proteins and enzymes utilised.

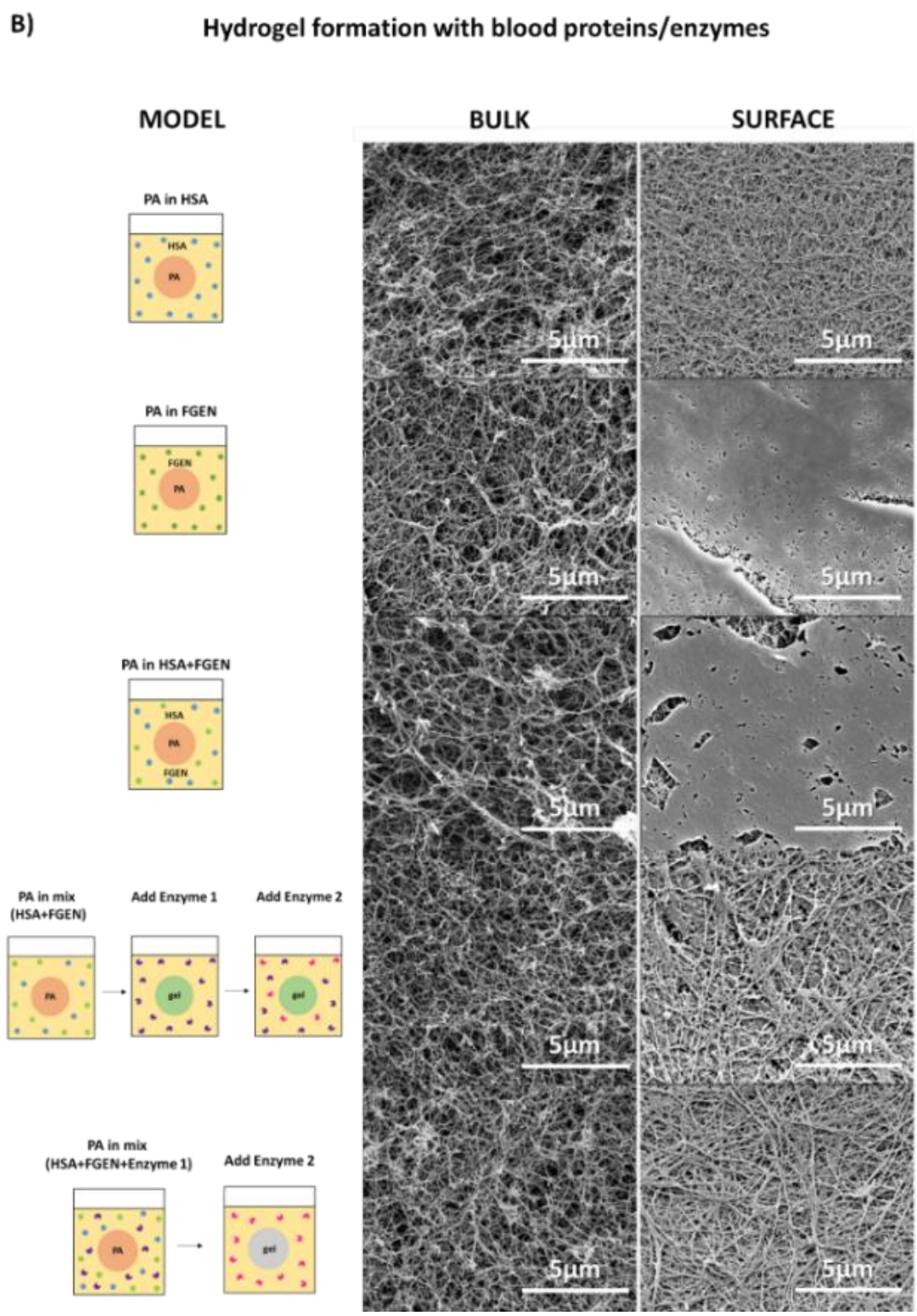

Figure 4.3. Evaluation of materials interaction with blood and derived products. A) Hydrogel formation with whole blood and fractions (Platelet rich plasma, plasma). SEM analysis of bulk and surface nano and microstructural changes. B) Hydrogel formation with blood proteins albumin (HSA) and fibrinogen (FGEN), and enzymes (enzyme 1: thrombin, enzyme 2: Factor XIII). Bulk and surface changes are dependent of the proteins and enzymes utilised.

Interestingly, the observed stiffness of the gels created by addition of proteins and enzymes is inferior compared to the ones created with blood and fractions. Gels created for this study are very weak and hard to handle. A possible reason for the change in mechanical properties is that all components mixed together are activated prior to PA addition whereas the natural blood clotting process is characterised by step by step activation of the components of the coagulation cascade. This can have an impact the way that both PA and proteins interact with each other as well as their polymerisation process. Moreover, it has been shown that platelets are a key component in the stabilisation of blood clots and contribute to their strength (Lam et al., 2011). We hypothesise that blood cells are directly involved in the modulation of these hydrogels stiffness.

Moving forward it is important to highlight that the multiple components that form these hydrogels give rise to heterogeneous zones in the materials which can also contribute to the change in their properties.

4.1.3.2.2 Hydrogels mechanical properties

The viscoelastic properties of the materials were measured using rheology. The comparison between the stiffness of hydrogels formed using a concentrated ionic solution (PBS 1X) that promotes self-assembling and hydrogels using blood proteins and human plasma is shown in Figure 4.4.

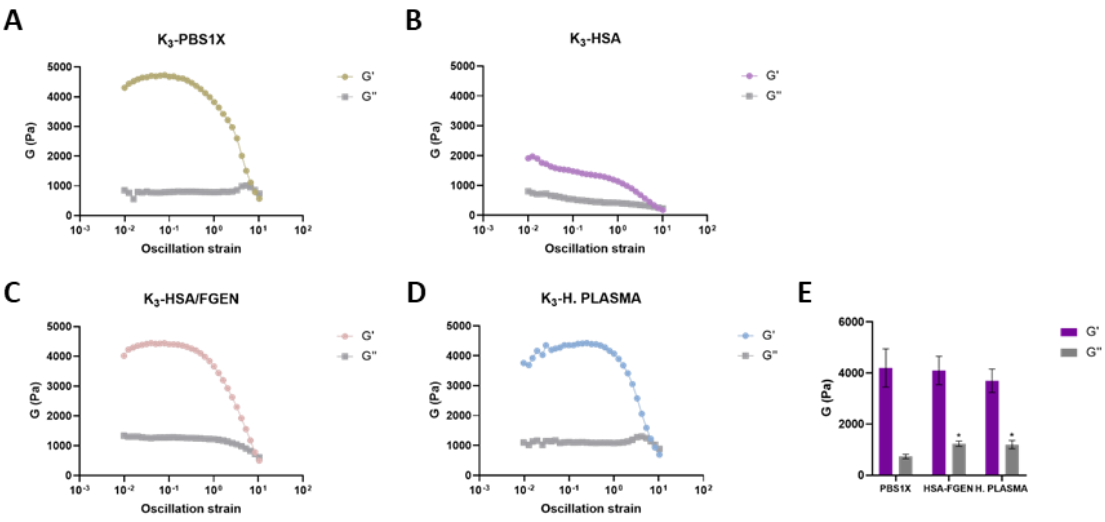

Figure 4.4. Evaluation of hydrogels viscoelastic properties with rheology. PA-K_3 hydrogel formation with an ionic solution (A), one protein (B), two proteins (C) and a complex protein sample of human plasma (D). The comparison of the different materials was done via ANOVA for multiple comparisons test (E).

Results show no statistically significant difference between hydrogels created with a concentrated ionic solution (Figure 4.4 A) and those created with protein mixtures (HSA/Fibrinogen) or human plasma (Figure 4.4 B-D). These hydrogels exhibit G' values of around 4 kPa (Figure 4.4 E). The viscoelastic plateau of the hydrogels is limited, which may indicate that the interaction with poly-ionic proteins is more limited than using mono-ions for gel formation.

When using HSA for gel formation (Figure 4.4 B), the results indicate that although there is nanofiber formation, these samples do not have a typical hydrogel behaviour. Thus, we observe there is protein aggregation but possibly no complete gelation (Schmidt et al., 1981). A possible explanation for the weakness of these materials is that although the self-assembling process is triggered, the nanofibers formed might be very short and their electrostatic interactions with HSA alone may not be strong enough to recover after applying stress (Redaelli et al., 2016). On the other hand,

when using 2 proteins (HSA and fibrinogen) or human plasma, PA-K_3 is able to show a typical gel-like behaviour and improved stiffness on the material was observed. This suggests fibrinogen is a key regulator in the hydrogels stiffness.

By having a multiple component self-assembling system, very complex morphologies can emerge with different properties. We hypothesise that in the case of PA-K_3 – HSA gels, the most favoured mechanism may be the co-assembly of the PA and the protein, where the building blocks interact with each other preferentially. However, in the case of PA-K_3 – FGEN or PA-K_3 – Plasma, we could have different gelation mechanisms acting together including: self-sorting, specific co-assembly and random co-assembly due to the existence of many different components in the gelator solutions. Further studies would be required to evaluate this hypothesis.

4.1.3.3 Study of co-assembly interaction kinetics

After initial macro and microscopic evaluation of hydrogels and determination of key components involved in the hydrogelation process, the co-assembly interactions and mechanisms were evaluated at the molecular level.

4.1.3.3.1 Selection of blood proteins as study models: Albumin and Fibrinogen

From the previous set of studies, we identified key blood proteins due to their high concentration in blood as well as their role in hydrogelation. Albumin represents about 55% of the total proteins in blood and has a key role in the balance of osmotic pressure in blood as well as nutrients transport. The previous studies have also

presented evidence that our hydrogels form a double network of cross-linked fibrinogen (fibrin network), this protein is a key component of the blood clotting process and its role in blood clots stiffness has been widely researched.

To validate our findings, PA-K_3 – Blood hydrogels were stained with primary and secondary antibodies and immunofluorescence analysis was carried out. Microscopy imaging identified a fibrin network in the surface of the gels as well as non-localised accumulation of human serum albumin (Figure 4.5). This agrees with previously documented responses to biomaterials where it has been identified that the first event occurring in the surface between different materials and blood upon contact is protein absorption. This leads to enzymes and platelet activation and fibrin deposition. Subsequently, the formation of a “conditioning film” is formed by these proteins, which could help integrate the biomaterials to the native tissues (Xu et al., 2014). However, previous results on our systems suggest that proteins are also migrating inside the PA solution, to help assemble the gels. Further studies using these model proteins were carried out to validate this hypothesis (Section 4.1.3.3.3)

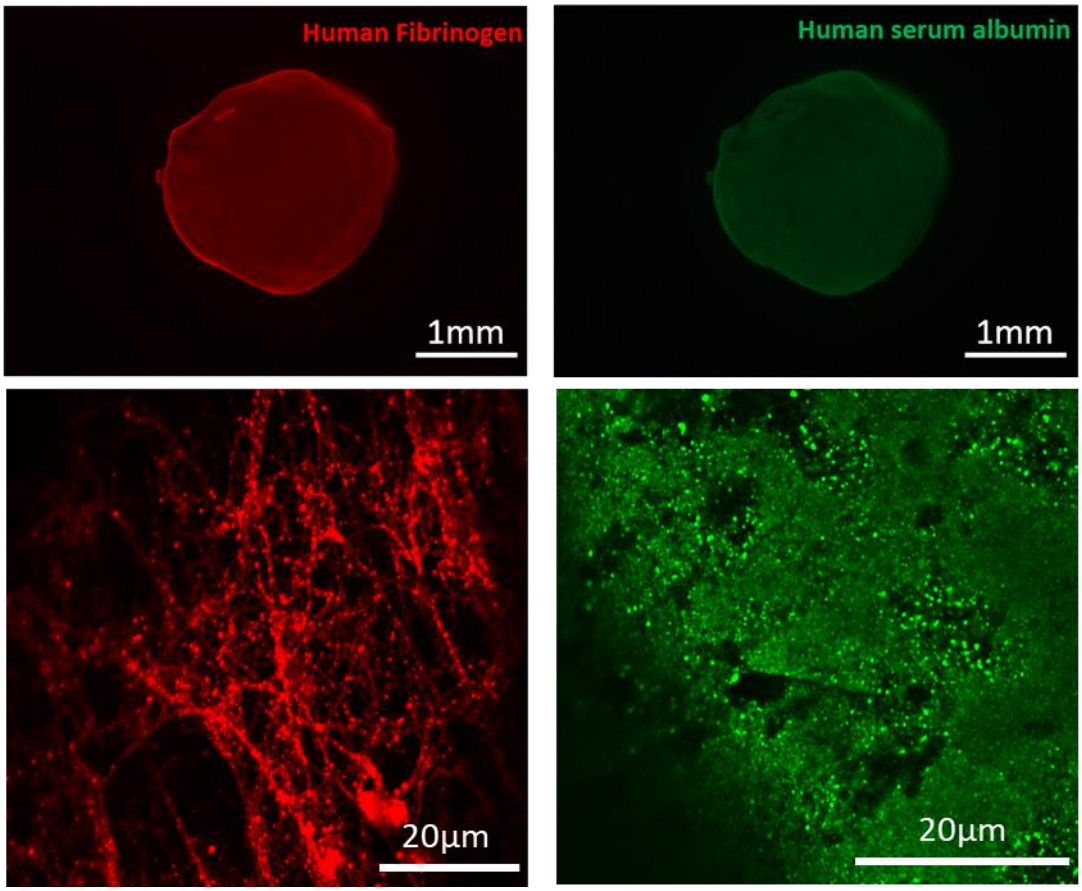

Figure 4.5. Immunofluorescence detection of blood proteins. Immunofluorescence microscopy showed human fibrinogen and human serum albumin presence in PA-K_3 – Blood hydrogel samples. Images obtained with Leica DMI4000 epifluorescence microscope 2.5X magnification show the hydrogels total surface and high magnification images of the hydrogels obtained with Zeiss Confocal microscope were obtained to analyse the surface in more detail. Images representative of n=3 independent repeats.

4.1.3.3.2 Evaluation of changes in the secondary structure of PA-K_3 and proteins during co-assembly

Circular dichroism was used to characterise blood proteins interaction with PA materials. This technique is based on the differential absorption of left and right circularly polarised light of optically active molecules with UV light (Johnson, 1996). This method can be used for determination of the secondary structure, folding and binding capacity of peptides or proteins in solution (Greenfield, 2006). The

characteristic CD spectral signature is dependent on the secondary structure of the molecule analysed (e.g. alpha-helix, beta-sheets) (Beychok, 1996).

We selected albumin and fibrinogen as protein models of this study to determine the extent of their interactions with PA-K_3. Albumin is a globular protein of 60 kDa that represents around 55% of the proteins present in serum, with a predominantly alpha helix structure and a negative net charge. Fibrinogen is a fibrillar protein of 350 kDa that represents 4% of the proteins in blood, it also has alpha helix structure and negative net charge (Berman et al., 2003).

Initially, the secondary structure of these proteins and PA-K_3 was confirmed by CD. As expected, PA- K_3 exhibited a β-sheet signature signal characterised by a positive maximum signal at around 202 nm and a negative minimum at around 219 nm. Albumin and fibrinogen exhibited an α-helix conformation characterised by two negative signals at around 208 nm and 222 nm as reported in the literature (Figure 4.6). These spectra were then compared to the spectrum of composites (PA-Protein 1:1 ratio, volume: volume) in order to observe any potential shifts in the signal.

The composite signal of PA-K_3 – HSA (1:1) exhibited pronounced differences compared to the pure PA and protein spectrum, indicating that conformational changes take place in the presence of each other. Focusing on the PA-K_3 – HSA graph (Figure 4.6 A) there is a negative absorption with increased intensity and shifted to the right for the composite compared to the pure PA-K_3 signal, and the negative peak observed around 205nm in HSA was no longer detected, indicating that these molecules are interacting and conformational changes are taking place as a result of this interaction.

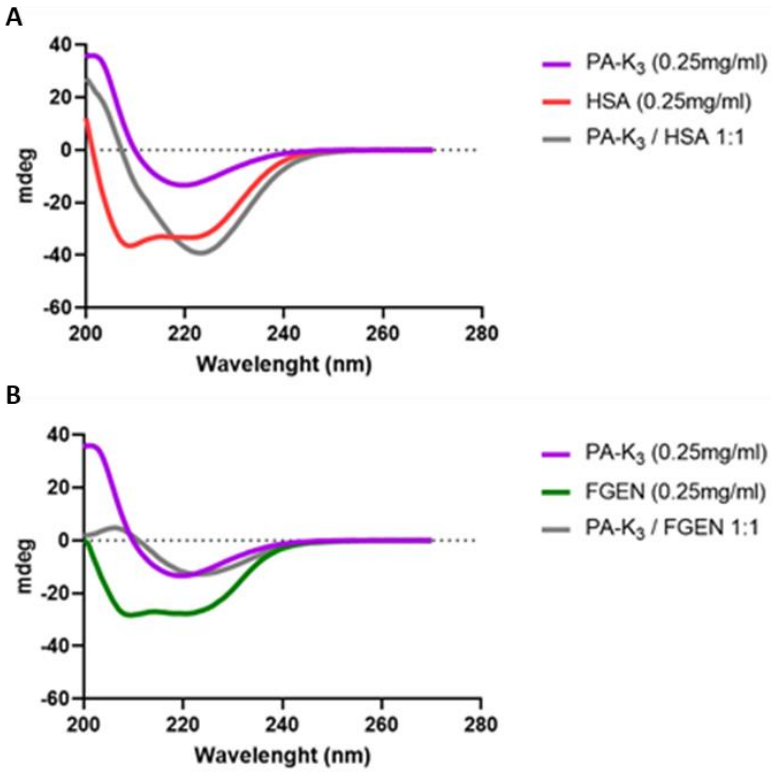

Figure 4.6. Study of blood proteins interaction with PA-K$_3$. A) CD spectra showing the secondary structure of PA-K$_3$ (β-sheet) and HSA (α-helix) as well as their interaction signature (1:1 v/v). B) CD spectra of the secondary structure of PA-K$_3$ (β-sheet) and Fibrinogen(α-helix) as well as their interaction signature (1:1 v/v).

The PA-K$_3$ – FGEN signal is considerably different compared to the peptide and protein spectra. The PA-K$_3$ – FGEN graph (Figure 4.6 B) showed that the composite spectrum presents a very low positive peak with a reduced intensity, around 205 nm and a low intensity peak around 220 nm. The distinctive signatures of β-sheet and α-helix are no longer detected. This is also an indication of interaction between these proteins and potential conformational changes. Additional studies like TEM imaging could help visualise these fibres and help confirm if they form hybrid systems.

Although these models serve as a starting point on characterisation of the protein-peptide systems, these do not accurately represent the complexity of PA interactions

with body fluids such as blood and derived products. Hence, further analysis need to be done in order to study the PA-Blood systems.

4.1.3.3.3 Protein diffusion assays

For the purpose of this study, albumin and fibrinogen were selected as study models to determine the extent of their diffusion through hydrogels due to their abundance in blood. Albumin is a globular protein of 60 kDa that is abundant in blood, whereas fibrinogen is a fibrillar protein of 350 kDa that represents around 4% of the proteins in blood (Tutwiler, et al., 2016).

In order to characterise the spatiotemporal location of these key components in hydrogels, fluorescent tagged proteins were utilised to determine the diffusion patterns through the gels. The protein diffusion assay was validated using a two-way microchannel slide (ibidi) to study the point of contact between protein and PA solution by using microscopy at different time points.

The diagram on Figure 4.7 A shows the channel with PA solution on the left and protein solution on the right. The two solutions were placed close to each other to allow the capillary forces to bring them together. As the solutions got into contact, there is immediate interface formation that triggers the gelation process. The gelation process was tracked for 24 hours and images were acquired at different time points.

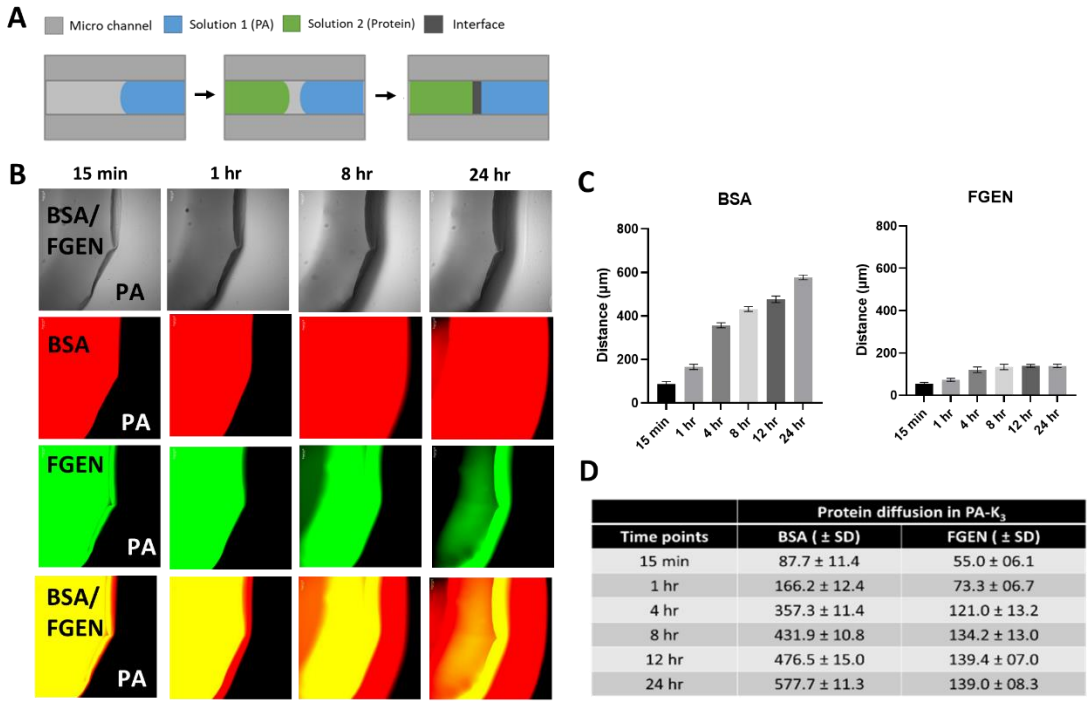

D

	Protein diffusion in PA-K_3	
Time points	BSA (± SD)	FGEN (± SD)
15 min	87.7 ± 11.4	55.0 ± 06.1
1 hr	166.2 ± 12.4	73.3 ± 06.7
4 hr	357.3 ± 11.4	121.0 ± 13.2
8 hr	431.9 ± 10.8	134.2 ± 13.0
12 hr	476.5 ± 15.0	139.4 ± 07.0
24 hr	577.7 ± 11.3	139.0 ± 08.3

Figure 4.7. Protein diffusion experiments. A) Diagram of experimental set up of micro channels for protein diffusion studies. B) Fluorescently tagged proteins (BSA and FGEN) were utilised to track the diffusion of biomolecules inside PA-K_3 hydrogels at different time points. C) The graphs show the maximum distance of diffusion over a period of 24 hours. D) Summary of protein diffusion distance (µm) over time.

This study showed that after the interphase formation between PA solution and protein solution formed, the diffusion process is directional from the protein solution into the peptide solution. Albumin appears to be diffusing into the PA gels for 577.7 ± 11.3 µm over a period of time of 24 hours whereas fibrinogen maximum diffusion occurs at 4 hours, and it stops at an approximate distance of 139 ± 0.83 µm. These results support our findings on blood and PRP gels microstructure (Section 4.1.3.1), where we hypothesise the blood clotting process is activated and the fibrin network polymerisation is triggered by polymerisation with blood enzymes. This network co-exists with the PA network, forming double network hydrogels, rather than this protein diffusing through the gels. In terms of albumin, a globular and smaller

protein, we hypothesise that this protein and similar ones, in terms of size and charge, are able to diffuse more freely through the gels and help the co-assembly process. An in depth analysis of molecule localisation on our hydrogels need to be carried out to complement these findings.

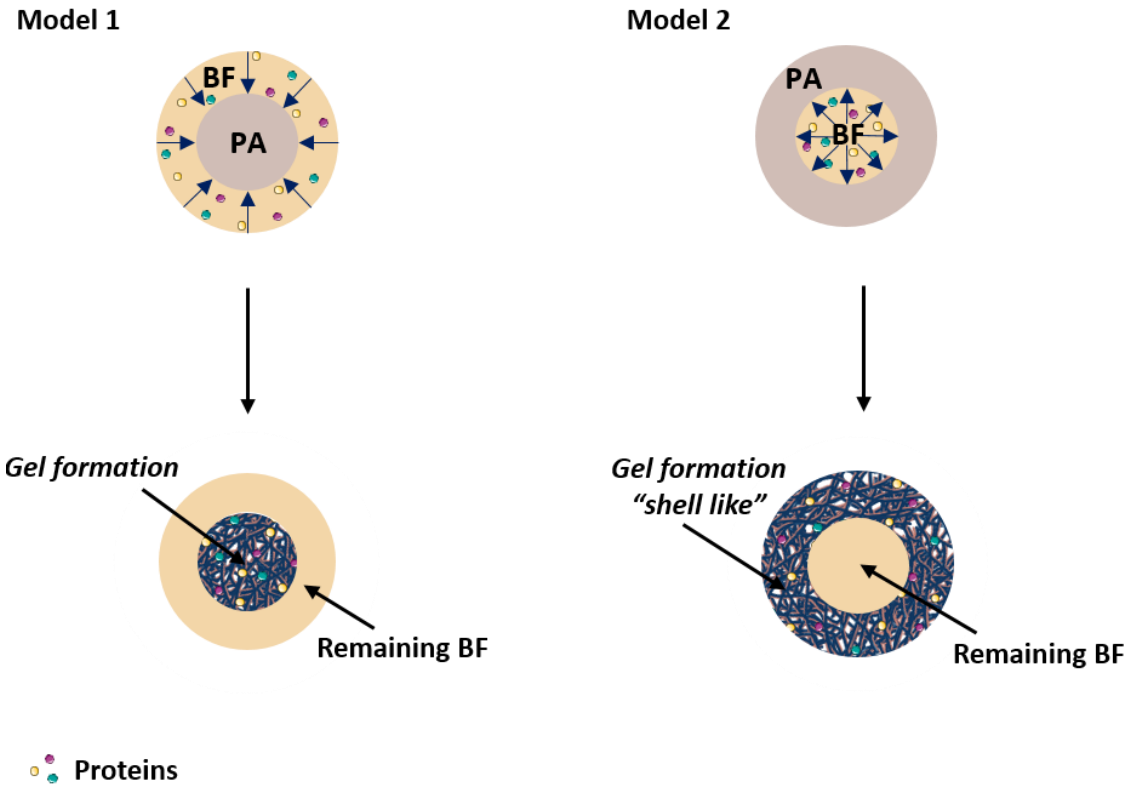

Figure 4.8. Proposed diffusion mechanism of the co-assembled hydrogels. Biomolecules present in the biological fluids are diffusing inside the PA solutions triggering the nanofibre and gel formation. Therefore, Model 1 creates a compacted hydrogel whereas Model 2 creates a "shell-like" gel with biological fluid encapsulated inside.

Altogether, results indicate that a mix of proteins and ions present in blood are diffusing inside the PA solutions triggering nanofiber formation. whereas cells remain on the surface of the assembled hydrogels where a biological network is formed with

entrapped cells and fibrin. Figure 4.8 shows the proposed mechanism of diffusion of these systems.

4.1.3.4 Comparison of clinically relevant buffers effect on hydrogels secondary structure and mechanical properties

Peptide solubility is determined by two main properties: a) peptide sequence and b) peptide environment. In general, peptides with a large proportion of non-polar amino acids will be difficult to dissolve in aqueous solutions, the more polar residues that are present, the easier it will be to dissolve a peptide (Sarma et al., 2018).

Biologically compatible buffers are of special interest for this work as hydrogels are constituted of 99% water and would be in close contact with cells on in vitro or in vivo settings.

HEPES buffer is widely used for cell biology research to mimic the buffering capacity of the body. It is an organic chemical buffer with a high capacity to maintain physiological pH in cell culture for extended periods of time (Good, et al.,1966). This buffer was used as a control for this studies.

Ringers lactate solution and normal saline solution were selected as test buffers due their wide spread use in the clinic. These are intravenous fluids used to treat different conditions including: a) blood loss due to trauma, b) burns, c) dehydration, d) fluid replacement during surgery, e) wound cleaning; and e) drug administration. These buffers are constituted by water and electrolytes.

Ringer's lactate solution and Saline solution can be administered at an initial rate of 500 ml to 3 litres/24 hr in adults, depending on the patient’s age, weight and current

health conditions. The recommended dosage when using these buffers as a vehicle or diluent ranges from 50 to 250 ml “per dose of medicinal product” that is administered (Electronic Medicines Compendium UK, 2018). Our hydrogels are created using microliters of the diluents. As an example, 30 microliters of PA mixed with 90 microliters of blood can create 5 mm diameter hydrogels. The volumes needed to create the materials are below the recommended dosage of these buffers for clinical use, therefore studies on the effect of these buffers in peptide amphiphiles and their ability to create hydrogels are relevant for future clinical applications.

Circular dichroism analysis showed that the β-sheet conformation of the PA is not affected by these different buffers (Figure 4.9 A-C). The CD spectra of PA-K_3 in Saline solution and Ringer’s buffer shows a stronger beta-sheet signal compared to HEPES buffer, indicating that the beta-sheet content and fibre length might be enhanced in these buffers. These results are encouraging as both of these solutions are routinely used in hospitals and considered as safe and cost- effective for clinical use according to the WHO Model List of Essential Medicines (World Health Organisation, 2017).

Results show hydrogel stiffness in the range of 3 to 4 kPa of hydrogels created with HEPES, Saline solution and Ringer’s lactate solution (Figure 4.9 D-G). Hydrogels created with HEPES and Ringers Lactate solution presented a similar stiffness. Hydrogels created with Saline solution show an overall decrease in stiffness of around 1 kPa compared to the later.

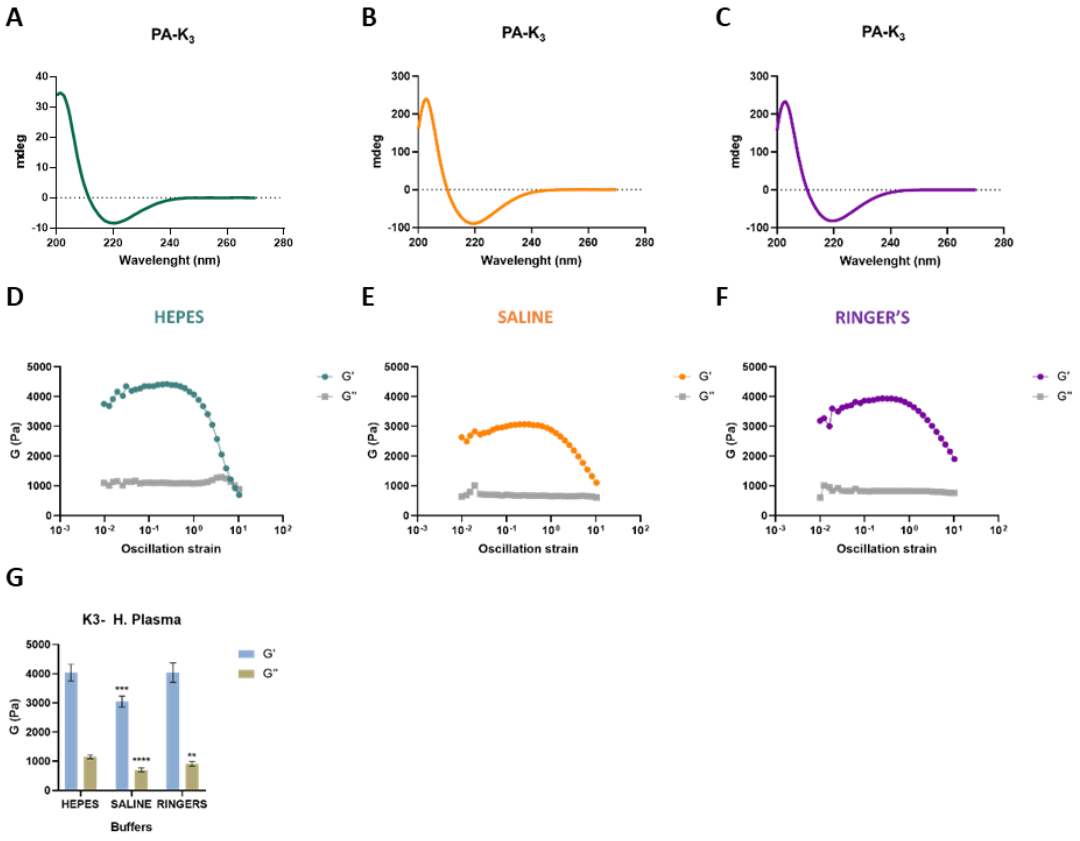

Figure 4.9. Comparison of different buffers used as solvents on PA secondary structure and mechanical properties of PA-K_3. A-C) CD signal shows that PA-K_3 maintains the β-sheet structure regardless of the buffer utilised as solvent. D-F) Rheology measurements of PA-K_3 viscoelastic properties in different buffers. G) The comparison of the viscoelastic properties of the hydrogels was done via ANOVA multiple comparisons test.

4.1.4 PA design of bioinspired sequences

After initial testing of different PA materials (positively and negatively charged), it was determined that positively charged materials were able to assemble into hydrogels after contact with blood and derived products.

From these initial observations, new specific sequences were designed with the idea to enhance blood components interaction with peptide amphiphiles and improve materials' mechanical properties. These sequences were designed to have a positive charge with three lysine residues to build on previous results. Additionally, glutamine

residues were incorporated into the sequences. The rational for selecting these particular amino acids is their potential to be cross-linked with human factor XIII enzyme, which is present in blood and plasma.

Human factor XIII is a transglutaminase that has a key role in blood coagulation (Mosesson et al., 2000). Its mechanism of action consists on the crosslinking of *lysine* and *glutamine residues* located in fibrin, which stabilises blood clots and provides them their strength. Factor XIII catalyses the formation of an isopeptide bond between a free amine group in a protein/peptide-bound lysine and the acyl group at the end of the side chain of a protein/peptide-bound glutamine, creating γ-glutamyl-Є-lysyl amide crosslinks (Figure 4.10).

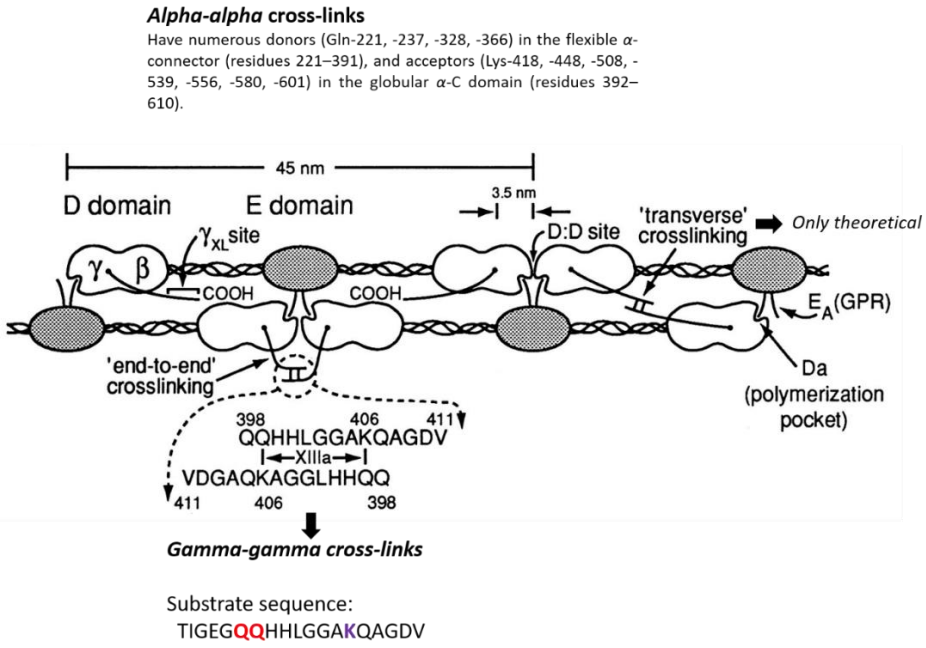

Figure 4.10. In vivo mechanism of crosslinking of fibrin networks. The design of the new PA sequences was inspired by the function of the blood enzyme Human Factor XIII which plays a key role in the blood clotting process. Its main function consists on the crosslinking of lysine (red) and glutamine (purple) residues located in fibrin, which stabilises the blood clot and enhances its strength. Image modified from Mosesson et al., 2000.

As previously mentioned, it is possible to improve PA hydrogels strength using crosslinking agents, however, it has been shown that most of the commonly used chemicals such as Glutaraldehyde and Paraformaldehyde are highly toxic for cells, thus limiting their use for biomaterials. Although other alternatives like genipin have emerged as potential candidates for crosslinking due to their less toxic activity against cells (Inostroza-Brito et al., 2017), our rationale was to incorporate key amino acids in the PA sequence in order to take advantage of a naturally occurring crosslinking mechanism already present in blood.

Our hypothesis was that inter and intra molecular crosslinking would occur due to the presence of these key residues and improve the materials stiffness. A new set of PAs (Table 4.4 A-B) was designed in order to test their interactions and the crosslinking ability of the Factor XIII present in human blood and plasma. These sequences were synthesised and purified by Biomatik company.

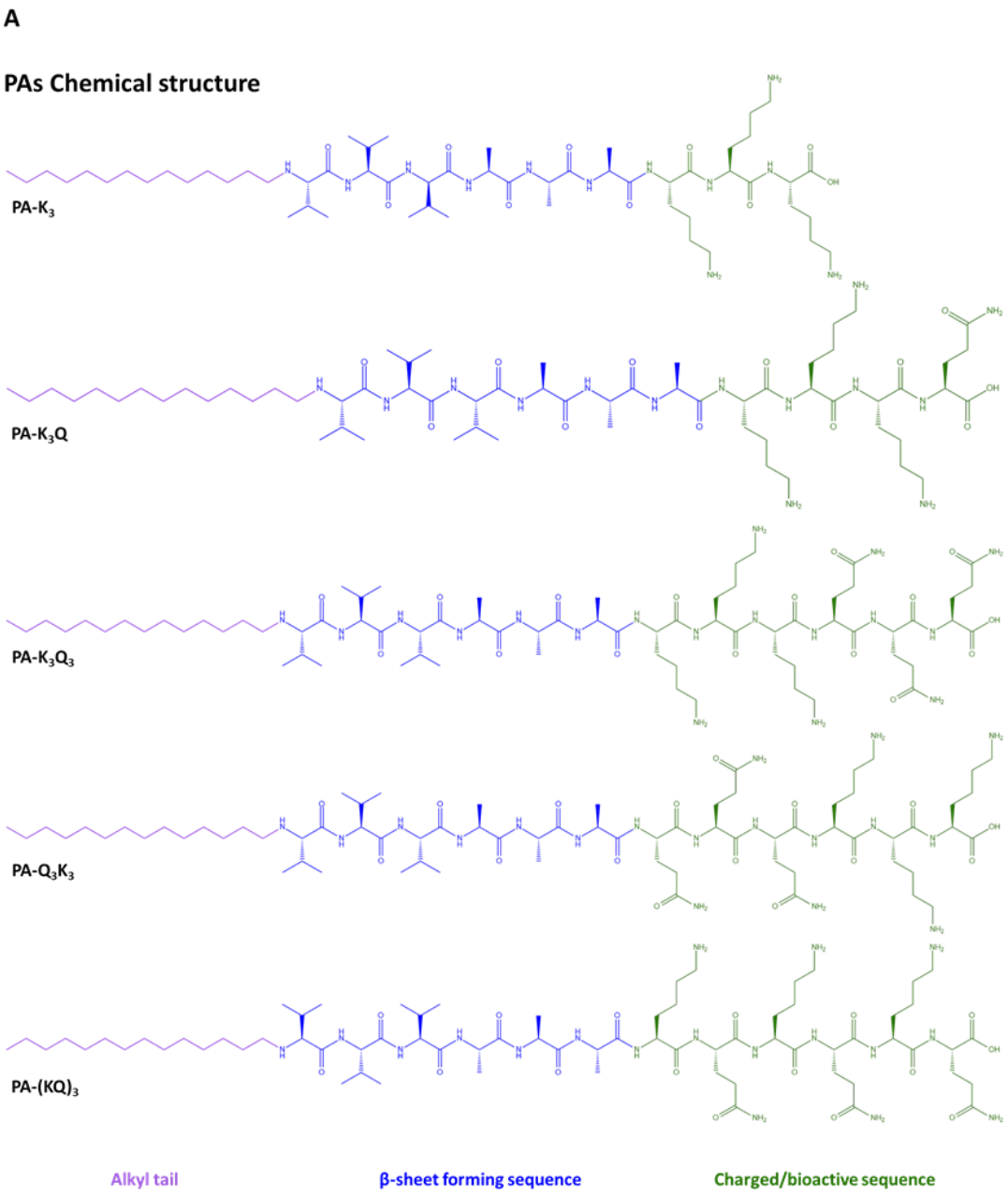

Table 4.4. Peptide amphiphiles designed to interact with blood components. A) Molecular structures of the new set of PAs using Chemdraw software. These peptides have 3 different distinctive regions: the alkyl tail hydrophobic sequence (purple), the β–sheet forming sequence (blue), and the charged or bioactive sequence (green).

B

PAs properties

Peptide Amphiphile Name	Sequence	Molecular weight (kDa)*	pI ł	Purity * (HPLC)
PA-K_3 (control)	$C_{15}H_{31}$CONH-VVVAAAKKK-$CONH_2$	1.15	**10.3**	96.65%
PA-K_3Q	$C_{15}H_{31}$CONH-VVVAAAKKKQ-$CONH_2$	1.27	**10.0**	96.06%
PA-K_3Q_3	$C_{15}H_{31}$CONH-VVVAAAKKKQQQ-$CONH_2$	1.53	**10.0**	96.51%
PA-Q_3K_3	$C_{15}H_{31}$CONH-VVVAAAQQQKKK-$CONH_2$	1.53	**10.0**	95.10%
PA-$(KQ)_3$	$C_{15}H_{31}$CONH-VVVAAAKQKQKQ-$CONH_2$	1.53	**10.0**	97.01%

Table 4.4. Peptide amphiphiles designed to interact with blood components. B) The table summarises the new materials' specific properties including the following: specific sequence, molecular weight (MW), isoelectric point (pI), and purity (%) by HPLC determined by Biomatik company. ł These are theoretical values calculated using Chemdraw software based solely on the chemical structure of the peptides. * Purity was obtained from Biomatik company HPLC analysis.

4.1.4.1 Characterisation of new PA sequences

4.1.4.1.1 Solubility assays

New PA sequences were tested for solubility in different biologically relevant buffers selected previously (Table 4.5). Briefly, PAs were prepared by dissolving them to a concentration of 10mg/ml and were put on sonication for 20 minutes.

From the sequences tested, PA-K_3Q, PA K_3Q_3 and PA-Q_3K_3 were easily solubilised in HEPES, Saline and Ringers Lactate solution as well as in water at lower pH (pH 3 and 5). When the peptides pH was adjusted to pH 7 the solutions turned turbid, which is regarded as a sign of aggregation. Sonication time was adjusted to 1 hour to help solubilisation; however, this did not have any visible effect. At pH 9, the peptide

solutions changed to a turbid white colour and some precipitation was observed. The peptides were treated with sonication for an hour but this did not improve the outcome either. These sequences showed a similar behaviour to the control peptide PA-K_3.

The pH testing range selected is below the isoelectric point (pI) of the PAs and therefore confers a net positive charge to the peptides. However, when PAs are in acidic pH, they tend to have a higher positive charge that will proportionally decrease to a net neutral charge (zero) as they approach their respective isoelectric points.

It has been demonstrated that it is imperative for the peptide amphiphiles solubility to keep the amino acids on the hydrophilic segment charged in order to maintain the balance with the hydrophobic core and therefore improve the peptides solubility.

PA-$(KQ)_3$ could not be dissolved in biologically compatible buffers other than water. This peptide showed no solubility in HEPES, Saline and Ringer's solutions and a strong tendency to form aggregates and precipitate in solution. We hypothesise that alternating the charged and neutral residues has had a direct impact on the peptide solubility by decreasing its overall hydrophilicity and affecting its ability to solubilise in buffers. By separating the lysine positive charges, this could have potentially hide these charged residues hence reducing the solubility of the peptide. In addition, secondary structure formation could have also contributed to the poor solubility of the peptide. Peptide and protein solubility software using computational models to predict solubility from the amino acid sequence is currently under development (Chen et al., 2021). This type of programs could become instrumental tools to tackle this issue when creating new synthetic sequences.

	HEPES	Saline Solution	Ringers Lactate Solution	Water	pH
PA-K_3					3
					5
					7
					9
PA-K_3Q					3
					5
					7
					9
PA-K_3Q_3					3
					5
					7
					9
PA-Q_3K_3					3
					5
					7
					9
PA-$(KQ)_3$					3
					5
					7
					9

Soluble
(fully dissolved, clear solution)

Not fully dissolved
(turbid solution)

Not soluble
(Not dissolved, precipitation)

Table 4.5. Solubility of new PA sequences containing lysine and glutamine residues. This table summarises the solubility results in a pH range of 3 to 9. Most of the peptides are soluble in the water and different buffers at pH 5 whereas at pH 7 and pH 9 the solubility decreases until they become insoluble. These results are in accordance with their theoretical calculated pI. In the case of PA- $(KQ)_3$, this peptide was only soluble in water but insoluble in the buffers tested.

From this set of studies, solubilisation of the peptides at pH 5 was selected for further analysis.

4.1.4.1.2 Evaluation of the secondary structure

Different buffers were tested to determine their impact in the secondary structure of the newly synthesised PAs (Figure 4.11). PA-K_3 in HEPES buffer was used as a control since it has previously been reported that this sequence presents a β-sheet structure

and a random-coil conformation when using water as a solvent (Inostroza-brito et al., 2015).

PA-Q_3K_3 showed a similar behaviour to PA-K_3 control in all buffers exhibiting a β-sheet structure in HEPES, Saline and Ringer's buffers and a random-coil conformation in water. PA-K_3Q was assayed in HEPES buffer and showed a β-sheet conformation very similar to PA-K_3 (Figure 4.11 A). This peptide could not be assayed in other buffers due to technical issues with equipment.

PA-$(KQ)_3$ spectrum was measured only in water due to solubility issues and revealed a weak signal resembling β-sheet structure conformation (Figure 4.11 B). On the other hand, although PA-K_3Q_3 was soluble in all buffers, it appeared to have an irregular or disordered structure instead of the signature of the β-sheet structure.

Interestingly, the CD spectra of PA-K_3 and PA-Q_3K_3 in Saline solution and Ringer's buffer show a stronger β-sheet signal compared to HEPES buffer (Figure 4.11 C-D), which may be an indicator of an increase in the organisation of the secondary structure and their β-sheet content in these buffers with different ionic contents. The co-assembly of PAs and blood proteins has been shown to be predominantly driven by the difference in electrostatic charge of these molecules (Section 4.1.2 and 4.1.3.2). However, it has been reported that PA nanofibre formation can also be initiated by ionic solutions (Stendahl et al., 2006). Therefore, the dissociated ions from the salts contained in these buffers may enhance nanofibre formation, thus increasing the network density and hydrogel stiffness. Further analysis is needed to study the impact of these buffers on the hydrogels properties.

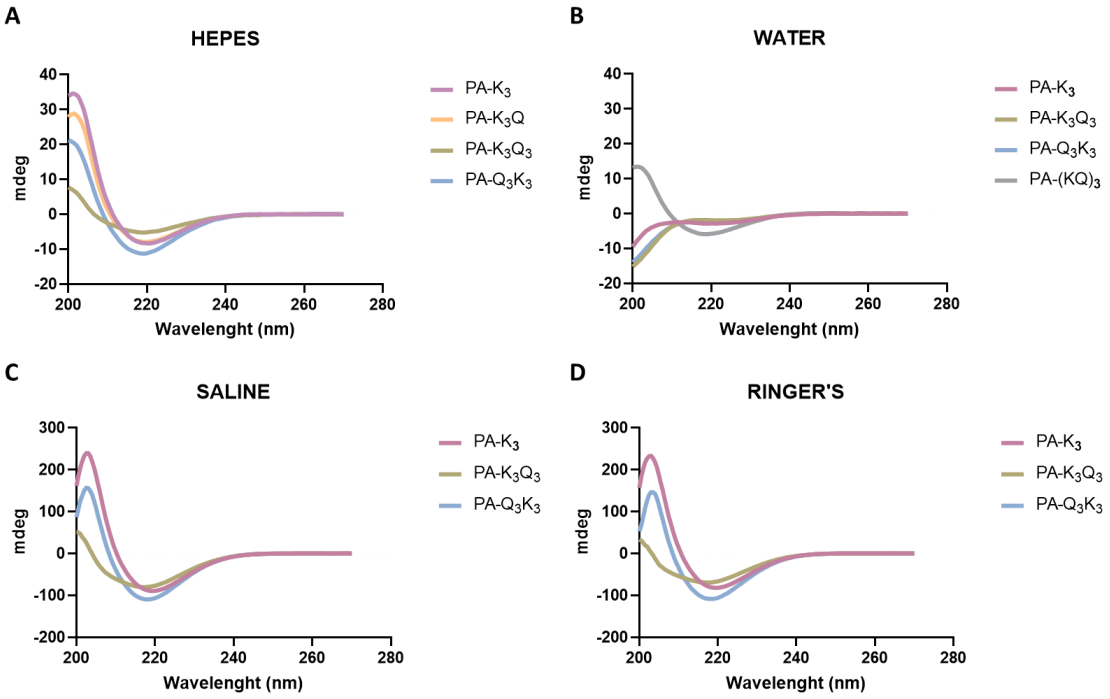

Figure 4.11. CD spectra of newly designed PA sequences in different buffers. PA-K_3 was used as a control for the evaluation of the new sequences as it has a characteristic β-sheet structure in HEPES buffer and a random coil structure in water. These buffers were selected for its clinical relevance. Results showed two of the new peptides (PA-K_3Q and PA-Q_3K_3) maintain their characteristic β–sheet secondary structure in HEPES and other buffers whereas some sequences have lost their signature structure (PA-K_3Q_3 and PA-$(KQ)_3$).

Previous studies have shown the formation of stable β-sheet secondary structures is essential for the peptides self-assembly (Löwik et al, 2004). Although the β-sheet secondary structure of PA-K_3 has been previously identified and characterised (Behanna et al., 2005), the inclusion of glutamine residues in the new PA sequences and their spatial location has had an impact in the molecular arrangement of some of the sequences (PA-K_3Q_3) and could consequently affect the hydrogel formation process, the stability of the assembly and the mechanical properties.

4.1.4.1.3 Determination of the electrokinetic potential

The materials synthesised zeta potential is above 30mV in all cases when dissolved in water and adjusted to pH 5 (Table 4.6), which has been regarded as an indicator of monodispersity and good colloidal stability of the particles (Gupta et al., 2018; Gumustas et al., 2017). Moreover, it has been demonstrated that strong particle charges, either positive or negative, are a good indicator of longer shelf life which represents an important quality of our materials for their translation to medical applications (Pate et al., 2022).

However, in the biological setting, particles with highly positive charges can interact more favourably with membranes and cause toxicity. Therefore, it is important to evaluate different aspects of the charges distribution in the PAs and their secondary structure in order to ensure biocompatibility.

Peptide Amphiphile Name	Molecular weight (kDa)	pI	pH	Concentration	Dispersant	ζ (mV)
PA-K_3 (control)	1.15	10.3	5	0.1mg/ml	Water	52.23±1.18
PA-K_3Q	1.27	10.0	5	0.1mg/ml	Water	55.68±2.29
PA-K_3Q_3	1.53	10.0	5	0.1mg/ml	Water	59.13±3.26
PA-Q_3K_3	1.53	10.0	5	0.1mg/ml	Water	65.46±3.70
PA-$(KQ)_3$	1.53	10.0	5	0.1mg/ml	Water	51.6±0.35

Table 4.6. Zeta potential of new PA sequences. All sequences present a highly positive zeta potential.

4.1.4.1.4 Hydrogel formation

For this study, the materials were dissolved in HEPES buffer and adjusted to pH 5. Hydrogel formation was studied using Model 1 (Section 4.1.2). Five microliters of each PA was injected into the different bio-fluids and incubated for a period of 24 hours before washing and testing qualitatively for gel formation and stiffness (Table 4.7).

PA	Whole Blood	Platelet rich plasma (PRP)	Plasma	Serum	Albumin (HSA)	Simulated body fluid (SBF)
PA-K_3						
PA-K_3Q						
PA-K_3Q_3						
PA-Q_3K_3						
PA-$(KQ)_3$*						

Strong
Medium
Weak
Aggregate
No gel

Table 4.7. Hydrogel formation with new PA sequences. Results showed that PA-K_3Q hydrogels present similar strength compared to PA-K_3. The rest of the peptides produced weaker hydrogels (PA-Q_3K_3) or aggregates (PA-K_3Q_3 and PA-$(KQ)_3$). All peptides were dissolved in HEPES buffer for this study. *PA-$(KQ)_3$ was dissolved in water.

PA-K_3Q presented a similar behaviour than PA-K_3. Initial macroscopic observation indicated the formation of robust hydrogels with blood fractions as well as good solubility in biocompatible buffers. This PA was selected for further testing.

PA-Q_3K_3 was able to form a weak hydrogel in all of the bio-fluids tested. The resulting hydrogels were able to maintain a shape after washing and handling.

Although PA-K_3Q_3 was dissolved in different bio-friendly buffers, CD results did not show a clearly defined β-sheet structure, indicating the peptide has an ill-defined secondary structure. Moreover, this peptide was only able to form very brittle

aggregates that broke down when handling. Therefore, this sequence was also excluded from further testing. A similar behaviour was observed with PA-$(KQ)_3$ which was not able to assemble into a hydrogel but instead formed aggregates. In addition, this peptide could not be dissolved in biologically compatible buffers other than water. Due to the lack of biocompatibility of this solvent with blood cells and the inability of this peptide to form hydrogels, this sequence did not undergo further testing either.

4.1.4.1.5 Mechanical properties

To characterise the mechanical properties of the new PA sequences (K_3Q and Q_3K_3), hydrogels were created on larger sizes, scaling up the initial volumes 6 times. For this, 30µl of PA was injected into 90µl of blood and gels were incubated and tested over a period of 24 hours. PA-K_3 was used as a control for the experiment and this set of hydrogels was create using the same donors' blood sample to avoid variability in terms of blood cell and protein content.

After gel incubation, PA-Q_3K_3 hydrogels were too brittle and broke down when moved. Due to this recurrent issue, rheological measurements were not acquired. Nevertheless, PA-K_3 and PA-K_3Q hydrogels mechanical properties were followed up during this study.

Gels were monitored over a period of 24 hours. PA-K_3 showed an initial storage modulus (G') of 1654.8 ± 134.5 Pa (Figure 4.12 A) whereas PA-K_3Q had an initial stiffness of 2329.02 ± 435.1 Pa (Figure 4.12 B) at 3 hours post incubation. The stiffness

of the hydrogels did not change significantly over time. However, a significant difference in stiffness between the different PAs was observed.

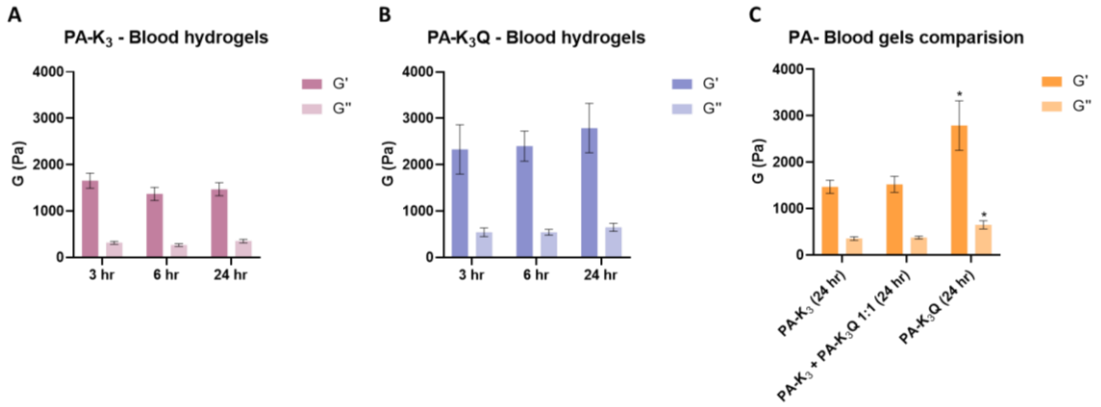

Figure 4.12. Mechanical properties of PA-Blood hydrogels. A) PA-K3 – Blood hydrogels stiffness monitored for 24 hours showed no significant difference over time. B) PA-K_3Q – Blood hydrogels showed no significant difference over time. C) Comparison of the effect on stiffness between blood and PA-K_3, PA-K_3Q and a mixture of them at 24 hours.

To determine whether the higher stiffness observed in PA-K_3Q hydrogels could be a result of the addition of the glutamine residue and potential crosslinking, PA-K_3 and PA-K_3Q were mixed at a ratio of 1:1 (v: v) and rheology measurements were carried out. After 24 hours of incubation time (Figure 4.12 C), results showed that the mixture of PAs had similar stiffness to PA-K_3 alone, thus confirming that the addition of a glutamine residue had improved the stiffness of the material. This change in stiffness suggests that mixing these PAs in different ratios could be used to regulate the hydrogels' stiffness, thus highlighting the potential to modulate their mechanical properties and tailor them to different applications. In addition, it has been reported that PA sequence has a key role in hydrogel stiffness, which supports the observed results (Pashuck et al., 2010). More specific analysis need to be done in order to

determine if PA-K_3Q stiffness is also being regulated by the Factor XIII enzyme crosslinking ability of the residues.

Previous research has shown that PA based hydrogels are relatively soft materials with stiffness on the range of Pa to kPa (Radvar & Azevedo, 2009), depending on their components and mechanism of assembly. PA hydrogels, formed in the presence of electrolytes, have a reported stiffness in the range of 20–80 kPa. In contrast, co-assembly hydrogels developed by Hedegaard et al. (2019), using PAs and keratin reported a stiffness in the range of 0.3-0.9 kPa. Other studies using PAs and hyaluronic acid have reported a stiffness of 9 kPa (Ferreira et al., 2013). This suggests the hydrogels developed on this research have enhanced stiffness properties compared to those assembled with other proteins, but are softer compared to hydrogels assembled with ionic solutions or polymers.

4.1.4.1.6 Selection of new bioinspired sequences: PA-K_3Q and PA-Q_3K_3

After evaluation of different parameters including solubility, electrokinetic potential, secondary structure, hydrogelation capability and mechanical properties, it was demonstrated that PA-K_3Q_3 and PA-$(KQ)_3$ were not viable candidates to undergo further testing due to issues with solubility and hydrogelation.

PA-K_3Q and PA-Q_3K_3 were identified as potential candidates for biological studies. PA-K_3Q presented a similar behaviour to PA-K_3 in most of their properties, but showed a higher stiffness compared to PA-K_3Q. On the other hand, PA-Q_3K_3 also exhibited similar properties to PA-K_3 with the exception of a higher positive charge and lower stiffness (not quantified). Given that cells can sense very small changes in stiffness,

and stiffness has high variation between organs and tissues (0.5 to 20,000 kPa) (Handorf et al., 2015), PA-K_3Q and PA-Q_3K_3 were selected for further testing.

4.2 Discussion and conclusion

This study explored the potential of PAs to assemble with blood and different blood fractions to create complex bioinspired materials that take advantage of the different properties of proteins present in blood.

To the best of our knowledge, this study demonstrated for the first time that positively charged PAs can co-assemble with blood or blood derived fractions to create hydrogels. The co-assembly process was studied by dissecting key components that contribute to the hydrogels' assembly. Positively charged peptides were able to form hydrogels by interacting with the negatively charged proteins in blood. This was demonstrated by the ability of PAs to form gels with the model proteins albumin or fibrinogen, which are abundant in blood and have a negative charge. By using other blood fractions like plasma and serum, it was also determined that blood cells and blood clotting factors are not essential to trigger the initial process of co-assembly and hydrogelation, however, they do contribute to their mechanical properties by forming a double network that strengthen the gels, as observed in SEM images of blood and PRP based hydrogels (Figure 4.2 and Table 4.2). In summary, these results confirmed the hypothesis that PAs can co-assemble with blood and it is inferred that the co-assembly process is driven by hydrophobic and electrostatic forces as well as by the interaction with blood cells.

From the tested peptides, PA-K_3 derived hydrogels were qualitatively more robust, thus validating the choice of this peptide as the main study molecule for further studies on co-assembly and mechanical properties.

After building up knowledge on how PA-K_3 interacts with blood, new sequences were designed in order to take advantage of potential interactions with blood proteins as well as improving their mechanical properties. Peptides with lysine and glutamine residues were designed. A set of tests including solubility, determination of secondary structure and charge, hydrogel formation capacity and mechanical properties revealed that the peptides' sequence influenced all of these properties. We hypothesise that the order of the charged and neutral residues has a direct and clear impact in the aforementioned peptides' properties. However, the exact reasons behind these changes were not investigated within the scope of this study.

In terms of use of clinically relevant buffers, it was demonstrated that peptides can be dissolved in Saline and Ringers Lactate solution, both of which are approved for use in patients by the WHO Model List of Essential Medicines. Moreover, our hydrogels are created by using microliters of PA solution. As an example, the hydrogels created for this study with 30ul of PA (dissolved in buffer) mixed with the 90ul of blood can create a 5 mm diameter hydrogel. Extrapolating these numbers, we assume using 300ul of peptide solution could yield gels in the range of 5 cm diameter. The volume of buffer required to achieve this is below the recommended doses of the buffers for clinical use and therefore could be regarded as safe for the patients. Further scale up studies need to be done in in vivo models to prove this theory and

the evaluation of other parameters like immune response and toxicity are needed in order to determine their safety for clinical use.

In summary, the work done in this chapter lead to the identification and characterisation of two new peptide amphiphiles sequences for further in vitro testing: K_3Q and Q_3K_3.

Chapter 5.

Tissue engineering applications

This chapter describes the evaluation of PA – Blood hydrogels suitability as candidates for tissue engineering and regenerative medicine applications. This chapter aims to provide insights into relevant biological interactions between peptide amphiphiles and blood components, the biocompatibility of the co-assembled materials and their effect on cell health and behaviour.

5.1 Biological interactions of blood components with peptide amphiphiles

The blood clot is a remarkably rich and functional environment that re-establishes homeostasis after injury and regenerates damaged tissues. The creation of biomaterials that emulate the structural complexity and functionality of this regenerative environment has not been achieved yet.

Our aim is to develop personalised materials that take advantage of key molecules and incorporate them into biomaterials to enhance their bioactive properties in order to tackle major regenerative challenges.

The studies presented in this chapter were used to address the third thesis objective (Section 2.6.3): Evaluate the biocompatibility of the new peptide amphiphiles and their potential to be used for tissue engineering and regenerative medicine applications.

The experiments conducted were divided in 3 main stages. First, the characterisation of relevant biological interactions between peptide amphiphiles and blood components. Second, to evaluate the biocompatibility of peptide amphiphiles and blood by determining their haemolytic potential, hydrogel degradation rate and protein release patterns. Third, to evaluate cell response to the biomaterials by in vitro testing of different cell types relevant to the wound healing process. For this, three different cell lines were selected: fibroblasts (NIH-3T3), endothelial cells (HUVECs) and mesenchymal stem cells (hMSCs).

5.1.1 The blood clotting process

A blood clot is the first step towards the process of regeneration of tissues with remarkable efficiency. Upon injury, blood creates a clot, which triggers and regulates inflammation, immunomodulation, cell recruitment, vascularization, and ultimately regeneration. The initial phase of this process is considered to be critical and there is emerging body of evidence highlighting the importance of a blood clot.

The blood clot is a highly dynamic environment that serves as a defence mechanism against pathogens, a regulator of biological processes, a medium to transport nutrients and waste, a structural support matrix, and a resource of key molecular and cellular components. Platelets are key components found on this environment, not only playing a direct role in its formation, but also regulating other key processes in inflammation, infection, and the healing response.

Activated platelets secrete a myriad of pro-inflammatory and immunomodulatory cytokines such as VEGF, PDGF, and TGF-β (Schmidt et al., 2012; Butterfield et al., 2006). The blood clot also establishes a hypoxic environment that supports pluripotency and stimulates leukocytes to release growth factors such as VEGF and PDGF (Shiu et al, 2018). This environment also stimulates monocytes to differentiate into macrophages, which secrete a variety of cytokines and growth factors such as TNF-α, IL-1, IL-4, IL-6, IL-13, TNF-β, PDGF, VEGF, and TGF-β (Marsell et al., 2011; Anderson et al., 2008) These factors then promote vascularization, cell recruitment, and granulation.

In addition, erythrocytes, which account for 95% of all the cell content of the blood clot, play a role in coagulation activation, clot formation and resistance to fibrinolysis, and clot porosity to facilitate cell migration (Litvinov et al., 2017; Carr et al., 1987). Altogether, the composition and the processes dictated by the blood clot play a key role in wound healing and the regenerative process. Furthermore, it is known that minor molecular and cellular changes have a significant effect on the blood clot's regenerative functionality (Hoff et al., 2016).

5.1.1.1 PAs trigger the blood clotting process

As previously demonstrated, the addition of PAs to blood and derived products appears to trigger the coagulation process (Section 4.1.3.1). In order to identify some of the key components of interest present in blood clots and PRP clots, SEM and immunofluorescence microscopy examination of hydrogel samples create with PA-K_3 was carried out. Platelets were the focus of these experiments due to their role in the blood clotting process and as a main source of growth factor secretion.

To determine initial interactions of blood cells with PAs, PA-K_3 – PRP and PA-K_3 – Blood samples were incubated for 30 minutes before washing and fixing with paraformaldehyde. For the determination of their interaction at a later stage, samples were incubated for 24 hours before washing and fixing with paraformaldehyde.

The main steps on platelet activation in vivo are comprised by: 1) platelet circulation in blood, 2) activation of platelets and binding to fibrin, 3) platelet spreading through the fibrin network, 4) blood clot contraction and strengthening (Figure 5.1 A). In PA-

K_3 – PRP samples incubated for a short period of time, platelet activation in different steps was observed: platelets attached to the hydrogel (Figure 5.1 B yellow arrows) and consecutive platelets morphology change and spreading to a star shaped form (Figure 5.1 B red arrows). In addition, PA-K_3 – PRP samples incubate for 24 hours showed evidence that platelets collapsed the fibrin network which is an indicator of clot contraction (Figure 5.1 B magenta arrows) (Kim et al., 2017; Brown et al., 2014)

PA-K_3 – Blood hydrogels incubated for a short period of time showed a variety of cells attached to the PA network (Figure 5.1 C, blue arrows) and were very brittle compared to gels created with PRP. Samples incubated for 24 hours also presented indications of clot contraction (5.1 C pink arrows), although these were not as apparent as the ones present in PRP hydrogels.

Immunofluorescence staining was performed in samples incubated for 24 hours. The platelet marker P-selectin (AK-6) marker is found inside the cytoplasm of platelets contained in α–granules when platelets are inactive and it translocates to the platelets membrane when they get activated (Schewertz et al., 2009; Vinik et al., 2001), and activated platelets can be found attached to the blood clot fibrin network. P-selectin (green) was localised on platelet membranes, which confirms platelet presence in the samples and their activated state (Figure 5.1 D-E). The fibrin staining (red) was used to confirm fibrin network formation in hydrogels.

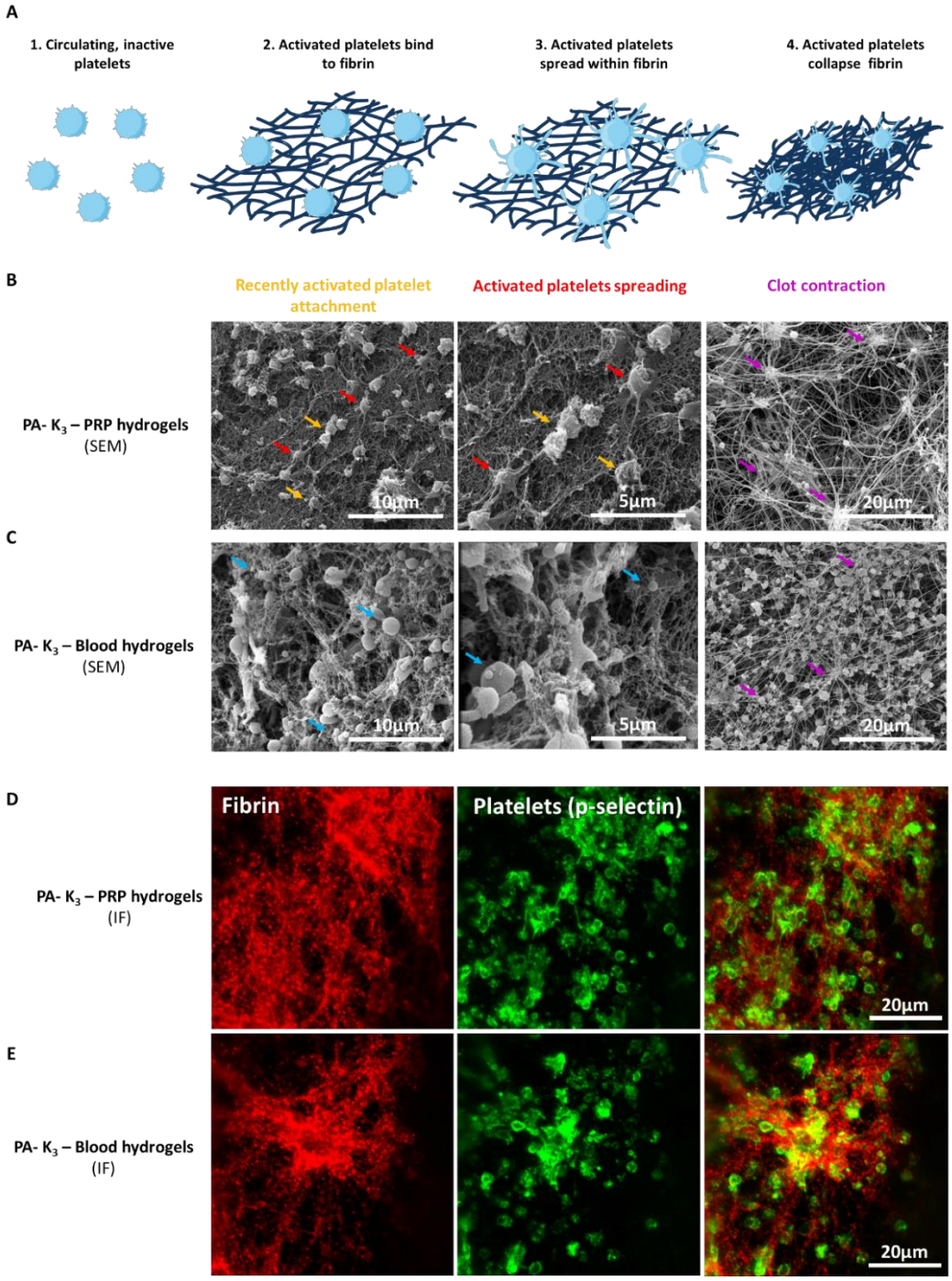

Figure 5.1. PAs trigger the blood clotting process. A) Diagram of platelet activation steps (adapted and modified from Brown et al. 2014), B) SEM microscopy showing PA-K_3 – PRP hydrogels with recently activated platelets (yellow arrows) and showing a round shape and activated platelets with star shape morphology (red arrows), as well as contraction points (pink arrows). C) SEM microscopy of PA-K_3 – Blood hydrogels with different types of blood cells (blue arrows) and clot contraction points (pink arrows), D) PA-K_3 PRP and E) PA-K_3 – Blood immunofluorescence microscopy of stained platelets with P-selectin (green) and fibrin (red) show the different morphology between activated platelets at different stages.

An additional test to confirm blood coagulation was set up by measuring the zeta potential of human plasma and PA-K_3. Zeta potential has been defined as a physical property exhibited by any particle or macromolecule in suspension, or a material's surface. The measurement of this parameter allows to determine the charge at the interface between a solid molecule surface and its liquid medium (Hunter et al., 1998). In this system, PAs are known to have a net positive charge and the proteins in blood are known to have a negative net charge. Solutions that present a charge and zeta potential values > 30 mV tend to be moderately stable whereas zeta potential values > 80-100 present extremely good stability (Riddick, 1968). Rapid coagulation or flocculation is characterised by mildly charged particles, which can be detected when the zeta potential is close to zero (Riddick, 1968).

The peptide amphiphile utilised for the study (PA-K_3) is positively charged whereas the human plasma has an overall negative charge. Fibrinogen and albumin zeta potential were also measured as they are the most abundant proteins in blood, both of which also showed a negative zeta potential, thus confirming the overall negative charge of key proteins involved in the co-assembly process.

After mixing human plasma with PA-K_3, a decrease in the zeta potential of both plasma and PA-K_3 is observed when solutions are mixed, thus indicating the materials trigger the clotting process (Figure 5.2 A-B). This is consistent with SEM microscopy images and immunofluorescence images showing activated platelets and a dense fibrin network co-existing with the PA nano-network.

A

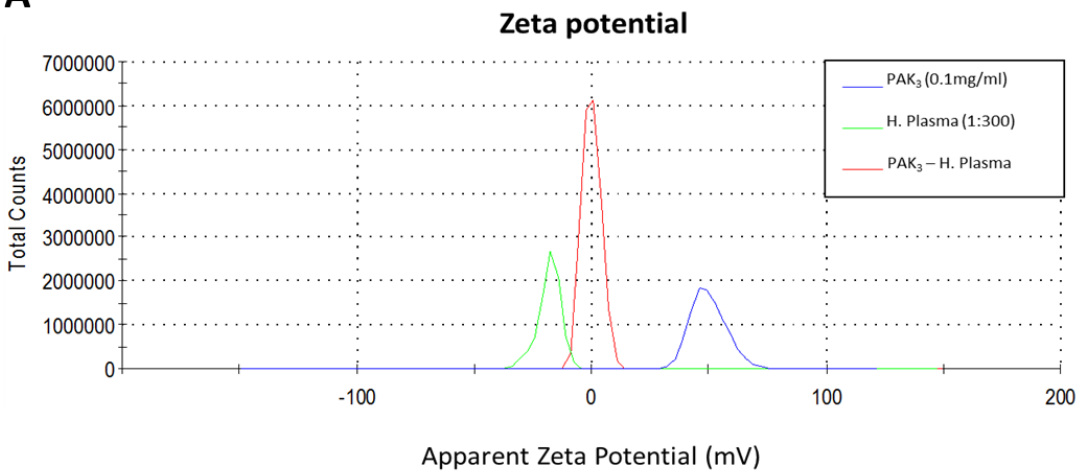

B

Material	MW (kDa) *	pI *	pH ǂ	ζ (mV) ǂ
PA-K_3	1.15	10.3	5	52.23±1.18
Human serum albumin (HSA)	66.50	4.7	7.4	-23.8±0.10
Human fibrinogen (FGEN)	340.00	5.5	7.4	-11.83±0.46
Human plasma	-	-	7.4	-30.06±0.80
PA-K_3 – Human plasma	-	-	-	0±4.00

* Theoretical value. ǂ Experimental value.

Figure 5.2. Zeta potential as an indicator of agglutination and clotting. A) Zeta potential measurements of PA-K_3 (in MilliQ water) and human plasma (in MilliQ water) when combined showed the neutralisation of their individual charges. This is an indicator of particle agglutination and clotting. B) Summary of peptides and proteins tested for the analysis.

5.2 Biocompatibility of PA – Blood hydrogels

Evaluating the biocompatibility of drugs and biomaterials when they come in contact with the human body is highly important in order to determine their potential use in a clinical setting as well as the chances of the treatment's success. Ensuring the safety of biomaterials is of utter importance for their translation into in vivo models and into the clinic.

5.2.1 Haemocompatibility studies

Haemolysis can happen in vivo and in vitro. There are a number of reasons why RBCs lysis occur in the body (e.g. disease, surgical procedures, haemodialysis, blood transfusion, certain therapies or apoptosis and cell renewal). When this happens, there is free haemoglobin (Hb), free heme and ROS species released that can cause inflammation and tissue damage. When this happens, mechanisms to prevent or repair the damage are activated, for example, the scavenger protein haptoglobin (Hp) can bind the haemoglobin, forming a complex. These Hb-Hp complexes are recognised and degraded by macrophages. There are other scavenger proteins that can also bind the free heme such as hemopexin (Hpx) in order to prevent its toxic effects (Dennis et al., 2001). However, if these systems fail, tissue damage and complications can result in negative health outcomes.

Positively charged materials are known to be able to interact with the negatively charged cell membranes and cause toxicity to different degrees. In the case of peptides, depending on their structure, this interaction can cause cell membrane damage to different extents, which could lead to cell death (Newcomb et al., 2014).

The peptides toxicity when interacting with blood was evaluated by testing their haemolytic potential in samples of human whole blood (HWB). For this study, samples of whole blood were injected with the different peptide amphiphile solutions at the concentration used for creating the hydrogels (10mg/ml) and PA and incubated for 1 hour. Samples were then centrifuged to the obtain the plasma

fraction. Haemoglobin concentration was then measured in the plasma samples and compared to a blood plasma control sample.

Control samples of blood plasma without exposure to PAs presented haemoglobin values of 100 ±10.02 mg/dL. Although normal levels in blood plasma are set around 50mg/dL, it is important to note that spontaneous haemolysis in blood samples can happen as a result from red blood cells lysis during the stages of sample collection, transport and routine handling of the blood sample (Heireman et al., 2017). Complete blood sample lysis can present values above 500mg/dL, therefore it was determined that the blood sample quality was acceptable to undergo further testing.

After incubation, PA-K_3 and PA-Q_3K_3 peptides did not significantly trigger haemolysis compared to the blood plasma control when they came in contact with the peptide materials. PA-Q_3K_3 presented a significantly higher value of haemoglobin concentration (Figure 5.3). We hypothesise this might be due to its higher positive charge compared to the other peptides, ζ= 65.46±3.70 (Refer to Section 4.1.4.1.3). PA-Q_3K_3 hydrogels have also shown to be softer materials compared with hydrogels formed with PA-K_3 and PA-K_3Q. This might be a consequence of blood cells damage when they come in contact with this PA which could be affecting the dynamics of the co-assembly process. Further studies are needed to determine the extent of blood cell damage and its effect on hydrogels mechanical properties.

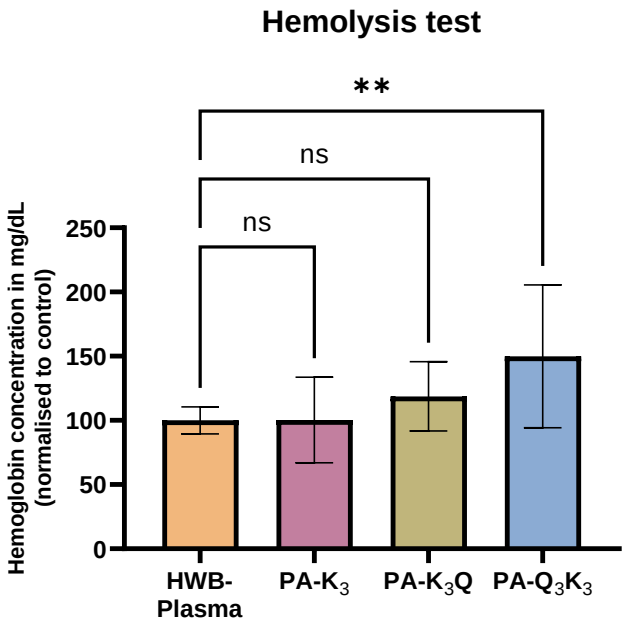

Figure 5.3. Haemocompatibility of biomaterials. A haemolysis test was performed by measuring the haemoglobin content in plasma (mg/dL) after blood samples incubation with peptide amphiphiles. Results showed that PA-K_3 an PA-K_3Q did not cause haemolysis when in contact with blood whereas PA-Q_3K_3 did show a significant increase compared to the plasma control (Statistical significance relative to human whole blood plasma control (HWB-Plasma); ** $p < 0.05$).

In terms of biocompatibility, hydrogel formation is triggered within seconds of the peptide and bio-fluids coming into contact and this interaction appears to neutralise the charges of the hydrogels as demonstrated by the zeta potential study before (Refer to Section 4.1.1.1). Therefore, it was hypothesised that after hydrogel formation the gels would be innocuous for further in vitro studies.

5.2.2 Degradation studies

One of the major challenges for the use of peptide based materials in the clinic is controlling their degradation rate in biological settings as proteolytic enzymes are abundant in biological fluids and triggered during different processes (López-Otín et

al., 2008). For regenerative medicine applications, an ideal scenario is having a temporary scaffold that helps regeneration but can eventually be substituted by the regenerated native tissue.

In addition, the ability of cells to interact and modify the temporary scaffold is crucial to trigger cell proliferation, migration and differentiation, essential cell activities to achieve tissue repair (Jun et al., 2005).

Peptide based hydrogels have different patterns of degradation that can vary from days to months, depending on the chemical composition and mechanical properties of the building blocks (Azevedo et al., 2004). For example, a peptide amphiphile and protein composite system shows a slow degradation rate of 3 months (Hedegaard et al., 2020) whereas a peptide amphiphile combined with hyaluronic acid and laponite is degraded in 50 days (Okesola et al.,2020). Previous research has also showed that peptide based hydrogels are highly susceptible to enzymatic degradation (Stupp et al., 2010).

The stability of the PA – Blood hydrogels was evaluated by using 2 different approaches: a) degradation in HEPES buffer and b) degradation using plasmin, a protease that degrades blood clots in nature by cleavage of lysine and arginine bound amino acid residues (Castellino et al., 2013).

PA – Blood hydrogels were relatively stable for 21 days and showed a similar degradation rate with a final mass loss of around 25% for both hydrogels without enzymatic treatment. When plasmin was added to the hydrogels, the hydrogels degradation rate was accelerated. PA-K_3 – Blood gels were fully degraded in 9 days

whereas PA-K_3Q – Blood gels were degraded within 7 days (Figure 5.4 B). Although in vivo settings would have a variation in enzymatic concentration and timing of enzymatic activity during the wound healing process, we hypothesise this can be regarded as a clear indication of the potential of these materials to degrade and undergo remodelling by cells as the wound healing process progresses.

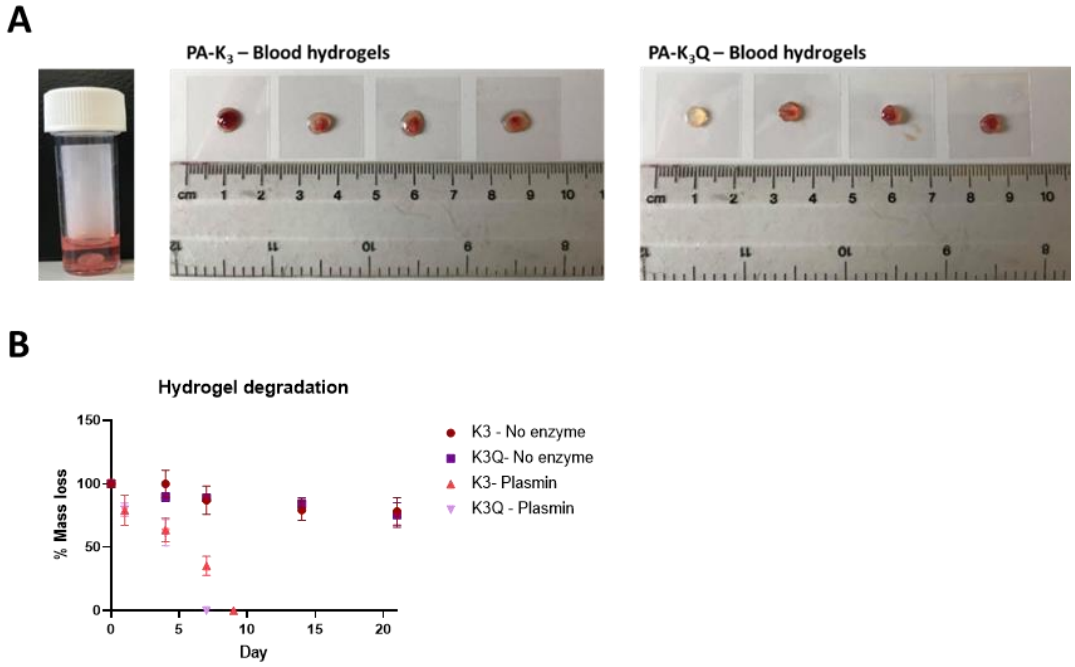

Figure 5.4. Degradation of PA – Blood hydrogels. A) Macroscopic images of PA-K_3 and PA-K_3Q – Blood hydrogels before treatment. B) Degradation of Blood hydrogels in HEPES buffer with and without enzymatic treatment with plasmin. The hydrogels degradation patterns changed in the presence or absence of the enzyme. In the absence of plasmin, hydrogels presented a final mass loss of around 25% at 21 days. Complete degradation of the hydrogels was observed at 7-9 days in the presence of plasmin.

Depending on the wound type, the timeline for the main stages of healing is (Uskoković et al., 2016):

a) Haemostasis, inflammation and cell migration (0-3 days)

b) Cell proliferation, ECM synthesis, angiogenesis (2-11 days)

c) Remodelling, contraction, wound closure (9 days- months)

By comparing the wound healing stages to the degradation rate we have observed when using plasmin, it is hypothesised that immune cells may be able to infiltrate the gel and remodelling by fibroblasts and other cell types could be possible. Further testing on in-vivo models need to be done to prove this hypothesis.

5.2.3 Protein release studies

One of the main key challenges of biomedical materials is in vivo protein delivery of key components to target sites. Peptide hydrogels have been created in two different approaches: a) Traditional hydrogels with non-specific binding of proteins and protein release mainly through diffusion, and b) affinity hydrogels that can retain and sustainably release specific proteins based mainly on diffusion and binding reaction (Koutsopoulos et al., 2009; Abune et al., 2021). Our hydrogels belong to the first category as the goal of this system is to incorporate different molecules and cells to help the wound healing process.

Total protein release from the hydrogels was measured to evaluate potential differences in hydrogels created with PA-K_3 and PA-K_3Q. For this, PA-Blood hydrogels were incubated in PBS 1X buffer and the supernatant was collected at 1, 4 and 7 days. Protein quantitation was done using the Bradford test. Three different aliquots of blood from the same blood donor sample were evaluated.

Results showed that there was a burst release of proteins on Day 1 for both PA-K_3 and PA-K_3Q hydrogels. Although the amount of protein release varied between

different hydrogels, it was possible to observe a pattern where PA-K_3Q hydrogels released more proteins than gels created with PA-K_3 over a period of 7 days (Figure 5.5).

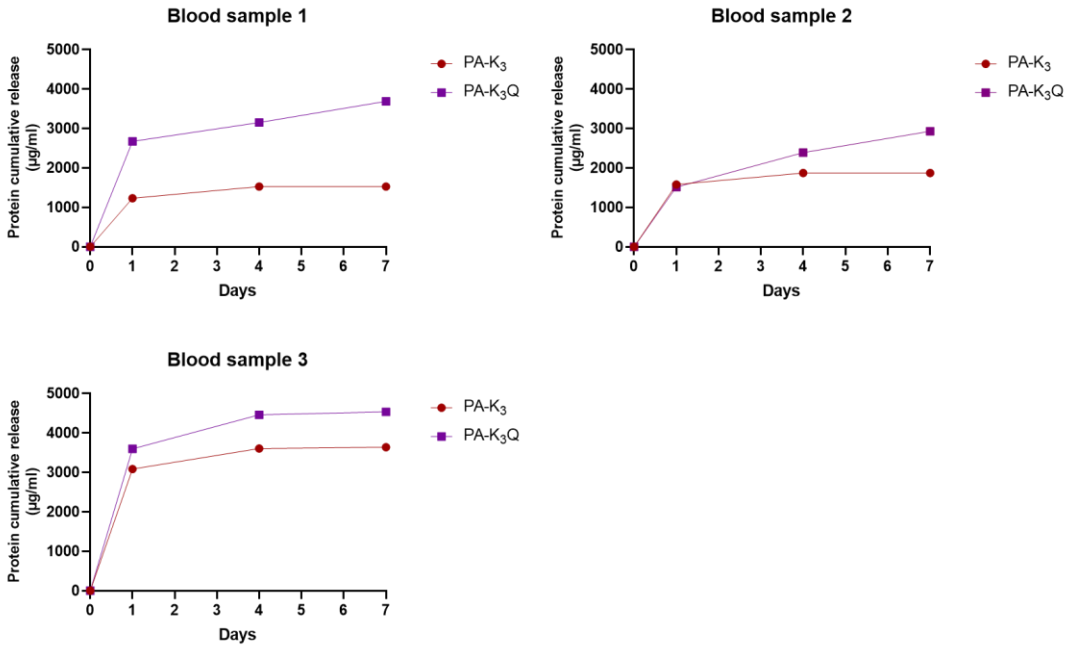

Figure 5.5. Protein release from PA-blood hydrogels. Total protein release from hydrogels was measured on supernatant fractions obtained on Day 1, 4, and 7. The study showed that PA-K_3Q – Blood hydrogels release higher amounts of protein compared to PA-K_3 – Blood.

It is important to note that the system created by using peptide amphiphiles and blood is highly complex and protein release is not a straight forward process as it is dependent on different sources:

a) Protein release of non-specific blood proteins bound to the materials (e.g. albumin, globulins)
b) Protein release of specific proteins from cells attached to the materials (e.g. growth factors and cytokines)
c) Protein release from the materials fibres degradation (e.g. fibrin and PA networks)

Therefore, the amount of proteins that bind to the material via non-specific ionic interactions, the amount and type of cells attached to the materials, and the degradation rate of the bio-networks, all have an impact on the total protein release.

5.2.4 Protein identification studies

The Human Protein Atlas project has identified 784 different proteins in blood (Uhlen et al., 2019). Given the complexity of blood, an exploratory study for the identification of blood proteins was carried out using a protein microarray in order to do an initial screening of potential proteins of interest.

Protein samples were evaluated to determine whether specific proteins from blood cells were released from the hydrogels. For this, PA – Blood hydrogels were incubated in PBS 1X buffer and the supernatant was collected every 2 days for a total of 7 days and pooled together. Samples were then incubated in a protein microarray with 42 target proteins. The supernatants from hydrogels were compared to a control blood sample (Figure 5.6 B).

Overall, it was possible to identify the 42 targets in the blood sample control and in the supernatant of the hydrogels samples. Immunomodulatory cytokines involved in the wound healing process like IL-1, IL-4, IL-6 and IL-13, TNF-α and TNF-β were found in the supernatants. In addition, growth factors of interest like EGF, IGF-1, VEGF and PDGF-BB, known to enhance cell proliferation, were detected in both PA-K_3 and PA-K_3Q supernatants.

Interestingly, two proteins, IL-8 and RANTES were found to be the most abundant in the blood sample and the supernatants from the hydrogels. IL-8 is a cytokine secreted

by macrophages and its primary role is to recruit and activate neutrophils to different tissues upon infection, inflammation, ischemia or trauma (Baggiolini et al., 1992). Other roles have been reported including its potential to stimulate cell migration and proliferation in keratinocytes and endothelial cells (Li et al., 2003; Jiang et al., 2011).

RANTES is a chemokine secreted by activated platelets and its main role is the recruitment of leukocytes to inflammation sites and activation of lymphocytes and neutrophils (Appay & Rowland, 2001) and it is involved in pathological inflammatory conditions. The RANTES receptor is also a major target of study for anti-HIV drugs that are based on blocking viral entry (Crawford et al., 2011).

These findings suggest that these materials are highly effective for nonspecific binding of proteins present in blood samples. Although some growth factors found in blood are essential for wound healing, other proteins like inflammatory molecules (e.g. interleukins and chemokines) in high concentrations could extend the inflammation stage and hamper the wound healing process. Further studies are needed in order to characterise the nature of these proteins-materials interactions and the specific binding of molecules of interest.

A

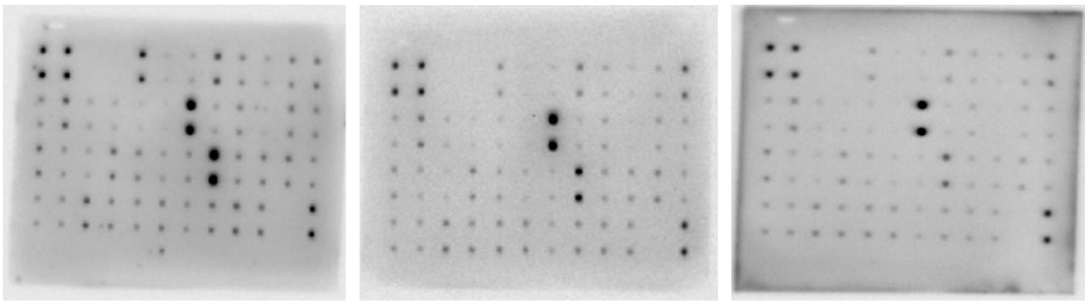

Blood sample | PA-K_3 – Blood hydrogel supernatant sample | PA-K_3Q – Blood hydrogel supernatant sample

B

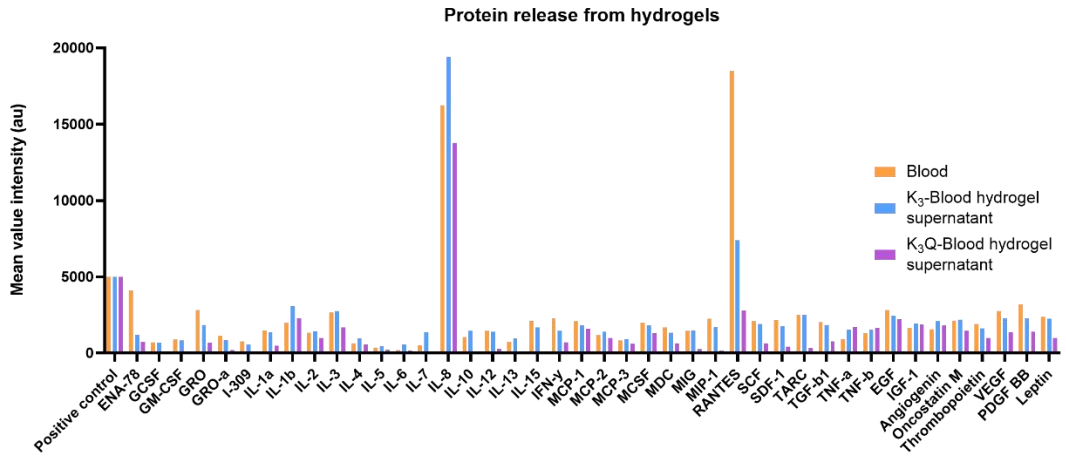

Figure 5.6. Blood proteins identification from supernatants. A) A protein microarray was used to detect proteins of interest in supernatant samples of PA-K_3 (blue) and PA-K_3Q – Blood (magenta) hydrogels collected for a period of 7 days compared to a blood sample (orange). B) Semi quantitation of proteins detected in supernatants showed that proteins were released from the hydrogels after 7 days (Samples were normalised to the positive control).

5.3 Cellular response to PA – Blood scaffolds

Wound healing is a complex process that involves multiple steps where different cell types work together to achieve tissue repair. The use of hydrogels with the ability to entrap and release blood proteins and blood cells offers an exciting possibility to

recreate a microenvironment with enhanced biological properties to support cell growth and organisation.

The potential of these biomaterials for their use in wound healing research was assessed by assessing fibroblasts, endothelial, and mesenchymal stem cell lines response to the biomaterials.

5.3.1 Fibroblasts

Fibroblasts play a key role in the early stages of the wound healing processes. These cells are involved in a) the breakdown of the fibrin clot, b) the creation of new extra cellular matrix (ECM) to support other cells associated with effective wound healing, and c) wound contraction (Bainbridge, 2013).

Fibroblasts (NIH-3T3) were seeded on top of the different PA – Blood scaffolds. Prior to the evaluation of cell behaviour and growth on hydrogels, it is critical to ensure that cells can survive and attach after the seeding on hydrogels and that they are viable for further follow up studies. A Live-Dead staining was used as a method to qualitatively visualise cell attachment, health and distribution in hydrogels. This assay consists of two different dyes, calcein-AM which indicates intracellular esterase activity and stains viable cells in green, and ethidium homodimer-1 which infiltrates the membranes of damaged cells and stains them in red (Ninan et al., 2018). Overall, fibroblast cultures did not seem to be significantly affected by the seeding into hydrogels. However, fibroblasts cultured in PA-Q_3K_3 hydrogels presented a rounded

morphology and appeared clumped together compared to cells cultured in tissue culture plastic (TCP) as a control (Figure 5.7 A).

After confirmation of cell viability, metabolic activity studies were used to monitor cell health and proliferation for 7 days in culture. Generally, metabolic activity tends to be higher in active proliferating cells cultured under optimal conditions and this assay can also indirectly reflect the increase on the number of viable cells or cell growth (Ninan et al., 2018). The Alamar blue test was used for the determination of metabolic activity. This reagent incorporates an oxidation-reduction indicator that both fluoresces and changes colour in response to chemical reduction of the compound in the cell media as a result of cell growth. Thus, continued growth maintains a reduced environment while inhibition of growth maintains an oxidized environment (Geier et al., 1964).

During injury, PDGF and TGF-β play a key role in fibroblast recruitment to the wound site, whereas IGF-1 and EGF have a role in fibroblast proliferation (Schultz et al., 2011). These molecules were detected in the supernatants of PA-K_3 and PA-K_3Q scaffolds (Refer to Section 5.2.4).

A significant increase in metabolic activity was observed in PA-K_3 and PA-K_3Q hydrogels compared to the TCP control on Day 1. We hypothesise this increase in metabolic activity may be related to the burst release of the aforementioned factors. There was no significant difference on the metabolic activity in the PA hydrogels for day 4 and day 7 (Figure 5.7 B).

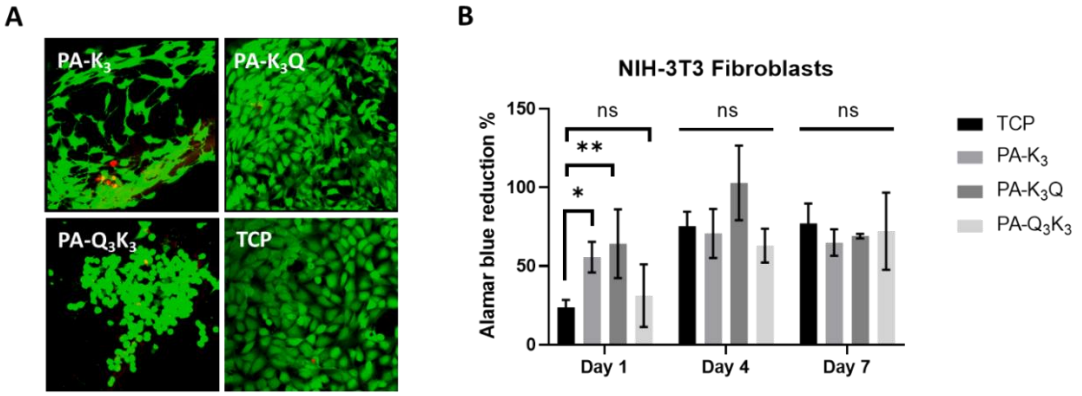

Figure 5.7. Study of the cell response of fibroblasts NIH-3T3 cultured in scaffolds. A) Live-Dead assay showing fibroblasts seeded on top of hydrogels and a TCP control. Results showed good cell viability after seeding (green) with some cell death (red). B) Metabolic activity using the Alamar blue assay to assess cell health and proliferation at Day 1, 4 and 7. An increase in metabolic activity on Day 1 was observed for PA-K_3 and PA-K_3Q –Blood hydrogels (Statistical significance relative to TCP control; * $p < 0.05$, ** $p < 0.001$)

Cells interactions with biomaterials can cause differences in cell behaviour. The surface morphology of a scaffold has been proven to have an effect on the morphology of adherent cells and their behaviour can be modified as a result of these interactions (Papenburg et al., 2017; Wang et al., 2016). To determine the impact of our hydrogels on cell morphology and behaviour, the cytoskeleton of cells was stained with a phalloidin-actin antibody and DAPI to identify cell nuclei.

A layer of cells was observed in PA-K_3 and PA-K_3Q based hydrogels from Day 1, suggesting the scaffolds enhanced cell attachment and growth. PA-Q_3K_3 scaffolds showed a less cell dense surface. Confocal imaging on samples from day 4 and 7 showed multiple layers of cells growing on top of each other in all the hydrogel materials (Figure 5.8).

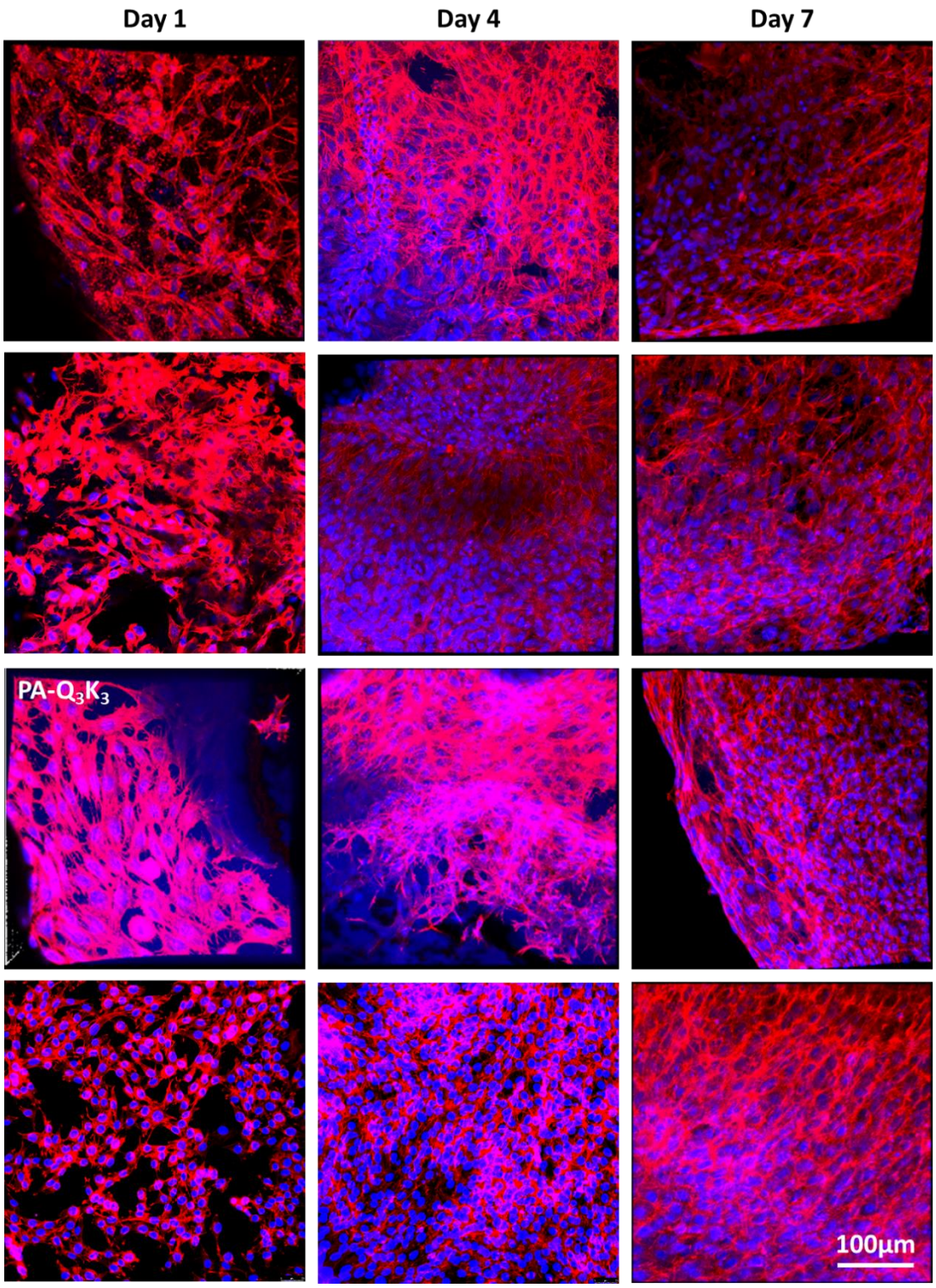

Figure 5.8. Study of cell morphology and proliferation of fibroblasts (NIH-3T3) in scaffolds over 7 days. Immunofluorescence images of NIH-3T3 fibroblasts cultured on PA-Blood hydrogels and TCP at Day 1, 4 and 7, showing their nuclei stained with DAPI (Blue) and cytoskeleton stained with F-actin (Red).

5.3.2 Endothelial cells

Tissue health depends on blood supply and after injury angiogenesis is activated to create new blood vessels. A burst of growth factors activates endothelial cells to start proliferating and repairing the damaged capillaries (Alberts et al., 2002). VEGF, FGF, and TGF-β, are known potent angiogenic factors that play an important role of this process (Li et al., 2003).

From previous experiments using the protein microarrays described before, VEGF and TGF-β were detected in the supernatant of Blood-PA hydrogels. We hypothesised that these factors release from the hydrogels could help promote the growth of human vein endothelial cells (HUVECs).

Similar to the previous cell experiments, Live-Dead staining was used for evaluation of cell viability and spreading when in contact with the hydrogels. Overall, endothelial cells were able to attach in the different materials. Cells seeded in hydrogels initially presented a more rounded morphology compared to cells cultured in TCP (Figure 5.9 A) and some cell death was observed (red).

Metabolic activity studies showed that although the initial attachment and morphology of the cells presented some differences compared to TCP, cells were able to recover and proliferate. On Day 1, cells culture in the PA-K_3Q – Blood hydrogels presented higher metabolic activity indicating that the hydrogel may have stimulated cells due to blood protein release, the other two materials did not show a difference in metabolism. No significant differences on metabolic activity levels were observed from Day 4 onwards (Figure 5.9 B).

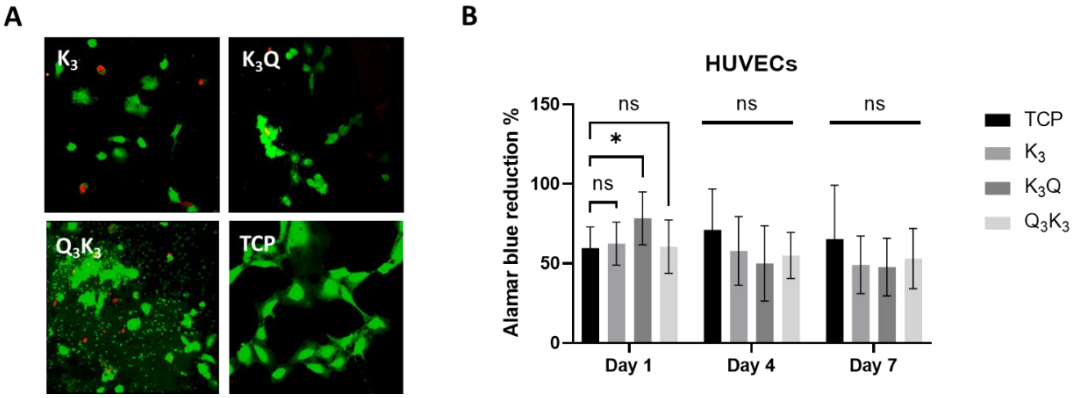

Figure 5.9. Study of the cell response of endothelial cells (HUVECs) cultured in scaffolds. A) Live-Dead assay showing endothelial cells seeded on top of hydrogels and a TCP control. Results showed good cell viability after seeding (green) with some cell death (red). B) Metabolic activity using the Alamar blue assay to assess cell health and proliferation at Day 1, 4 and 7. An increase in metabolic activity on Day 1 was observed for PA-K_3Q –Blood hydrogels (Statistical significance relative to TCP control; * $p < 0.05$)

HUVECs presented a spread morphology on the hydrogels resembling the TCP control from Day 1. An increase in cell population on the scaffolds was also observed from day 1 to day 7. Endothelial cells initially expanded through the scaffolds forming a monolayer (Figure 5.10).

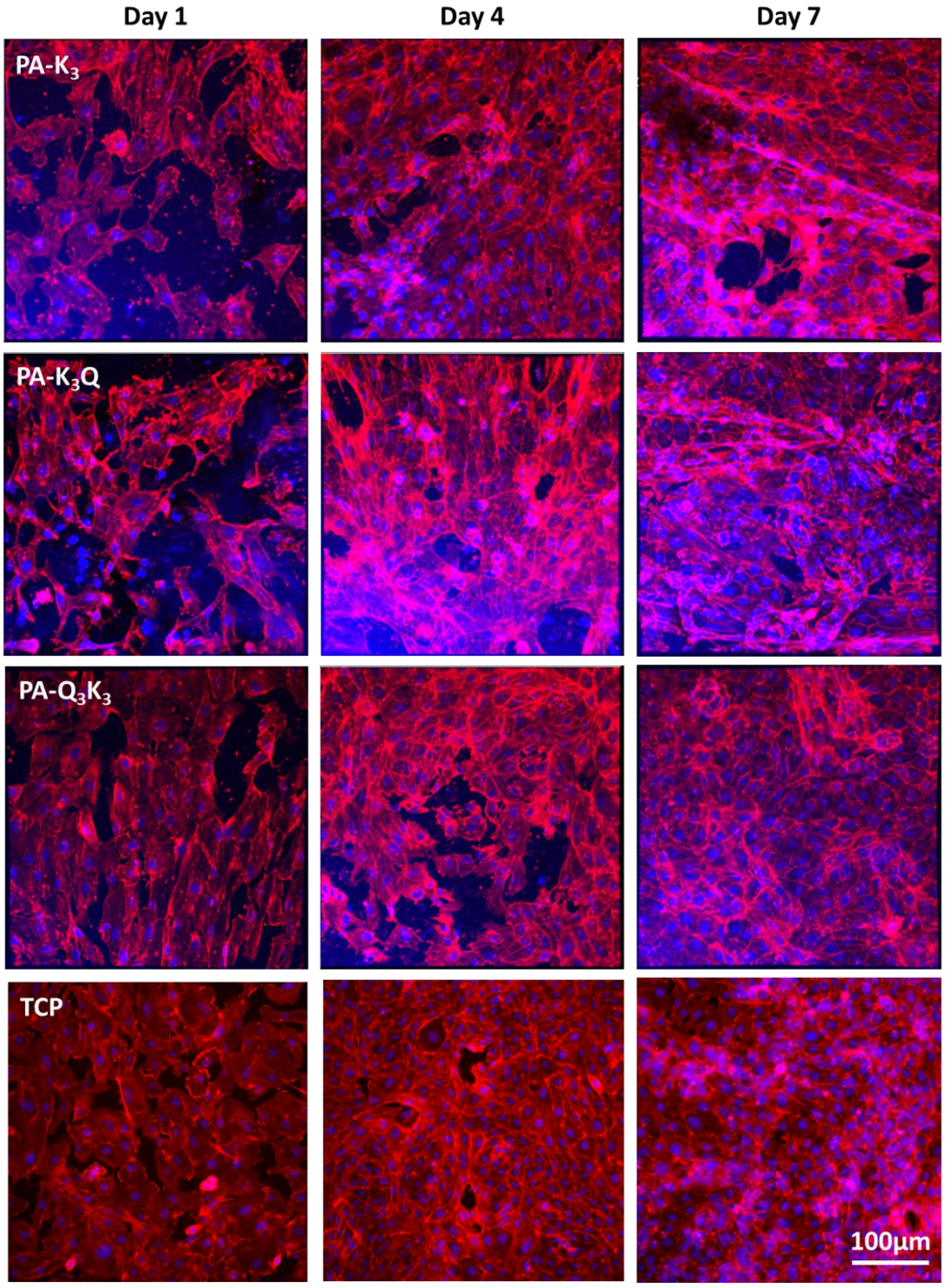

Figure 5.10. Study of cell morphology and proliferation of endothelial cells (HUVECs) in scaffolds over 7 days. Immunofluorescence images of endothelial cells cultured on PA-Blood hydrogels and TCP at Day 1, 4 and 7, showing their nuclei stained with DAPI (Blue) and cytoskeleton stained with F-actin (Red).

By day 7, indications of cell alignment and 3D organisation resembling immature tubular-like structures were detected in PA-K_3 and PA-K_3Q - Blood hydrogel samples (Figure 5.11). Angiogenin is another key stimulator of angiogenesis, this protein interacts with endothelial cells and triggers important biological process including proliferation, migration, invasion, thus initiating the process of blood vessel formation (Pyatibratov et al., 2012). In addition, IL-8 has also been reported to stimulate endothelial cell proliferation, migration and capillary tube formation in HUVECS and human dermal microvascular endothelial cells treated with IL-8 and FGF2 (Li et al., 2003). These molecules were detected in the supernatant of PA-K_3 and PA-K_3Q (Refer to Section 5.2.4). It is hypothesised that these molecules could have played a role in the formation of tubular-like structures observed by Day 7 (Figure 5.11: white dotted lines indicating tubular like formation).

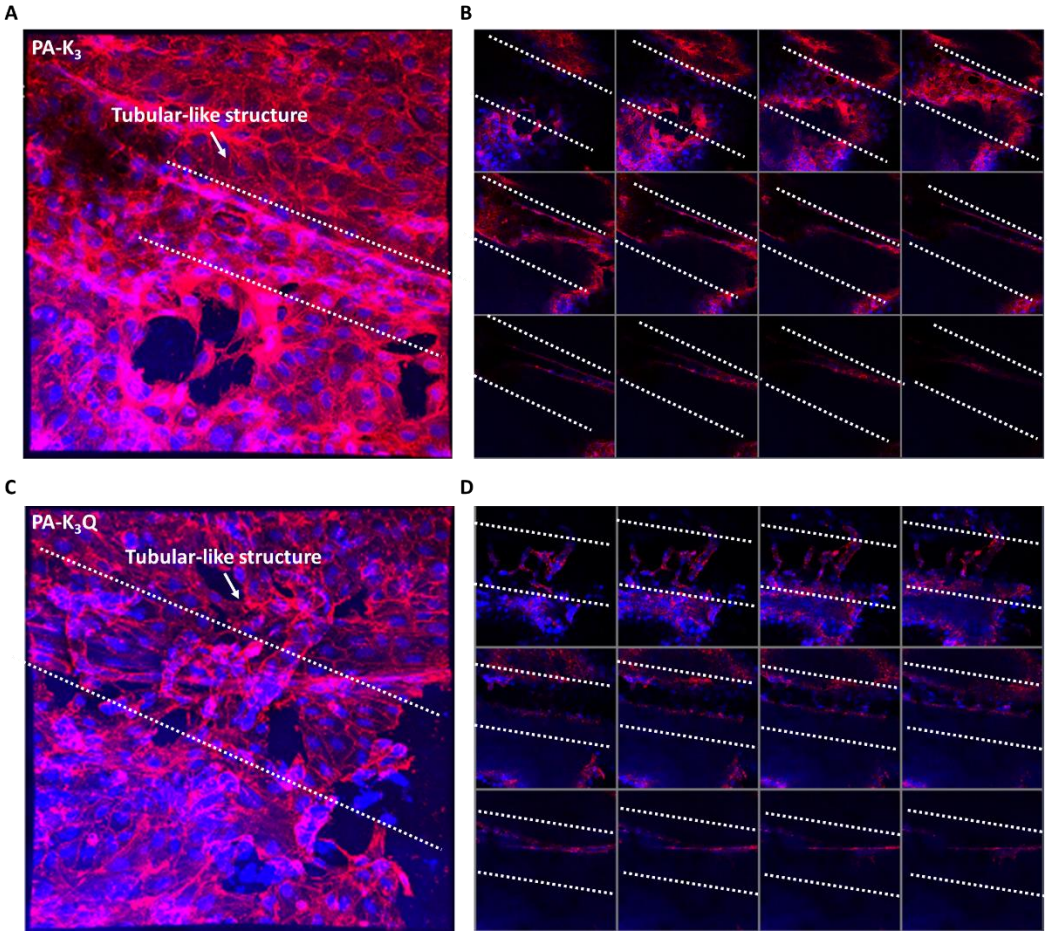

Figure 5.11. Endothelial cells (HUVECs) organisation into 3D tubular-like structures. A-B) PA-K_3 – Blood scaffolds cultured for 7 days, C-D) PA-K_3Q – Blood scaffolds cultured for 7 days. B and D z-stacks images indicate the tubular-like structures (white dotted lines).

5.3.3 Mesenchymal stem cells

Mesenchymal stem cells (MSCs) are involved in the wound healing process of different tissues. These cells have been the focus of intensive research for regenerative medicine and tissue engineering applications including burn wound healing, bone and dental tissue engineering applications.

Human mesenchymal stem cells (hMSCs) were seeded onto the different scaffolds and their response was evaluated. Live-Dead staining showed cells were able to attach to the hydrogels after seeding on hydrogels. PA-Q_3K_3 – Blood hydrogels

showed a change in morphology with less spreading through the scaffolds but cells were viable (Figure 5.12 A).

PA-K_3 – Blood hydrogels showed an increase on metabolic activity during Day 1 compared to the TCP control whereas PA-K_3Q – Blood hydrogels showed a decrease in metabolic activity (Figure 5.12 B). PA-Q_3K_3 – Blood hydrogels did not show a difference in metabolic activity compared to TCP. Nevertheless, no significant changes on metabolic activity were observed from Day 4 onwards. This suggests that there may be an adaptation period when cells first come into contact with the materials.

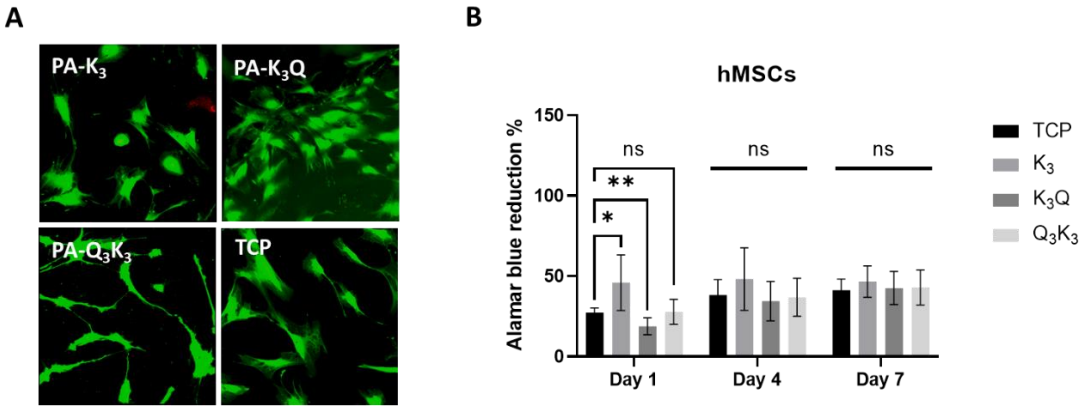

Figure 5.12. Study of the cell response of mesenchymal stem cells (hMSCs) cultured in scaffolds. A) Live-Dead assay showing human mesenchymal stem cells (hMSCs) seeded on top of hydrogels and a TCP control. Results showed good cell viability after seeding (green) with some cell death (red). Differences in morphology were observed in PA PA-Q_3K_3, B) Metabolic activity using the Alamar blue assay to assess cell health and proliferation at Day 1, 4 and 7. An increase in metabolic activity on Day 1 was observed for PA-K_3 and PA-K_3Q – Blood hydrogels (Statistical significance relative to TCP control; * $p < 0.05$, **$p < 0.001$)

Mesenchymal stem cells have demonstrated an increase in proliferation and cell spreading when cultured on stiff hydrogels compared with softer hydrogels. Available binding sites and their distribution in hydrogels are important as they facilitate cell

spreading influencing cell shape and cytoskeletal organisation (Figure 5.13). Cells cultured in hydrogels with binding sites present a spread out morphology and actin stress fibres. In contrast, cells cultured in scaffolds without binding sites would often present a rounded morphology and lack of actin stress fibres.

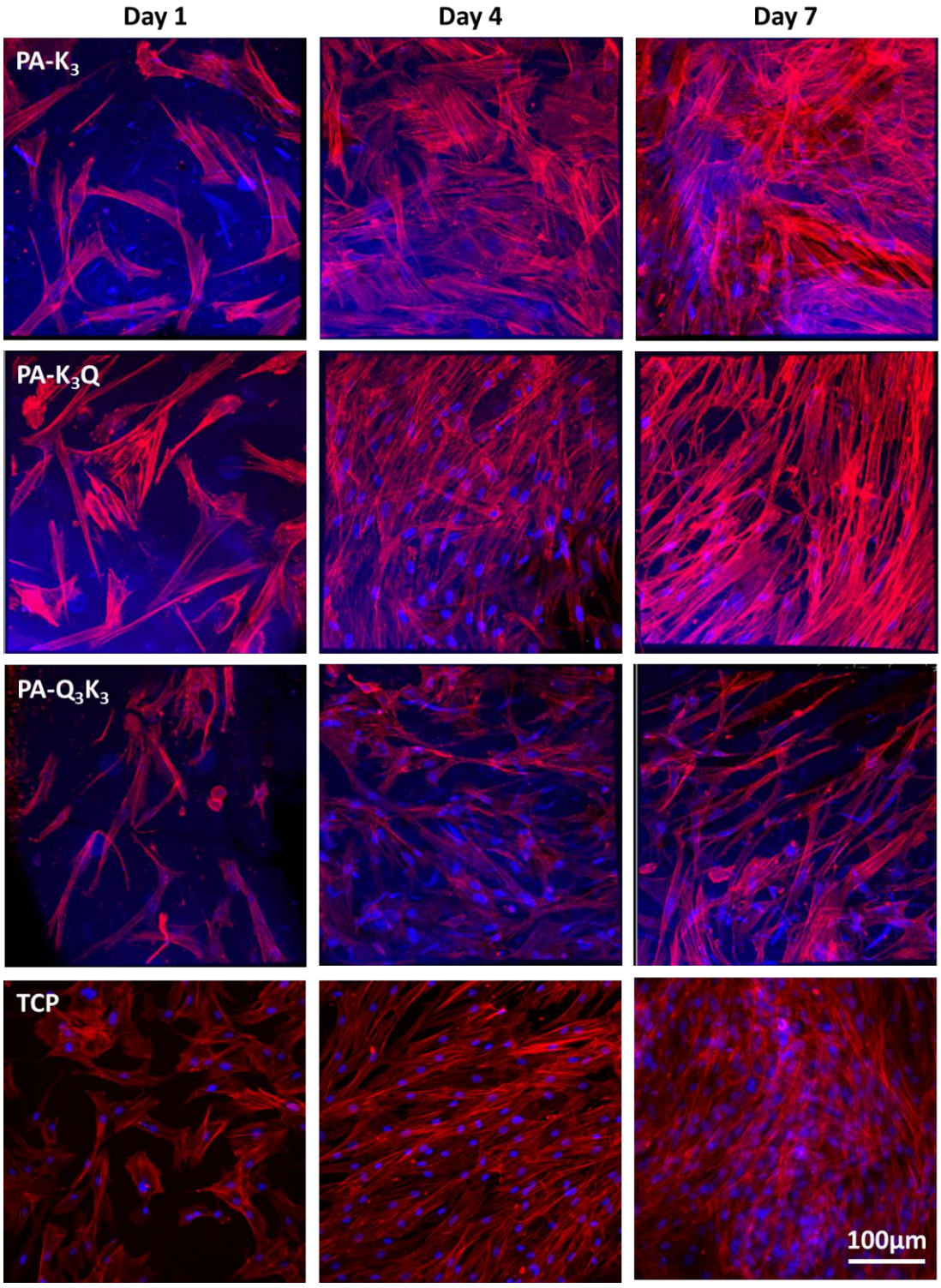

Figure 5.13. Study of cell morphology and proliferation of mesenchymal stem cells (hMSCs) in scaffolds over 7 days. Immunofluorescence images of human mesenchymal stem cells cultured on PA-Blood hydrogels and TCP at Day 1, 4 and 7, showing their nuclei stained with DAPI (Blue) and cytoskeleton stained with F-actin (Red).

Cell mobility and migration in hydrogels depends on different factors that include: a) contractile and adhesive forces in the cell, b) available binding sites in the hydrogel, c) matrix remodelling, and d) hydrogels stiffness (Ahearne et al., 2014).

Different approaches have been studied to promote mesenchymal stem cell motility in biomaterials. Chemotaxis is driven by biochemical stimulation of cells where said stimuli can be incorporated into the hydrogels to enhance cell migration in a particular direction. Another approach is durotaxis, where the substrate stiffness regulates the direction of cell migration (Vincent et al, 2013). Incorporating different degrees of stiffness into the hydrogels can also modulate cell migration.

Cell protrusions migrating inside the gels were observed on PA-K_3 and PA-K_3Q scaffolds (Figure 5.14 A-B), suggesting the cells are able to sense and explore their environment. In some cases, full cells were able to migrate through the scaffold and morphology changes to a star-like shape were observed (Figure 5.14 B, white arrows). It has been shown that most of the adherent cell types would migrate from softer to stiffer regions of hydrogels, therefore we hypothesise that there may be a gradient of stiffness within our hydrogels that stimulates this cell behaviour. We hypothesise that hMSCs were not able to migrate or move inside PA-Q_3K_3 scaffolds due to their softness whereas PA-K_3 and PA-K_3Q provided sufficient stiffness for the cells to explore the inner regions of these hydrogels.

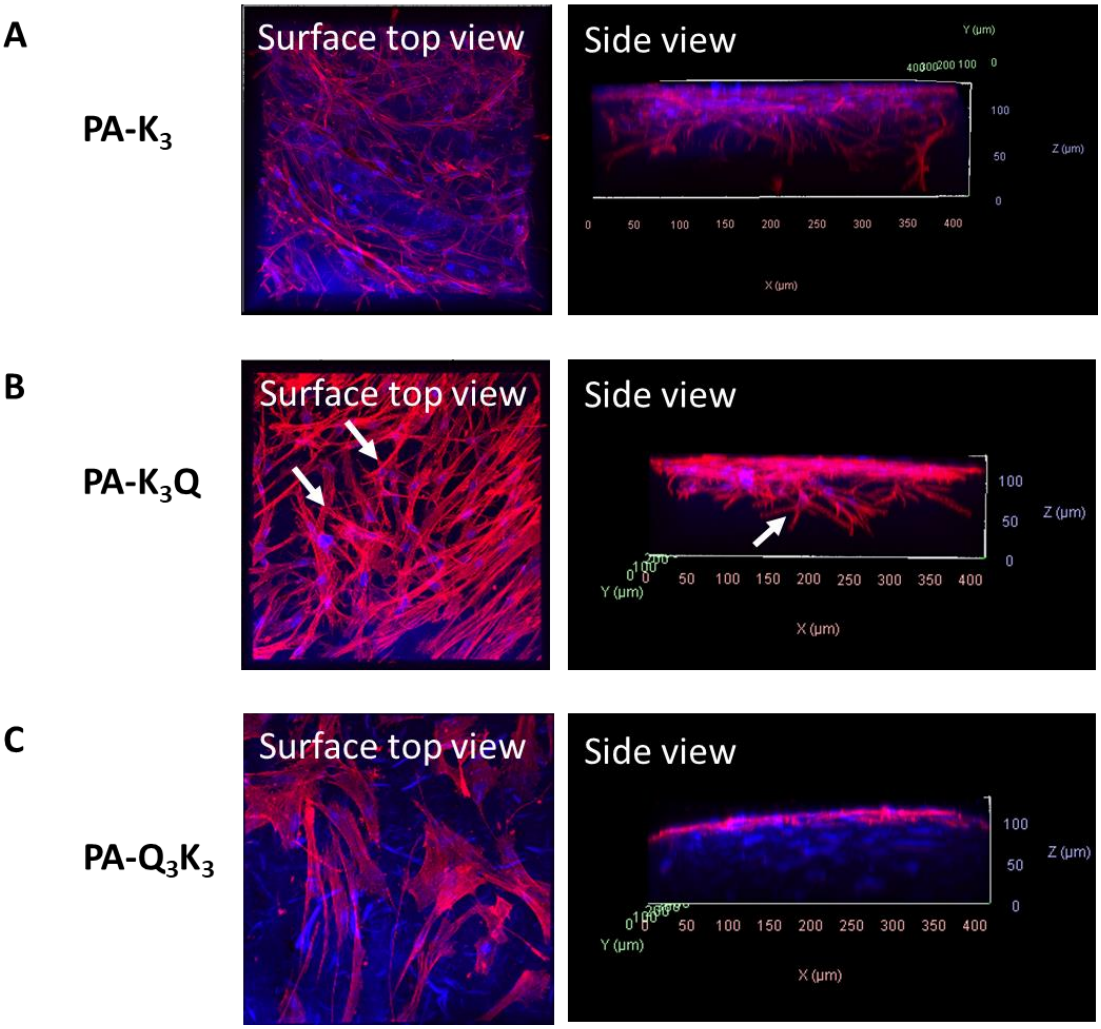

Figure 5.14. Human mesenchymal stem cell (hMSCs) migration inside hydrogels. PA-K_3 – Blood scaffolds (A) and PA-K_3Q – Blood scaffolds (B) cultured for 7 days showed cell infiltration inside the hydrogels whereas PA-Q_3K_3 – Blood scaffolds (C) cultured for 7 days did not show signs of cell migration inside the materials.

Although the hydrogels were not degraded by cells, we have previously showed that when adding enzymes, the patterns of gel degradation change dramatically. More complex follow-up studies including enzymes and cells or in vivo models could help determine the impact of the biological microenvironment on gel remodelling.

5.4 Discussion and conclusions

This study offers insights on the potential of these biomaterials as a reservoir of growth factors and blood cells to help the wound healing process. Peptide amphiphiles were able to trigger the blood clotting process and interact with blood proteins and cells, creating a microenvironment rich in a wide variety of signalling molecules that resembles the natural environment and progression of wound healing after injury.

In terms of biocompatibility, haemolysis studies were performed to determine the impact of the materials on blood cells. It was shown that peptide amphiphiles PA-K_3 and PA-K_3Q do not cause haemolysis, thus supporting their use for further research in vitro.

Studies on the degradation of the scaffolds showed that the inclusion or exclusion of a specific enzyme (plasmin) has a significant effect on the time of degradation of the gels. A point of optimisation is to explore the degradation rates of these scaffolds with different enzymes and on in vivo models.

An initial screening of the protein identification was performed and bioactive molecules of interest including EGF, PDGF-BB, IGF-1, and VEGF growth factors were identified in the supernatants of the hydrogels. These proteins have been extensively studied for their effects on proliferation and cell migration in different cell types including fibroblasts, epithelial and endothelial cells and stem cells. They have also been identified as important growth factors that are released into the wound site and enhance the healing process (Grazul et al., 2003).

Follow up studies on: a) the type of proteins bound to the hydrogels, b) the identification and quantitation of blood cells that are activated and attach to the different materials, and c) the quantity of factors release from those cells, are required in order to have a better understanding of the protein release mechanics of these systems. By using techniques like liquid extraction surface analysis (LESA) it would be possible to determine which proteins remain attached to hydrogels surface and their identification by mass spectroscopy could help to have a more comprehensive overview on the proteome of these materials.

It is hypothesised that the burst release of growth factors from the hydrogels had different effects on the cell types used for this research. In the case of fibroblasts, the burst release on Day 1 seemed to help cell attachment to the scaffolds and increased their metabolic activity/proliferation.

Cell organisation into 3D tubular-like structures was observed in HUVECs, suggesting PA-K_3 and PA-K_3Q scaffolds have the potential to help cells organise differently than TCP by providing an environment that resembles native tissues. Angiogenesis and tube formation in-vitro has been observed to occur in hours to days, while this process in in-vivo models has been reported to occur in 4-14 days, depending on the model used (Tahergorabi et al., 2012). Long term tracking (>7 days) of tube formation using 3D-microscopy techniques and quantification of capillary-like networks using specific markers (e.g. VE-cadherin and PECAM-1) and software like Angiotool can be used to assess the number, length, and branching sites of these tubular-like structures (Andrée et al., 2019; Zudaire et al., 2011). In addition, functional assays to assess tube lumen formation and connectivity using fluorescently tagged dextran can

help evaluate the extent of maturation of these structures and determine the role of PA – Blood scaffolds in cell organisation.

In hMSCs, migration inside the hydrogels was observed, suggesting that cells are able to interact with and modify the scaffolds. Different strategies to modulate protein release from hydrogels can be pursued, such as: a) adding of bioactive sequences to bind specific proteins, and b) using higher concentrations of the peptide amphiphiles to create the hydrogels, thus modifying their protein release patterns. Complementary studies to determine the effect of these biomaterials on MSCs differentiation could help determine the best application for tissue regeneration. A further step towards the study of the potential of these materials as wound healing aids would be to establish a co-culture model with different cell lines to explore their interaction together, as well as in vivo models.

In addition, further studies to address the immune response to the materials and the effect on the wound healing process in vivo would be beneficial to determine the ability of the gels to enhance tissue regeneration.

In summary, these studies show that peptide amphiphiles are able to incorporate new bioactive properties by co-assembling with blood proteins to form composite hydrogels. These new materials are capable to support cell attachment, proliferation and initial organisation of different cell types and have shown a potential to be explored as alternative materials for wound healing applications.

Chapter 6.

Bioprinting potential of the PA – Blood co-assembly system

This chapter describes the evaluation of the peptide amphiphiles and blood co-assembly system suitability for three dimensional printing. This chapter aims to provide insights into a proof of concept study focused on the validation and optimisation of the peptide amphiphiles to be used as bioinks.

6.1 Tissue engineering and bioprinting

Tissue engineering is a rapidly expanding field that merges biomaterials science and cell biology to create new strategies to repair and regenerate damaged tissues and organs. Although there has been a steady progress in this field over the past years, there are key aspects that have hampered the translation of these technologies to clinical settings. The major challenges for TE include the development of scaffolds that recreate the microenvironment of complex tissues and support cell growth and organisation, the development of mature vascularisation, compatibility with the host immune response and functionality of complex tissue constructs.

An increasingly attractive approach is three-dimensional (3D) printing, a new technique of biofabrication that allows precise positioning of materials and biological components (e.g. living cells and proteins) in order to create highly reproducible scaffolds that resemble the complex architecture of organs and tissues. This technological platform presents a number of advantages over other approaches such as control of the micro and macrostructure, high reproducibility, and high precision in terms of shape and geometry (Hedegaard et al., 2020). However, the bioinks currently used for 3D-printing are still under development and in need of refinement.

For example, ECM based bioinks such as collagen, hyaluronic acid and decelluarised ECM (dECM) have remarkable properties that enhance cell growth and proliferation. The main limitation is that their mechanical properties are not well suited for 3D printing, as they require time for crosslinking or gelation in order to increase their

stiffness (Gopinathan, 2018). Although the use of chemical crosslinkers to improve stiffness of these materials has been successful, it has shown to be toxic for cells.

On the other hand, natural polymer based bioinks such as alginate, agarose and silk have excellent mechanical properties that allow well defined shapes and hence, reproducibility of 3D-printed constructs. However, they lack the biological cues that allow tissue growth and organisation. Their slow biodegradability can also hamper the biological process of tissue development.

In order to overcome the limitations mentioned above, research has shifted its focus to the development of "advanced bioinks" by using different types of supramolecular, multi-material and nanocomposite hydrogels (Mendes et al., 2020). The ability to design "smart materials" that can respond to stimuli in real time mimicking, for example, cell response to injury, is one of the reasons hydrogels have been catalogued as a promising solution to adapt to the highly variable changes that occur during the healing process.

Over the past years, self-assembling peptide hydrogels have emerged as leading candidates for tissue regeneration due to their molecular and structural versatility of design, which allows them to mimic specific aspects of the extracellular matrix and to support cell adhesion, proliferation and differentiation in vitro and in vivo. The ability to control and tailor specific properties of these materials such as bioactivity, porosity, stiffness, topography, elasticity, gelation time and degradation, makes them suitable for different medical applications.

Previous research by the Mata group has shown that by combining top down (3D-printing) and bottom up (self-assembling) technologies, it is possible to exploit the capabilities of the two approaches in order to recreate diverse aspects of native tissues. Work developed by Hedegaard et al. (2018), have combined the properties of PAs and a range of biomolecules (including collagen, fibronectin, and keratin) with inkjet 3D-printing to fabricate microgels with defined micro and nanostructure and improved biological properties. In addition, Wu et al. (2020), have explored a different system consisting on the co-assembly of ELPs and graphene oxide to create 3D-printed capillary-like fluidic microstructures. This system allows the creation of robust tubular structures with a resolution down to around 10 μm in diameter, capable of withstanding continuous flow, demonstrating its improved mechanical properties and biocompatibility.

The studies presented in this chapter were used to address the fourth thesis objective (Section 2.6.3): Develop a new 3D-printing system by using peptide amphiphiles as bio-inks for 3D printing of scaffolds. The experiments conducted in this chapter were designed as proof of concept study to: a) explore the peptide amphiphiles potential to act as a bioink, b) evaluate the emerging properties of PA – Blood 3D-printed scaffolds, and c) determine their suitability for tissue engineering applications.

6.1.1 Initial screening to determine PA – Blood and PA – PRP co-assembly systems potential as bio-inks for 3D-printing

Previous work has showed that liquid into liquid 3D-printing is possible with inkjet and extrusion methods by using a liquid bioink that can be jetted or extruded inside a bath of a second solution (Faulkner-Jones et al., 2015; Highley et al., 2015).

For this, peptide amphiphile solutions (PA-K_3) were injected in wells containing blood or PRP to determine the ability of these materials to be used as inks for 3D-printing. Hydrogel formation was detected after a couple of minutes. The gels were left under incubation for different periods of time (Figure 6.1 A).

After a couple of hours, hydrogels showed adhesive properties that allowed for the individual hydrogels to attach together without detaching when subjected to manual stretching and relaxation cycles (Figure 6.1 B). Although macroscopic observation of gel formation occurs after a couple of seconds, hydrogels strength improved with time and the adhesive properties of the gels were observed after 3-hours incubation time for PA – PRP gels and 6-hours incubation time for PA – Blood gels.

Several components of blood including fibrin, Factor XIII and platelets are known to contribute to the blood clot adhesive properties (Chan et al., 2020). We hypothesise that these properties are then acquired by the co-assembled materials. The difference in time observed between materials created with Blood or PRP could be explained by the composition of these two biofluids. The excess of platelets and fibrin concentration in PRP could be helping the resulting hydrogel acquire the adhesive properties faster than those created with blood.

In humans, the clotting time is 8-15 minutes in healthy individuals. This measurement is determined by detection of fibrin clot formation in clinical in-vitro tests. It has been determined that a fibrin clot is formed when a 3D-network of fibrin fibres is assembled. However, the clotting time occurs early in the fibrin polymerisation process, when only around 15-20% of fibrinogen has been deposited into the network (Weisel et al., 2013). It is hypothesised that as time passes and more fibrinogen is deposited in the surface of the hydrogels, a stronger layer of fibrin is formed, which confers the gels the increasing strength as well as their adhesive properties.

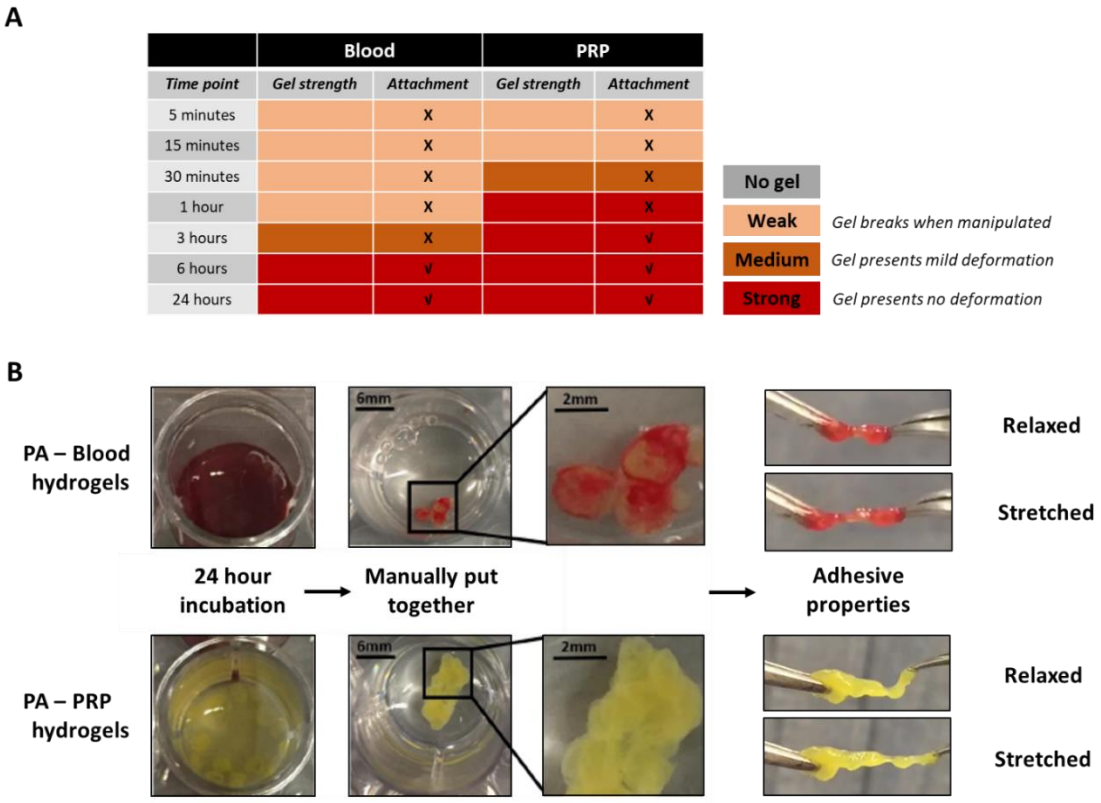

Figure 6.1. Pilot experiments to determine printing ability of PAs in biological fluids. A) Summary of the times to obtain gel formation and attachment of the PA gels. Results indicated that hydrogels created with blood took 6 hours to develop adhesive properties whereas hydrogels created with PRP took 3 hours to develop adhesive properties. B) Macroscopic images of the PA gels attached together and their adhesive properties when manually stretched.

The attachment sites of the hydrogels were examined by using SEM imaging of multiple gels attached together (Figure 6.2 A-B, white arrows). In both, PA – Blood and PA – PRP hydrogels attachment sites between different gels, a network that contributes to holding the gels together was observed. We hypothesise, that although there might be initial protein diffusion and fibrin deposition into the gels at earlier time points it might not be enough to display the sticky properties observed at later incubation times. The time that takes the hydrogels to acquire the adhesive properties could be related to the effect of the material on platelet activation, fibrin deposition and network formation. Further analysis is needed to understand the dynamics of these systems and the effect of PAs in blood clotting.

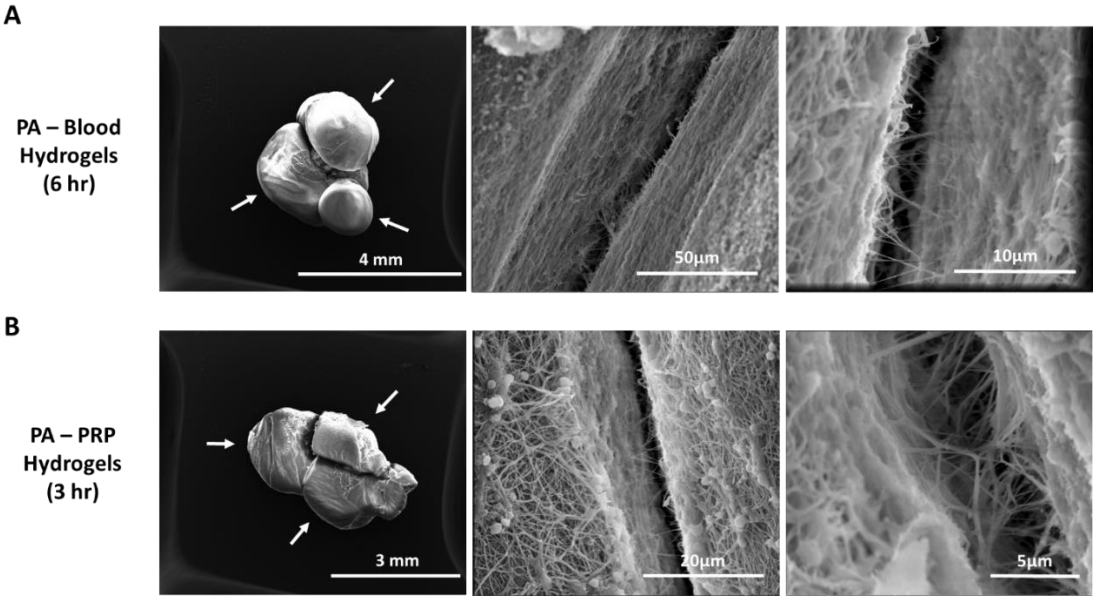

Figure 6.2. Hydrogels adhesive properties. SEM imaging presenting A) PA – Blood and B) PA – PRP hydrogels adhesive network at the attachment site between gels. White arrows indicate different gels attached together by fibrin fibres.

6.1.2 Extrusion three dimensional bioprinting

Our approach of printing materials incorporating blood components raises the possibility to incorporate blood proteins and molecules present in the body that help wound healing and create a personalised scaffold. This would also enable the creation of complex microenvironments with better control over the nano and micro structure of the materials as well as changes in topography.

Three dimensional bioprinting technologies allow the automated hierarchical fabrication of scaffolds with high precision (Cui et al.,2020). Extrusion 3D-printing is one of the most commonly used printing technologies as it presents a number of advantages including: a) ability to fabricate complex and hollow constructs, b) automated layer by layer hierarchical fabrication, c) high precision, d) affordability, and e) versatility. Previous studies have used self-assembling and peptide based materials as inks for extrusion based bioprinting (Loo et al., 2015).

6.1.2.1 Evaluation of PA-K_3 potential as a bioink for extrusion printing in a one-layer model

A RegenHU 3D-printer was used to carry out pilot extrusion experiments to determine the potential of PAs and biological fluids as a liquid in liquid 3D-printing via extrusion.

The printability of the PA bioink was assessed by printing a single filament one-layer model of PA-K_3 into the supporting bath (blood) using a 30G needle (160um inner diameter) and different printing parameters (Figure 6.3 A). For this, the first test carried out was to vary the printing speed. The optimisation of the printing

parameters was determined as follows: the pressure was maintained constant (0.02MPa) and the feed rate (speed) was increased 5mm/sec for each test. Samples were incubated for 15 minutes at room temperature before removing the blood bath solution to examine the printed structures (Figure 6.3 B).

The PA solution was easily extrudable through the syringe small nozzle (160µm) due to its low viscosity and required a relatively low pressure for the printing. The viscosity of the PA-K_3 solutions has been reported to be 5.1 ± 1.1 mPa.s (Hedegaard et al., 2018). Extrusion based printing can usually work with viscous bioink formulations of up to > 10^7 mPa.s (Ozbolat et al., 2016; Murphy et al., 2014).

Examination of samples S1 to S5 demonstrated that the printed filament structures had a uniform shape (Figure 6.3 C). A trend of decrease in thickness of the structures as the printing speed increased was observed. However, a speed of 35 and 40mm/sec (S6 and S7) showed the tubular structures had irregular shapes and sizes (Figure 6.3 C, S6 and S7).

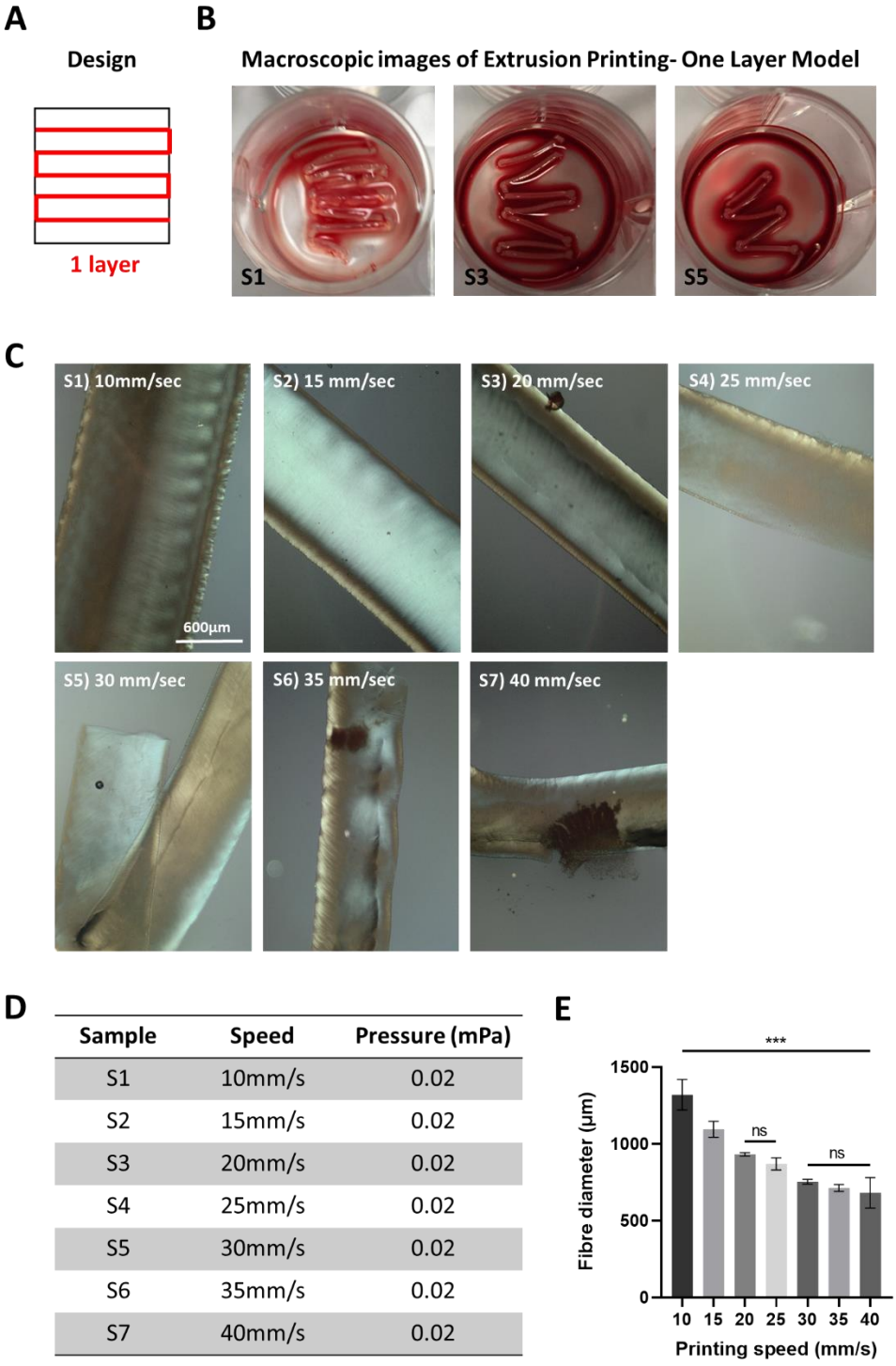

Sample	Speed	Pressure (mPa)
S1	10mm/s	0.02
S2	15mm/s	0.02
S3	20mm/s	0.02
S4	25mm/s	0.02
S5	30mm/s	0.02
S6	35mm/s	0.02
S7	40mm/s	0.02

Figure 6.3. Speed test to determine the potential of PA-K_3 as a bioink. A) One-layer single filament design diagram. B) Examples of macroscopic images of printed filaments. C) Light microscopy images of filaments printed at different speeds. D) Summary of parameters used for the different samples printed. PA-K_3 was printed from the lowest (10mm/sec) to highest speed (40mm/sec) allowed by the RegenHu printer to determine its potential as a bioink. Images show that the tubular printed structures maintain a good and regular shape up to 30mm/sec. E) Changes observed in filaments diameter (µm) printed at different speeds.

Further analysis using optical microscopy images showed that the thickness of the printed filaments (1319.5 ± 90.8 to 681.8 ± 90.7μm) could be controlled depending on the printing speed (Figure 6.3 D-E). No significant differences were found between the diameters of fibres printed at 20 and 25 mm/s and between filaments printed at 30 to 40 mm/sec (Figure 6.3 E). This indicated that although the shape fidelity was maintained, the hydrogel expanded around 4 to 8 times the size of the syringe nozzle that it was extruded from. Nevertheless, it was possible to continuously print a simple one-layer model of rectilinear lines reproducibly with rapid hydrogel formation. Moreover, the formation of reproducible hydrogels confirmed that the speed at which the co-assembly is triggered is sufficiently fast to support this method of fabrication.

From the conditions tested, the filaments printed at 35 mm/sec showed the highest fidelity and stability, and were therefore selected for the subsequent bioprinting assays.

The printing speed also had an effect on the topographical features of the surface of the printed materials, which could be an advantage towards the manufacturing of scaffolds with different levels of complexity.

The external topography of the filaments was imaged using SEM. As observed in Figure 6.4, the shear forces generated during printing not only guide the PA – Blood co-assembly into its tubular shape but they also allowed the creation of grooves and ridges-like micro topographies on the surface of the tubes.

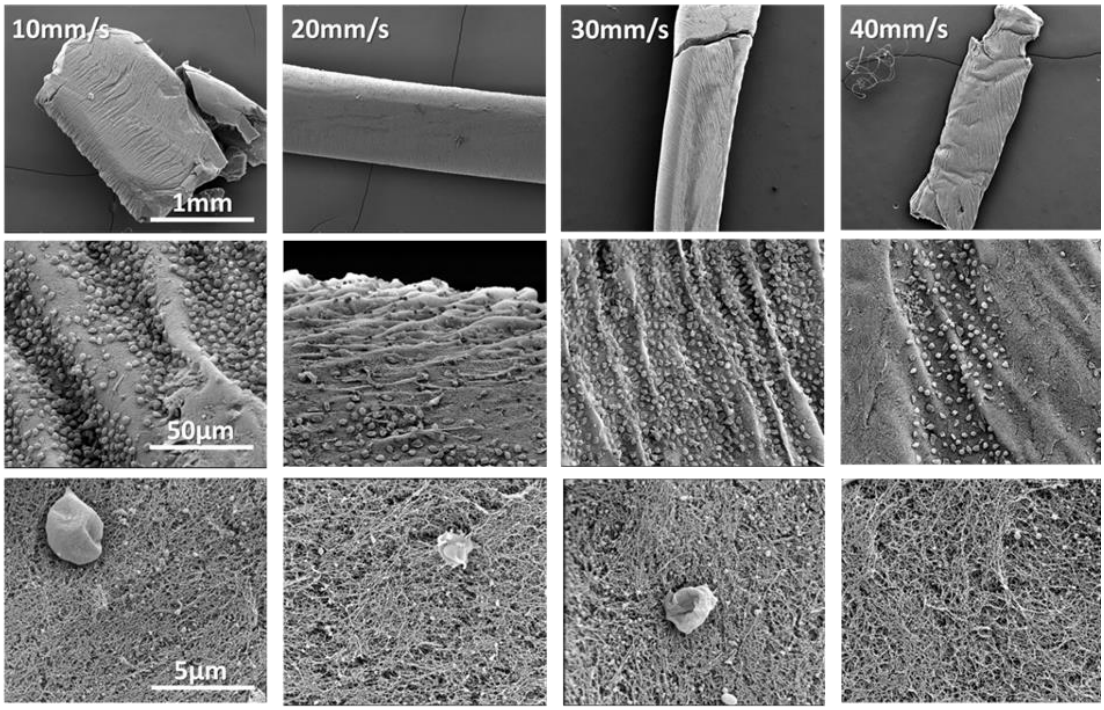

Figure 6.4. Surface topography of filaments printed at different speeds. Grooves and ridges were observed as an effect of different printing speeds. The orientation of these features was also determined by the printing speed.

In general, samples printed at lower speeds showed these channel-like structures were perpendicular to the tubular shapes whereas at high speeds they start to become parallel to the direction of the printed structures. It is hypothesised that the pressure and speed utilised may contribute to the way the PA solution is ejected and its initial contact with blood may create perturbations in the liquids that contribute to the formation of these microstructures.

6.1.2.2 Evaluation of extrusion printing parameters for the creation of scaffolds in two and four layer models

The parameters used for sample S5 (Pressure: 0.02mPa, Feed rate: 30mm/s) were utilised to create a two-layer scaffold model. In order to determine the best height

for maintaining contact between the first and second layer and improving the stability of the printed structures, the distance between layers (height) was varied.

It was observed that the constructs presented a good resolution despite the variation of distance between layers (Figure 6.5). Upon further examination of the samples, it was observed that the layers were not firmly adhered together and separated easily during manipulation of the constructs. These samples were incubated for 15 minutes before blood excess removal which may not be enough time for the constructs to incorporate the blood components and develop adhesion properties strong enough to keep the layers together as previously reported (Figure 6.1). By adjusting the time of incubation to a minimum of 1 hour, the delamination issue was resolved. It has been reported that the use of fibrin in bioink components help the delamination process by promoting adherence between layers (Mendes et al., 2020), thus it is expected that the blood clotting process and fibrin network formation is highly important for the adhesiveness of these constructs.

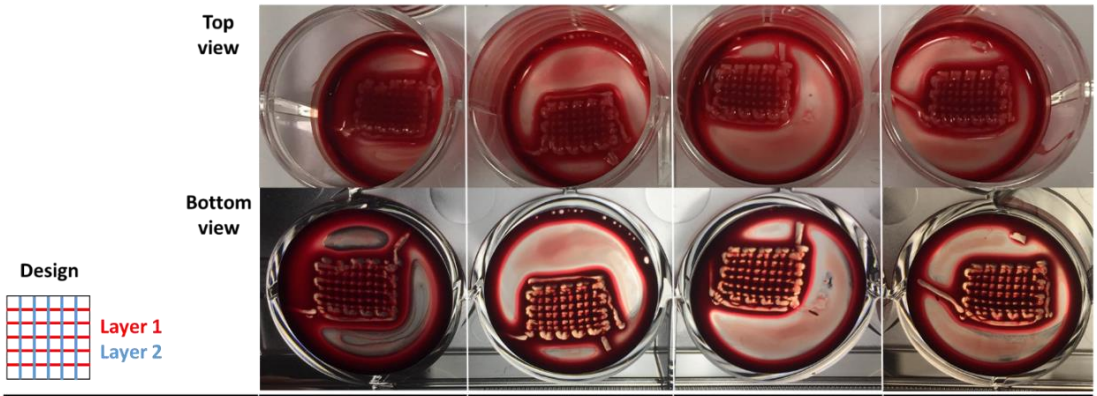

Two-Layers Model	TL-1	TL-2	TL-3	TL-4
Feed rate (mm/sec)	30	30	30	30
Pressure (Pa)	0.02	0.02	0.02	0.02
Distance between layers (µm)	450	500	550	600

Figure 6.5. Optimisation of a two-layer printed structure with PA-K_3. The distance between layers was modified to determine the best model for the printing of two-layers scaffolds.

For these experiments, blood from three different donors was used to replicate the different conditions of the scaffolds (TL-1 to TL-4). After incubation, it was observed that there was visible variability on the scaffolds mechanical properties of Donor 3 compared to Donor 1 and 2 (Table 6.1).

Scaffolds created with blood from Donor 3 were highly flexible and they did not hold their squared shape but rather acquired the well shape upon movement without breaking. This could be due to blood properties (such as protein content), which can differ depending on the donor. Unfortunately, blood samples are from anonymous donors and are provided without any type of analysis in terms of protein or cell content. Therefore, more in depth studies on blood content need to be done to determine the source of variability as this will determine the mechanical properties of the final scaffolds.

Donor	Model	Observations
Donor 1	2 layers	• Stable gel formation. • Good resolution printing. • Stiff gels- Scaffolds maintain their squared shape upon movement.
Donor 2	2 layers	• Stable gel formation. • Good resolution printing. • Stiff gels- Scaffolds maintain their squared shape upon movement.
Donor 3	2 layers	• Stable gel formation. • Good resolution printing. • Flexible gels- The scaffold moulds to the well plate shape upon movement without breaking.

Table 6.1. Effect of blood variability between donors on scaffolds mechanical properties. Summary of observations on mechanical properties of two-layer scaffolds depending on blood donor samples.

Initial SEM microscopy of the samples at low magnifications did not show clearly defined pores on the two-layer structures as planned on the design (Figure 6.6 A). Upon further examination, a close up of the pores showed that a relatively dense

fibrin network created by the triggering of the blood clotting process is covering them up. It was also possible to identify different blood cell types like RBCs, leukocytes and plates in the samples (Figure 6.6 B). It is hypothesised that the presence of this fibrin layer on the pores is also contributing to maintaining the layers adhered together.

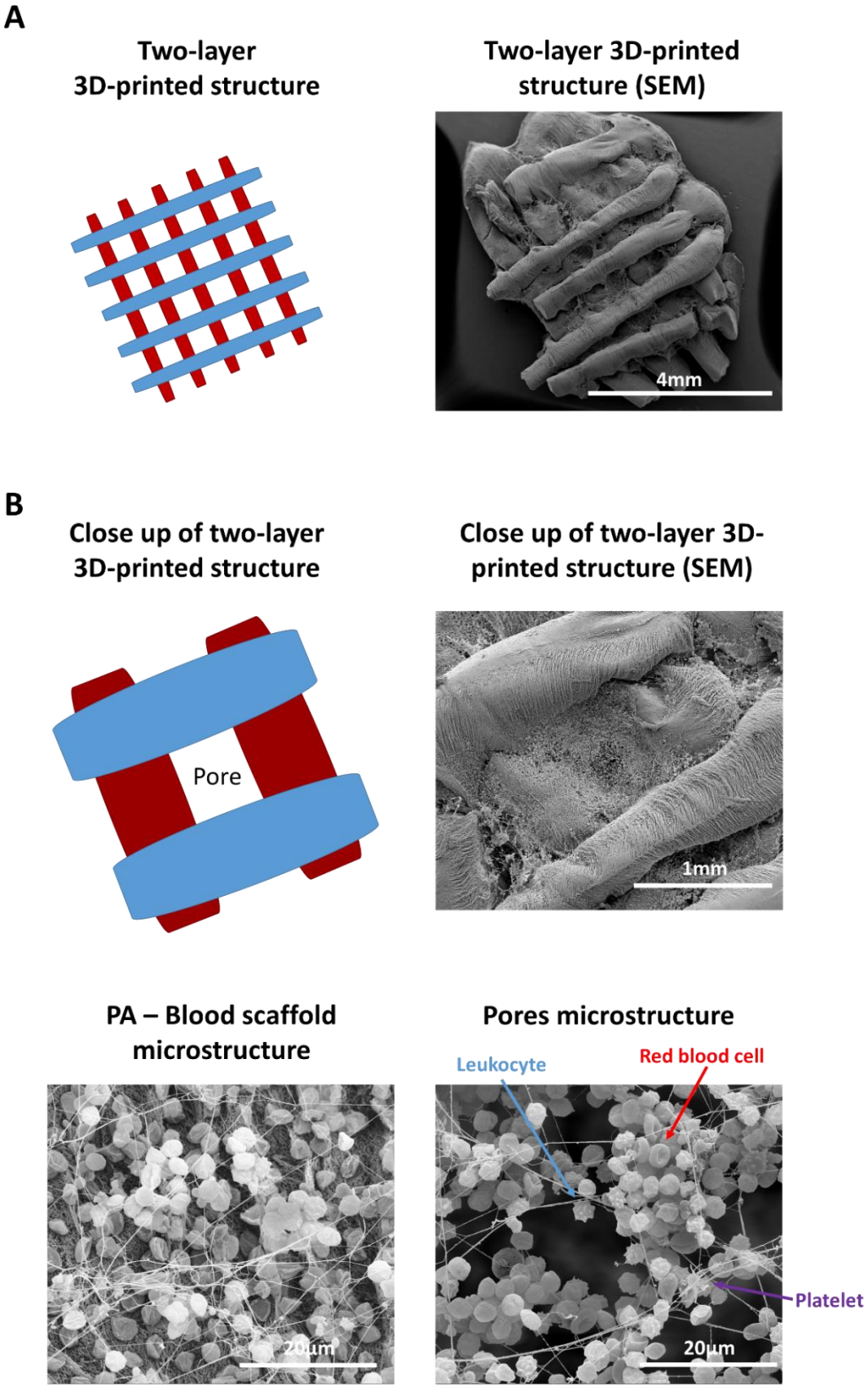

Figure 6.6. SEM analysis of the two-layer model. A) The construct showed no identifiable pores at low magnifications. B) A close-up of the scaffolds showed that the pores were covered by a fibrin layer with different types of blood cells.

For further examination of the two-layer scaffold design, the two layers of the scaffolds were carefully separated in order to inspect their shapes and structure. As observed in Figure 6.7, the first layer maintained the filament structure as planned whereas the filaments of the second layer seem to have collapsed between the spaces of the first layer filling in these spaces.

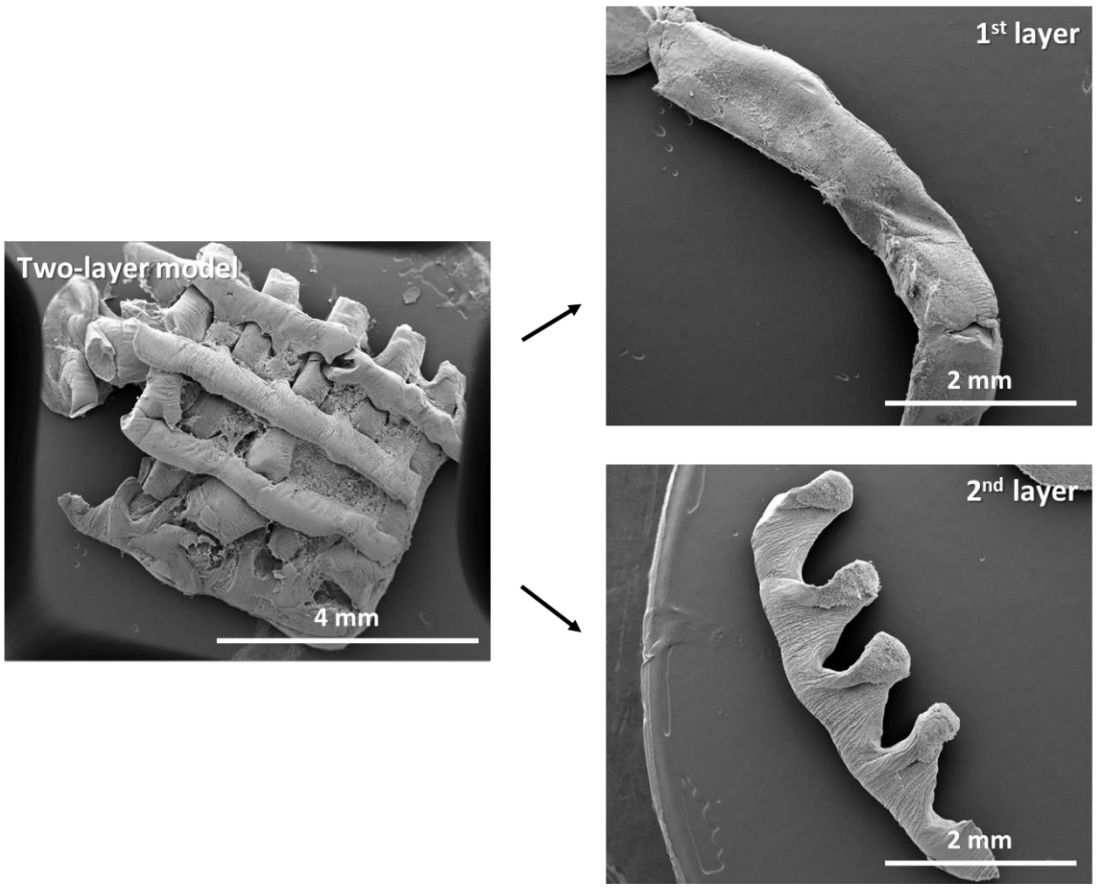

Figure 6.7. SEM analysis of the first and second layer of the two-layer model. The first layer shows that the filaments of the first layer maintained their structure according to the design, whereas the filaments of the second layer seem to have collapsed between the spaces of the first layer filling in the spaces.

There are a number of associated factors that may be contributing to this behaviour including: a) the diffusion between PA and blood solutions, b) the time of transition from the initial liquid components (PA and Blood) to solid hydrogels, c) the hydrogels

swelling behaviour observed after printing, and d) the relatively long time until the hydrogels are mechanically strong enough to withstand deformation (hours).

Building up on the information acquired from the two-layer model, the parameters of the scaffold TL-3 were selected to create a four-layer model in 2 different designs showed in Figure 6.8.

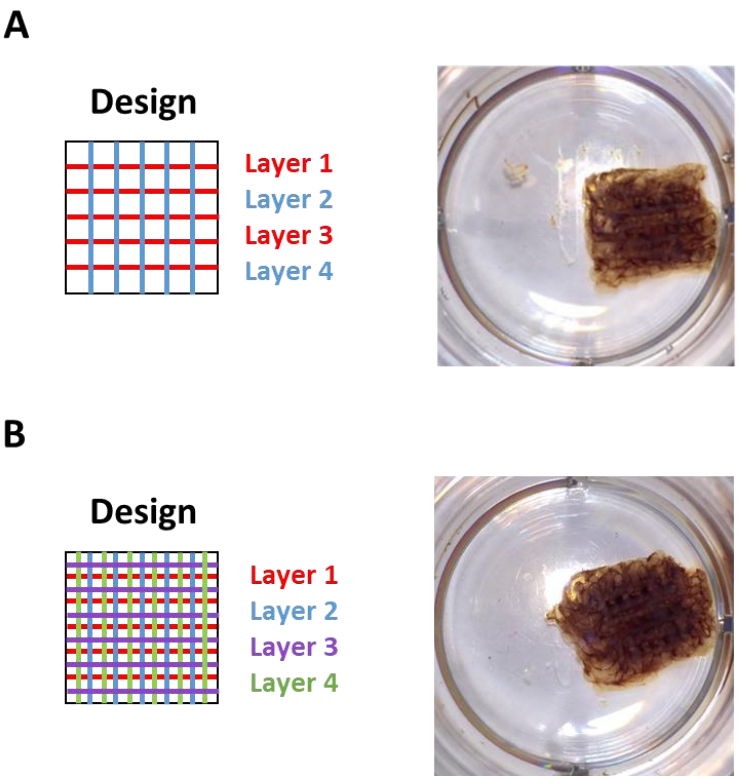

Figure 6.8. Testing of four-layer printed structures with PA-K_3. Two different designs were selected where the layers are printed on top of each other (A) or intercalated between each other (B) to determine the best configuration to obtain stable constructs.

Both models showed good resolution on XY, whereas Z resolution was poor. The stability of the scaffold was better on the central part whereas the edges seemed to collapse slightly. These constructs were incubated for 1 hour before removing the blood excess and upon further analysis the layers seem to be firmly attached together. The challenges presented here can be attributed to a number of factors

including: the nature of the material, the gelation time, the viscosity, and the printing method selected (Li et al., 2018).

These preliminary experiments show that the co-assembled hydrogels can withstand the weight of stacked layers without collapsing and can maintain their shape relatively well. These models serve as a proof of concept of the feasibility to print multi-layer scaffolds with this co-assembly system. Further studies need to be done to optimise this fabrication method.

6.2 Discussion and conclusion

In this work, a new method of biofabrication with biological fluids was proposed. By integrating the extrusion 3D-printing technology with the PA – Blood co-assembly system, this approach enables the possibility to build scaffolds with distinct and reproducible features on the nano, micro and macro scale. Furthermore, extrusion 3D-printing allows the ability to print reproducible structures in larger scale sizes.

The results presented in this chapter demonstrated the feasibility of using the PA-Blood co-assembly system as a liquid in liquid extrusion based 3D-printing method. The rapid co-assembly of PA and blood components confirmed the suitability of this material to be used as a bioink, where the rate of gelation is a key element to obtain high-resolution printed structures. By modulating the printing parameters, different scaffold features including size, shape and surface topography can be modified with a high level of control (Figure 6.3).

One of the main advantages demonstrated by the use of this system is the ability to incorporate a variety of blood components (e.g. proteins, growth factors) including

key biomolecules and different types of blood cells that can enhance the wound healing process. This ability of recreating the way these molecules and cells are presented in vivo during injury represents an advantage over other systems that are based on the incorporation of only one or two biomolecules.

In addition, the interplay between the extruded and bath solutions could also be optimised to modify the hydrogel surface in order to introduce reproducible features on the surface's microtopography (Figure 6.4) which could have important effects on cell behaviour. Moreover, this system represents the possibility of creating personalised scaffolds assembled by the patient's own blood, reducing the risk of immune reaction and disease transmission.

Although two and four layer models were successfully printed, collapsing of the layers above the first layer was observed (Figure 6.7). Interestingly, recent work has reported that there is a variety of "suspended manufacturing techniques" that allow 3D-printing of hydrogels with minimal reliance on their rheological properties. These techniques are based on the use of viscous supporting baths that allow the inks to remain in the 3D-printed space position with minimal diffusion (Moxon et al.,2017; Hinton et al., 2015). From this perspective, this system could benefit from further optimisation on the viscosity of the bioink and bath solution to allow the formation of more stable 3D-structures, which could help prevent the collapse of structures. Moreover, the resolution achieved in this work remains in the order of 600 µm diameter filaments due to hydrogel diffusion and swelling. Further optimisation of the printing parameters and the use of smaller nozzles could help improve this.

In summary, this co-assembly system enabled the biofabrication of interconnected hierarchical fibrillary structures across multiple size scales, including: a) the co-assembly of PAs with blood proteins into a bulk nano-network, b) the fibrin micro-network formation due to blood clotting, and c) the macro–scale creation of printed filaments. The ability of recapitulating structural and biological aspects of the native ECM allows the possibility of better directing cell behaviour compared to other polymer based hydrogels. Furthermore, the creation of these complex materials using blood components combined with 3D-printing demonstrates the potential of this system as an alternative to be explored for biofabrication the of personalised scaffolds.

Chapter 7.

Conclusions and future work

This chapter summarises the key findings of the research into the PA – Blood co-assembly system. The chapter is divided into four parts addressing each of the research objectives. These sections contain a summary of main findings, a perspective on the significance of the work, and suggestions for future work based on the limitations of the research.

7.1 Summary of the project

Current research on biomaterials that help the wound healing process has focused on generating materials and scaffolds that take advantage of specific blood derivatives such as serum, fibrin, albumin, or enzymes that play a key role in blood clotting and wound healing (Section 2.4.1). However, these materials exhibit a variety of important limitations such as the need for large quantities of blood, poor mechanical properties, animal sourced, elevated costs, and limited control of their bioactivity. Furthermore, these materials do not recreate the evolving properties of the natural blood clot that are necessary for the wound healing process. In this work we present the possibility to use the patient's own blood as a readily available and living material with the capacity to be processed in order to engineer personalised implants with defined geometries and bioactive properties.

The work done on this thesis presents the development of a novel method for the creation of a biomaterial that integrates self- assembling peptides and blood molecules in order to build bioactive scaffolds. This research demonstrated the feasibility to build these scaffolds as well as the possibility to use this system for biofabrication purposes. The biological relevance of these materials was validated by in vitro testing of different cell types relevant to the wound healing process.

This chapter provides a review of the experimental objectives, main findings and limitations of the research, as well as future work that could help develop this project further.

7.1.2 A multi-component based hydrogel using a biological fluid

The first thesis objective was 'to assess the potential of peptide amphiphiles to interact with blood and blood fractions and to determine key components involved in these potential interactions'. The studies presented in Chapter 4 aimed to address this objective.

7.1.2.1 Summary of findings, perspective and future work

A novel co-assembly system based on the interaction between PAs and blood components was developed. This work has demonstrated the possibility to use self-assembling peptides and complex biological fluids to trigger the organisation of a wide variety of biomolecules in order to create functional biomaterials.

The initial screening of a PA library with blood and blood fractions indicated that negatively charged proteins (e.g. albumin and fibrinogen) present in blood and PRP play a key role in the co-assembly with positively charged PAs for hydrogels formation. Moreover, it was determined that neither the ionic component nor the positively charged proteins concentrations alone were able to trigger the hydrogelation process when using negatively charged PAs.

PA-K_3 was selected for further testing due to its performance and mechanical properties observed in pilot experiments. CD analysis was used to determine initial interactions between blood and highly abundant proteins in blood (albumin and fibrinogen). The study showed that the PA and blood proteins exhibit conformational changes on their secondary structures in the presence of each other as a result of

their interaction. However, the exact conformational changes at the molecular-level remain to be elucidated. Nuclear magnetic resonance spectroscopy (NMR) and small-angle neutron scattering (SANS) have been previously used to elucidate changes on the molecular level of co-assembling systems (Redondo et al., 2019; Wu et al., 2020) and could prove useful for studying this system using representative blood proteins like albumin or fibrinogen and PAs.

Diffusion studies using fluorescent tagged model proteins like albumin and fibrinogen were used to provide some insight into the patterns of diffusion between blood proteins and PAs (Section 4.1.3.3.3). Results suggested that proteins are migrating inside the PA solutions enabling the process of nanofiber formation. In general, diffusion within hydrogels is a highly complex process to study due to the different interactions that a molecule can undergo while diffusing through the hydrogel mesh (Hagel et al., 2013). In this system this is further complicated by a number of factors including: a) biomolecules from blood co-assemble with PA molecules to create the gels, b) blood is a complex mixture of molecules that can interact with each other as well as with the forming hydrogel, c) blood biomolecules have different sizes, conformations and abundance in blood. Thus, prediction and modelling of diffusion is challenging due to the high complexity of molecules interactions. Tools like computational simulations and modelling could help provide a better understanding of this diffusion process (Axpe et al., 2019).

Analysis of the microstructure of these hydrogels was carried out using SEM microscopy. PA – Blood and PA – PRP hydrogels showed that the hydrogel was composed by two different networks, one that resembles the characteristic PA-

nanofibre network and a second one that resembles a fibrin network with different cells like the one present in blood or PRP clots. Immunofluorescence microscopy confirmed the presence of a fibrin network on the hydrogels' surface. The use of techniques like transmission electron microscopy (TEM) could help the characterisation of these networks in the nanoscale size.

Follow up experiments to determine key components needed for the hydrogel formation using blood proteins and enzymes demonstrated that negatively charged proteins like albumin and fibrinogen are required to trigger the gelation process. The addition of enzymes like thrombin and Factor XIII demonstrated that they are essential in order to trigger the blood clotting process and fibrin network formation (Section 4.1.3.2). Although the observed fibrin network is not a key component for hydrogel formation, it was established that it contributes to the overall strength of the gels. This finding is supported by research on the characterisation of naturally occurring blood clots, were it has been established that fibrinogen concentration and fibrin network formation have a direct effect on the mechanical strength of the clots. For example, a contracted blood clot has a reported stiffness of 3.21±1.97 (Mercado et al.,2018), whereas a fibrinogen clot created with a concentration of 15mg/ml can have a strength of up to 45 kPa (Alston et al., 2007). Platelets have also shown to play a key role in the clots stiffness, platelet rich clots have been reported to have a stiffness of 600 Pa whereas platelet free clots stiffness is only 70 Pa (Jen et al., 1982), this is also depending on the preparation methods of PRP and can have high variations between methods.

Hydrogels have a water content of 99% of their total composition. As such, clinically relevant solutions were used to dilute PA-K_3 solutions and characterisation of its secondary structure and effect on gelation was assessed. HEPES buffer, Ringer's lactate solution and Saline solution had no significant impact on the PA solubility, secondary structure or gelation properties. These results are encouraging for the future translation of these systems to in vivo models and clinical settings.

Altogether, these results presented initial insights into the understanding of the synergy established between PAs and biological fluids. Follow up studies on the molecular dynamics of these systems, including assays to determine the effect of different biomolecules on the assembly process and the properties of these new biomaterials could help build up a more in depth understanding of these materials behaviour.

7.1.3 Design of new PA sequences

The second thesis objective was 'to tailor and design a set of new self-assembling peptides to enhance interactions with blood components'. The studies presented in Chapter 4 aimed to address this objective.

7.1.3.1 Summary of findings, perspective and future work

PAs were designed to display lysine and glutamine amino acids in order to be selectively cross-linked with fibrin via clotting Factor XIII during the triggering of blood coagulation. The use of this enzyme to crosslink fibrin to peptides has been previously demonstrated (Ehrbar et al.,2007), and in this case, our rationale is that it would

enable PA nanofibre-fibrin integration and regulation of structural and mechanical properties of the resulting material.

Four different materials displaying these two key amino acid residues in different order named PA-K_3Q, PA-K_3Q_3, PA-Q_3K_3 and PA-$(KQ)_3$ were characterised and tested (Section 4.1.4). Due to lack of solubility in biologically compatible buffers or inability to create hydrogels, PA-K_3Q_3 and PA-$(KQ)_3$ were not used for further testing.

The estimated Young's moduli of highly retracted and mildly retracted human blood clots is 3.21 ± 1.97 and 0.79 ± 0.21 kPa, respectively (Mercado et al., 2019). By using different types of PAs we were able to create hydrogels that represent these variations in stiffness. For example, PA- Blood scaffolds created using PA-K_3 showed a storage modulus of 1.65 ± 0.13 kPa whereas scaffolds created with the new sequence PA-K_3Q showed a stiffness of 2.32 ± 0.43 kPa after 3 hours of incubation. PA-Q_3K_3 gels were very brittle and could not withstand mechanical testing. The addition of cysteine residues in the PA molecules could be used as strategy to create disulphide bonds in the materials, thus strengthening their mechanical properties. This type of covalent bonds is present in nature and is well known for its role in stabilising protein structures (William et al.,2000). Moreover, the combination of different peptides could also help the creation of materials that strengthen over time and more closely mimic the natural progression of healing of an injury. This could be useful to establish new biologically relevant in vitro models to help study the wound healing process as well as the mechanics behind non-healing injuries.

Furthermore, PAs could also be designed to selectively bind other structural and signalling cues. For example, the sequence *DICLPRWGCLW* binds albumin (Dennis et

al., 2002), which could further manipulate the coagulation process and control clotting properties, or the short peptides *AGD* (Sanchez et al., 2009) and *GRGDS* (Haverstick et al., 1985) which have been shown to regulate platelet binding, could help to modulate their activation and aggregation as well as their integration to the PA – Blood material. These modifications could enable temporal control of platelet activation and release of key cytokines and growth factors, which represent critical point of optimisation of the bioactivity and functionality of the resulting PA – Blood materials. PAs displaying growth factor binding sequences such as *DRVQRQTTTVVA*, which can selectively bind VEGF, could also help to control the growth factor distribution on the hydrogels as well as its controlled release to enhance angiogenesis (Adini et al., 2017). Moreover, the heparin molecule has been studied for its ability to bind growth factors such as VEGF and FGF-2. Peptide sequences like *LRKKLGKA* have demonstrated its ability to bind heparin (Rajagam et al., 2006; Rajagam et al., 2008). Other short peptide sequences such as *REDV* have shown to promote endothelial cell recruitment (Ippel et al.,2018; Ceylan et al., 2011)

The findings of this first part of the research suggest that the versatility of design of peptide amphiphiles represent an attractive tool to improve mechanical and structural features in PA-based hydrogels, but also to incorporate bioactive sequences to further direct the interaction with blood molecules of interest.

7.1.4 Tissue engineering applications

The third thesis objective was ‘Evaluate the biocompatibility of the new peptide amphiphiles and their potential to be used for tissue engineering and regenerative

medicine applications'. The studies presented in Chapter 5 aimed to address this objective.

7.1.4.1 Summary of findings, perspective and future work

PAs compatibility with blood was a key step of evaluation for their potential use in biological settings. Biomaterials can cause haemolysis, which leads to RBCs rupture and haemoglobin release. Some peptides have shown to trigger haemolysis and can be harmful depending on the degree of damage caused. For this application, haemolysis would be detrimental for the use of PAs in clinical applications as it would both damage blood cells causing toxicity and also, affect the materials' properties. Studies on haemolysis showed that PA-K_3 and PA-K_3Q did not present an increase in haemoglobin concentration in plasma after incubation with blood, an indication of their haemocompatibility, whereas PA-Q_3K_3 did show a slight increase on haemoglobin concentration in plasma. Follow up analysis to validate the biological effect of PA-Q_3K_3 would be required to determine the extent of its potential toxicity in vivo.

A major advantage of the project is the capability to incorporate and cooperatively work with endogenous blood cell populations to enhance inflammation, immunomodulation, and regeneration. The different blood cell populations were identified by SEM (RBCs, WBCs, platelets) and confocal microscopy (platelets). Further studies using specific markers for these cells could be helpful to detect and quantify specific blood cells types of interest.

Protein release studies showed that a burst release of proteins occurs on Day 1. Immunomodulatory molecules involved in wound healing (IL-1, IL-4, IL-6, IL-13, TNF-α, and TNF-β) were found in the supernatants. In addition, growth factors of interest like EGF, IGF-1, VEGF and PDGF-BB, know to enhance cell proliferation were also detected in supernatant samples. It is hypothesised that this initial release had different effects on cell behaviour. For example, fibroblasts cells showed fast growth and multiple layers of cells growing on the scaffolds, whereas endothelial cells (HUVECs) presented organisation into tubular-like structures. In the case of mesenchymal cells (hMSCs), cell migration was observed.

While the studies confirmed cell health and proliferation of different types of cells on the PA – Blood scaffolds, additional longer term studies on the effect of these scaffolds in cell organisation and differentiation would be beneficial to determine its suitability for a specific tissue engineering application. In addition, translation of these in vitro models into in vivo models would allow the study of immune reaction as well as wound healing capacity of these materials.

7.1.5 Potential for biofabrication

The fourth thesis objective was to 'Develop a new 3D-printing system by using peptide amphiphiles as bio-inks for 3D-printing of scaffolds'. The studies presented in Chapter 6 aimed to address this objective.

7.1.5.1 Summary of findings, perspective and future work

A 'liquid-into-liquid' bioprinting method was developed using extrusion 3D-printing. The potential of this co-assembly system to be used as a liquid in liquid bioprinting

technology was investigated by using PA-K_3 as a bioink printed into a bath of blood or blood fractions.

There are a number of examples of peptide-based bioinks and blood fractions-based bioinks (Section 2.4.2), however the use of peptide amphiphiles and whole blood has not been explored before to the best of our knowledge. An example of a comparable method of bioprinting to the one proposed in this work, is the development of PA-based bioink by using an inkjet method to print a peptide amphiphile on a pool of protein (Hedegaard et al., 2018).

Initial testing of PAs potential as bioink was evaluated by a simple test of manually injecting PA solution into a blood or PRP bath. This study showed that the co-assembly system gelation speed was fast enough to promote hydrogel formation in the form of drops on the bath solutions. It was also demonstrated that gels were able to remain attached together due to their glue-like properties. Further analysis using atomic force microscopy (AFM) may shed light on the adhesive properties and potential differences between materials.

For extrusion experiments, the initial evaluation of different parameters including printing pressure and speed were tested. Further optimisation of the PA bioink properties such as adjustment of viscosity and concentration is needed to improve the scaffolds' properties. A follow up study on the effect of the use of higher PA concentrations could help speed up the process of gelation and improve mechanical properties. Furthermore, it has been reported that higher viscosity of bioinks or supporting baths can help improve shape fidelity (Moxon et al.,2017; Hinton et al., 2015).

A key aspect of the developed biofabrication method is the ability to direct the internal (nanofibres) and external (grooves and ridges) features of the scaffolds at different levels. A follow up in vitro study with cells may highlight how these features affect the cellular response to the 3D-printed scaffolds. For example, previous studies haven show cells tend to directionally align with aligned nanofibres (Zhang et al., 2010). However, it remains to be studied how the observed microstructures created by the printing process may affect the cells response.

The results of this proof of concept study suggest that this method could be explored further for the creation of more complex scaffolds and opens up the possibility for larger scale automated production and reduction of the manufacturing process costs by printing the materials into biological fluids of patients. A key advantage of the development of this technology is the presentation of an alternative personalised, reproducible and scalable material that reduces the need to use animal-based or donor-based materials.

7.2 Closing statement

The incorporation of ions and biomolecules present in blood as building blocks is the central piece to develop our materials. We believe that by mimicking key aspects related to ECM properties, structure and protein location present in naturally occurring scaffolds (e.g. fibrin clots) we will be able to create personalised, biocompatible and highly smart materials that enhance tissue regeneration.

The research work presented in this thesis is part of an emerging field within self-assembling systems and bioprinting. The aim was to demonstrate the merits of combining self-assembling peptides with biological fluids and bioprinting technologies to illustrate the potential benefits of having a myriad of bioactive molecules incorporated into a scaffold and hierarchical levels of control (molecular to macroscale) that could prove helpful for tissue engineering applications.

In summary, the development of these PA – Blood scaffolds opens up the possibility of exploring the generation of new alternative materials for regenerative medicine by creating a bio-cooperative design and fabrication platform with the potential to harness and optimise the regenerative capabilities of the human body.

Bibliography

Abelseth E., Abelseth L., De la Vega L.,Beyer S., Wandsworth S.,Willerth S. (2018).ACS Biomater. Sci. Eng. 2019, 5, 1, 234–243

Abune L, Wang Y. (2021). Affinity Hydrogels for Protein Delivery,Trends in Pharmacological Sciences, 42 4, 300-312, https://doi.org/10.1016/j.tips.2021.01.005.

Adini, A., Adini, I., Chi, Z. L., Derda, R., Birsner, A. E., Matthews, B. D., & D'Amato, R. J. (2017). A novel strategy to enhance angiogenesis in vivo using the small VEGF-binding peptide PR1P. Angiogenesis, 20(3), 399–408. https://doi.org/10.1007/s10456-017-9556-7

Ahearne M. (2014). Introduction to cell-hydrogel mechanosensing. *Interface focus*, *4*(2), 20130038. https://doi.org/10.1098/rsfs.2013.0038

Ajovalasit A, Redondo-Gómez C, Sabatino MA, Okesola BO, Braun K, Mata A, Dispenza C. Carboxylated-xyloglucan and peptide amphiphile co-assembly in wound healing. Regen Biomater. 2021 Aug 11;8(5):rbab040. doi: 10.1093/rb/rbab040. PMID: 34386265; PMCID: PMC8355605.

Alberts B, Johnson A, Lewis J, et al. Molecular Biology of the Cell. 4th edition. New York: Garland Science; 2002. Blood Vessels and Endothelial Cells. Available from: https://www.ncbi.nlm.nih.gov/books/NBK26848/

Alves R, Grimalt R: A Review of Platelet-Rich Plasma: History, Biology, Mechanism of Action, and Classification. Skin Appendage Disord 2018;4:18-24. doi: 10.1159/000477353

Anderson JM et al. Foreign body reaction to biomaterials. Seminars in Immunology 2008, 20(2), 86-100, 10.1016/j.smim.2007.11.004.

Anderson, J. M., Kushwaha, M., Tambralli, A., Bellis, S. L., Camat, R. P., Jun, H. W. (2009). Osteogenic differentiation of human mesenchymal stem cells directed by extracellular matrix-mimicking ligands in a biomimetic self-assembled peptide

amphiphile nanomatrix. Biomacromolecules 10(10):2935-44. doi: 10.1021/bm9007452.

Andrée, B., Ichanti, H., Kalies, S. et al. Formation of three-dimensional tubular endothelial cell networks under defined serum-free cell culture conditions in human collagen hydrogels. Sci Rep 9, 5437 (2019). https://doi.org/10.1038/s41598-019-41985-6

Appay, V., & Rowland-Jones, S. L. (2001). RANTES: A versatile and controversial chemokine. Trends in Immunology, 22(2), 83–87. https://doi.org/10.1016/S1471-4906(00)01812-3

Ashton NJ, Hye A, Rajkumar AP, Leuzy A, Snowden S, Suárez-Calvet M, Karikari TK, Schöll M, La Joie R, Rabinovici GD, Höglund K, Ballard C, Hortobágyi T, Svenningsson P, Blennow K, Zetterberg H, Aarsland D. An update on blood-based biomarkers for non-Alzheimer neurodegenerative disorders. Nat Rev Neurol. 2020 May;16(5):265-284. doi: 10.1038/s41582-020-0348-0. Epub 2020 Apr 22. PMID: 32322100.

Atala A et al. Principles of Regenerative Medicine (Third Edition) 2019, Preface, Academic Press, Elsevier Inc., ISBN: 978-0-12-809880-6.

Aurora A, Wrice N, Walters TJ, Christy RJ, Natesan S. A PEGylated platelet free plasma hydrogel based composite scaffold enables stable vascularization and targeted cell delivery for volumetric muscle loss. Acta Biomater. 2018 Jan;65:150-162. doi: 10.1016/j.actbio.2017.11.019. Epub 2017 Nov 8. PMID: 29128541.

Avent ND, Reid ME. The Rh blood group system: a review. Blood. 2000 Jan 15;95(2):375-87. Erratum in: Blood 2000 Apr 1;95(7):2197. PMID: 10627438.

Axpe E, Chan D, Offeddu GS, Chang Y, Merida D, Hernandez HL, Appel EA. A Multiscale Model for Solute Diffusion in Hydrogels. Macromolecules. 2019 Sep 24;52(18):6889-6897. doi: 10.1021/acs.macromol.9b00753. Epub 2019 Sep 3. PMID: 31579160; PMCID: PMC6764024.

Azevedo, H., da Silva, R. (2018). Self-assembling Biomaterials. Molecular Design, Characterization and Application in Biology and Medicine. Chapter 18:371-390.

Baggiolini, Marco and Clark-Lewis, Ian(1992), Interleukin-8, a chemotactic and inflammatory cytokine, FEBS Letters, 307, doi: 10.1016/0014-5793(92)80909-Z

Bailey SR and Maus MV. Gene editing for immune cell therapies. Nature Biotechnology 2019, 37, 1425-1434, 10.1038/s41587-019-0137-8.

Bainbridge P. (2013). Wound healing and the role of fibroblasts. *Journal of wound care*, *22*(8), 407–412. https://doi.org/10.12968/jowc.2013.22.8.407

Basu, D., & Kulkarni, R. (2014). Overview of blood components and their preparation. *Indian journal of anaesthesia*, *58*(5), 529–537. https://doi.org/10.4103/0019-5049.144647

Bates I, Bain B. Approach to the diagnosis and classification of blood diseases Dacie and Lewis Practical Haematology. 2006 Jan:609-624. PMCID: PMC7152454.

Behanna, H. A., Donners, J. J. J. M., Gordon, A. C., & Stupp, S. I. (2005). Coassembly of amphiphiles with opposite peptide polarities into nanofibers. Journal of the American Chemical Society, 127(4), 1193–1200. https://doi.org/10.1021/ja044863u

Beniash, E., Hartgerink, J. D., Storrie, H., Stendahl, J. C., & Stupp, S. I. (2005). Self-assembling peptide amphiphile nanofiber matrices for cell entrapment, Acta Biomaterialia, 1, 387–397. http://doi.org/10.1016/j.actbio.2005.04.002

Berman, K. Henrick, H. Nakamura (2003) Announcing the worldwide Protein Data Bank Nature Structural Biology 10 (12): 980.

Beychok S. (1996). Circular dichroism of biological macromolecules. Science 9; 154(3754): 1288-99.

Bhadra, A. When life played dice with royal blood. *Reson* **20,** 769–787 (2015). https://doi.org/10.1007/s12045-015-0237-9

Bonhome-Espinosa AB, Campos F, Durand-Herrera D, Sánchez-López JD, Schaub S, Durán JDG, Lopez-Lopez MT, Carriel V. In vitro characterization of a novel magnetic fibrin-agarose hydrogel for cartilage tissue engineering. J Mech Behav Biomed Mater. 2020 Apr;104:103619. doi: 10.1016/j.jmbbm.2020.103619. Epub 2020 Jan 9. PMID: 32174386.

Brassard JA and Lutolf MP. Engineering stem cell self-organization to build better organoids. Cell Stem Cells 2019, 24(6), 860-876, 10.1016/j.stem.2019.05.005

Broughton, G., Jeffrey, E. J., Attinger, C. E. (2006). The Basic Science of Wound Healing. Plast Reconstr Surg. 117(7 Suppl):12S-34S. DOI: 10.1097/01.prs.0000225430.42531.c2

Brown, A. C., Stabenfeldt, S. E., Ahn, B., Hannan, R. T., Dhada, K. S., Herman, E. S., Barker, T. H. (2014). Ultrasoft microgels displaying emergent platelet-like behaviours. Nature Materials, 13(12), 1108–1114. https://doi.org/10.1038/nmat4066

Burnouf T, Goubran HA, Chen TM, Ou KL, El-Ekiaby M, Radosevic M. Blood-derived biomaterials and platelet growth factors in regenerative medicine. Blood Rev. 2013 Mar;27(2):77-89. doi: 10.1016/j.blre.2013.02.001. Epub 2013 Feb 19. PMID: 23434399.

Burnouf, T., Su, C.-Y., Radosevich, M., Goubran, H. and El-Ekiaby, M. (2009), Blood-derived biomaterials: fibrin sealant, platelet gel and platelet fibrin glue. ISBT Science Series, 4: 136-142. https://doi.org/10.1111/j.1751-2824.2009.01222.x

Butterfield T. A. The dual roles of neutrophils and macrophages in inflammation: A critical balance between tissue damage and repair. Journal of Athletic Training 2006, 41(4), 457–465.

Buscail E, Chiche L, Laurent C, Vendrely V, Denost Q, Denis J, Thumerel M, Lacorte JM, Bedel A, Moreau-Gaudry F, Dabernat S, Alix-Panabières C. Tumor-proximal liquid biopsy to improve diagnostic and prognostic performances of circulating tumor cells. Mol Oncol. 2019 Sep;13(9):1811-1826. doi: 10.1002/1878-0261.12534. Epub 2019 Jul 25. PMID: 31216108; PMCID: PMC6717761.

Carr Jr ME and Hardin CL. Fibrin has larger pores when formed in the presence of erythrocytes. Heart and Circulatory Physiology 1987, 253(5), H1069-H1073, 10.1152/ajpheart.1987.253.5.H1069.

Castelo-Branco, C., & Soveral, I. (2014). The immune system and aging: a review. Gynecological endocrinology : the official journal of the International Society of Gynecological Endocrinology, 30(1), 16–22. https://doi.org/10.3109/09513590.2013.852531

Cattaneo, M., Lecchi, A., Loredana Zighetti, M., Lussana, F. (2007). "Platelet aggregation studies: autologous platelet-poor plasma inhibits platelet aggregation when added to platelet-rich plasma to normalize platelet count". Haematologica, 92(05).

Cavalli S., Albericio, F., Kros A. (2010). Amphiphilic peptides and their cross-disciplinary role as building blocks for nanoscience. Chem Soc Rev. (1):241-63. doi: 10.1039/b906701a.

Ceylan H., Ayse B. Tekinay, Mustafa O. Guler. (2011). Selective adhesion and growth of vascular endothelial cells on bioactive peptide nanofiber functionalized stainless steel surface, Biomaterials 32: 34. ISSN 0142-9612. https://doi.org/10.1016/j.biomaterials.2011.08.018

Chan, K.Y.T., Yong, A.S.M., Wang, X. *et al.* The adhesion of clots in wounds contributes to hemostasis and can be enhanced by coagulation factor XIII. *Sci Rep* **10,** 20116 (2020). https://doi.org/10.1038/s41598-020-76782-z

Chang CY, Chan AT, Armstrong PA, Luo HC, Higuchi T, Strehin IA, Vakrou S, Lin X, Brown SN, O'Rourke B, Abraham TP, Wahl RL, Steenbergen CJ, Elisseeff JH, Abraham MR. Hyaluronic acid-human blood hydrogels for stem cell transplantation. Biomaterials. 2012 Nov;33(32):8026-33. doi: 10.1016/j.biomaterials.2012.07.058. Epub 2012 Aug 13. PMID: 22898181; PMCID: PMC3432174.

Chapter 5 - Effect of Polymer-Based Nanoparticles on the Assay of Antimicrobial Drug Delivery Systems. Multifunctional Systems for Combined Delivery, Biosensing and Diagnostics, Elsevier, 2017, Pages 67-108, https://doi.org/10.1016/B978-0-323-52725-5.00005-8.

Chen, J., Zheng, S., Zhao, H. et al. Structure-aware protein solubility prediction from sequence through graph convolutional network and predicted contact map. J Cheminform 13, 7 (2021). https://doi.org/10.1186/s13321-021-00488-1

Cheng SY, Heilman S, Wasserman M, Archer S, Shuler ML, Wu M. 2007. A hydrogel-based microfluidic device for the studies of directed cell migration. *Lab Chip* **7**, 763–769. (10.1039/b618463d)

Cheng, T., Chen, M., Chang, W., Huang, M., & Wang, T. (2016). Neural stem cells encapsulated in a functionalized self-assembling peptide hydrogel for brain tissue engineering. Biomaterials, 34(8), 2005–2016. http://doi.org/10.1016/j.biomaterials.2012.11.043

Chernysh IN et al. Fibrin clots are equilibrium polymers that can be remodelled without proteolytic digestion. Scientific Reports 2012, 2, 879, DOI: 10.1038/srep00879.

Codreanu, Florina. (2015). BLOOD UTOPIA. EXPERIMENTATION WITH BLOOD IN CONTEMPORARY ART.

Cohen JD, Li L, Wang Y, Thoburn C, Afsari B, Danilova L, Douville C, Javed AA, Wong F, Mattox A, Hruban RH, Wolfgang CL, Goggins MG, Dal Molin M, Wang TL, Roden R, Klein AP, Ptak J, Dobbyn L, Schaefer J, Silliman N, Popoli M, Vogelstein JT, Browne JD, Schoen RE, Brand RE, Tie J, Gibbs P, Wong HL, Mansfield AS, Jen J, Hanash SM, Falconi M, Allen PJ, Zhou S, Bettegowda C, Diaz LA Jr, Tomasetti C, Kinzler KW, Vogelstein B, Lennon AM, Papadopoulos N. Detection and localization of surgically resectable cancers with a multi-analyte blood test. Science. 2018 Feb 23;359(6378):926-930. doi: 10.1126/science.aar3247. Epub 2018 Jan 18. PMID: 29348365; PMCID: PMC6080308.

Cui, H., Webber, M. J., & Stupp, S. I. (2010). Self-assembly of peptide amphiphiles: From molecules to nanostructures to biomaterials. Peptide Science 94(1), 1–18. http://doi.org/10.1002/bip

Culver, H. R., Clegg, J. R., & Peppas, N. A. (2016). Analyte-Responsive Hydrogel: Intelligent Materials for Biosensing and Drug Delivery. Accounts of Chemical Research. http://doi.org/10.1021/acs.accounts.6b00533

da Silva, R., van der Zwaag, D., Albertazzi, L. et al. Super-resolution microscopy reveals structural diversity in molecular exchange among peptide amphiphile nanofibres. Nat Commun 7, 11561 (2016). https://doi.org/10.1038/ncomms11561

Davidson, C. (1997). Sacred Blood and the Late Medieval Stage. *Comparative Drama 31*(3), 436-458. doi:10.1353/cdr.1997.0039.

Dehsorkhi, A., Castelletto, V., & Hamley, I. W. (2014). Self-assembling amphiphilic peptides. Journal of Peptide Science, 20(7), 453–467. http://doi.org/10.1002/psc.2633

Dennis, C. Haemoglobin scavenger. *Nature* 409, 141 (2001). https://doi.org/10.1038/35051680

Dennis, M. S., Zhang, M., Meng, Y. G., Kadkhodayan, M., Kirchhofer, D., Combs, D., … Thromb, D. (2002). Albumin Binding as a General Strategy for Improving the Pharmacokinetics of Proteins *, 277(38), 35035–35043. doi:10.1074/jbc.M205854200

Derkus, B., Okesola, B. O., Barrett, D. W., D'Este, M., Chowdhury, T. T., Eglin, D., & Mata, A. (2020). Multicomponent hydrogels for the formation of vascularized bone-like constructs in vitro. Acta Biomaterialia, 109, 82–94. https://doi.org/10.1016/j.actbio.2020.03.025

Diegelmann R.F., Evans, M. C. (2004). Wound healing: An overview of acute, fibrotic and delayed healing. Frontiers in Bioscience 9, 283-289

Ding Y, Li Y, Qin M, Cao Y, Wang W. (2013). Photo-cross-linking approach to engineering small tyrosine-containing peptide hydrogels with enhanced mechanical stability. Langmuir 29(43):13299-306. doi: 10.1021/la4029639.

Edwards-Gayle, C.J. C. & Hamley I. H. (2017). Self-assembly of bioactive peptides, peptide conjugates, and peptide mimetic materials Org. Biomol. Chem. 15, 5867-5876. DOI: 10.1039/C7OB01092C

Electronic Medicines Compendium UK, 2018. https://www.medicines.org.uk/emc/product/1869/smpc#gref

El-sherbiny, I. M., & Yacoub, M. H. (2013). Review article Hydrogel scaffolds for tissue engineering: Progress and challenges. Global Cardiology Science and Practice 2013:38 http://dx.doi.org/10.5339/gcsp.2013.38

Engler, A. J., Sen S, Sweeney HL, Discher DE. (2006). Matrix elasticity directs stem cell lineage specification. Cell 25;126(4):677-89.

Everts, P. A., Knape, J. T., Weibrich, G., Schönberger, J. P., Hoffmann, J., Overdevest, E. P., Box, H. A., & van Zundert, A. (2006). Platelet-rich plasma and platelet gel: a review. The journal of extra-corporeal technology, 38(2), 174–187.

Farhud, D. D., & Zarif Yeganeh, M. (2013). A brief history of human blood groups. *Iranian journal of public health*, *42*(1), 1–6.

Faulkner-Jones A, C. Fyfe, D.-J. Cornelissen, J. Gardner, J. King, A. Courtney, and W. Shu. Bioprinting of human pluripotent stem cells and their directed differentiation into hepatocyte-like cells for the generation of mini-livers in 3D. Biofabrication, 7(4):044102, 2015.

FDA, 2020. https://www.fda.gov/vaccines-blood-biologics/cellular-gene-therapy-products/approvedcellularand-gene-therapy-products

Williams DF. Challenges with the development of biomaterials for sustainable tissue engineering. Frontiers in Bioengineering and Biotechnology 2019, 7(127), 10.3389/fbioe.2019.00127.

Ferreira, D. S., Marques, A. P., Reis, R. L., & Azevedo, H. S. (2013). Hyaluronan and self-assembling peptides as building blocks to reconstruct the extracellular environment in skin tissue. Biomaterials Science, 1(9), 952–964. https://doi.org/10.1039/c3bm60019j

Francis J. Castellino, in Handbook of Proteolytic Enzymes (Third Edition), 2013.

Fu, I. W., Markegard, C. B., Chu, B. K., Nguyen, H. D. (2013). The role of electrostatics and temperature on morphological transitions of hydrogel nanostructures self-assembled by peptide amphiphiles via molecular dynamics simulations. Adv Healthc Mater. 2(10):1388-400. doi: 10.1002/adhm.201200400.

Fu, I.W., Markegard, C.B., Chu, B.K., and Nguyen, H.D. (2014). Role of Hydrophobicity on Self-Assembly by Peptide Amphiphiles via Molecular Dynamics Simulations. Langmuir 30, 7745–7754.

Furukawa, T. (1930). A study of temperament and blood-groups. *The Journal of Social Psychology, 1,* 494–509. https://doi.org/10.1080/00224545.1930.9714153

Geier, Steven, Ph. D. 1994. Personal Communication: Analysis of alamarBlue Overlap: Contribution of Oxidized (ABOlOD6OOnm) to Reduced (ABRlOD570) OD.

Gerberding JL. Management of occupational exposures to blood-borne viruses. N Engl J Med. 1995 Feb 16;332(7):444-51. doi: 10.1056/NEJM199502163320707. PMID: 7824017.

Giangrande, P.L.F. (2000), The history of blood transfusion. British Journal of Haematology, 110: 758-767. https://doi.org/10.1046/j.1365-2141.2000.02139.x

Good NE, Winget GD, Winter W, Connolly TN, Izawa S, Singh RMM. Hydrogen ion buffers for biological research. *Biochem Int.* 1966;5(2):467–477. doi: 10.1021/bi00866a011.

Gopinathan, J., & Noh, I. (2018). Recent trends in bioinks for 3D printing. *Biomaterials research*, *22*, 11. https://doi.org/10.1186/s40824-018-0122-1

Grazul-Bilska, A. T., Johnson, M. L., Bilski, J. J., Redmer, D. A., Reynolds, L. P., Abdullah, A., & Abdullah, K. M. (2003). Wound healing: the role of growth factors. Drugs of today (Barcelona, Spain: 1998), 39(10), 787–800. https://doi.org/10.1358/dot.2003.39.10.799472

Greenfield, N. J. (2006). Using circular dichroism spectra to estimate protein secondary structure. Nature protocols 1(6): 2876-2890. doi:10.1038/nprot.2006.202.

Guerrero, R. B., Salazar, D., & Tanpaiboon, P. (2018). Laboratory diagnostic approaches in metabolic disorders. *Annals of translational medicine*, *6*(24), 470. https://doi.org/10.21037/atm.2018.11.05

Guler, M.O., Hsu, L., Soukasene, S., Harrington, D.A., Hulvat, J.F., and Stupp, S.I. (2006). Presentation of RGDS Epitopes on Self-Assembled Nanofibers of Branched Peptide Amphiphiles. Biomacromolecules 7, 1855–1863.

Gumustas, Ceyda T. Sengel-Turk, Aysen Gumustas, Sibel A. Ozkan, Bengi Uslu,

Gupta A. (2017). Bio-inspired nanomedicine strategies for artificial blood components. *Wiley interdisciplinary reviews. Nanomedicine and nanobiotechnology*, *9*(6), 10.1002/wnan.1464. https://doi.org/10.1002/wnan.1464

H. Azevedo and R. Reis. Understanding the Enzymatic Degradation of Biodegradable Polymers and Strategies to Control Their Degradation Rate. In Biodegradable Systems in Tissue Engineering and Regenerative Medicine, pages 177{202. CRC Press, 2004

Handorf AM, Zhou Y, Halanski MA, Li WJ. Tissue stiffness dictates development, homeostasis, and disease progression. Organogenesis. 2015;11(1):1-15. doi: 10.1080/15476278.2015.1019687. PMID: 25915734; PMCID: PMC4594591.

Hartgerink, E. Beniash, and S. I. Stupp. (2002). Peptide-amphiphile nanofibers: A versatile scaffold for the preparation of self-assembling materials. Proceedings of the National Academy of Sciences, 99(8):5133{5138

Hartgerink, E. Beniash, and S. I. Stupp. (2001). Self-Assembly and Mineralization of Peptide-Amphiphile Nanofibers. Science, 294(5547):1684{1688.

Hedegaard C L and Mata A 2020 Integrating self-assembly and biofabrication for the development of structures with enhanced complexity and hierarchical control Biofabrication 12 032002

Hedegaard, C. L., Collin, E. C., Redondo-Gómez, C., Nguyen, L. T. H., Ng K.W., Castrejón-Pita, A. A., Castrejón-Pita, J. R., Mata, A. (2018). Hydrodynamically Guided Hierarchical Self-Assembly of Peptide–Protein Bioinks. Advanced Functional Materials (28): 1703716. https://doi.org/10.1002/adfm.201703716

Heireman, L., Van Geel, P., Musger, L., Heylen, E., Uyttenbroeck, W., & Mahieu, B. (2017). Causes, consequences and management of sample hemolysis in the clinical laboratory. *Clinical biochemistry*, *50*(18), 1317–1322. https://doi.org/10.1016/j.clinbiochem.2017.09.013

Hendricks, M.P., K. Sato, L. C. Palmer, and S. I. Stupp. (2017). Supramolecular Assembly of Peptide Amphiphiles. Accounts of Chemical Research, 50(10):2440-2448.

Her GJ, Wu HC, Chen MH, Chen MY, Chang SC, Wang TW. (2013). Control of three-dimensional substrate stiffness to manipulate mesenchymal stem cell fate toward neuronal or glial lineages. Acta Biomater. 9(2):5170-80. doi: 10.1016/j.actbio.2012.10.012.

Highley C. B., C. B. Rodell, and J. A. Burdick. Direct 3D Printing of Shear-Thinning Hydrogels into Self-Healing Hydrogels. Advanced Materials, 27(34):5075{5079, 2015.

Hinton T J, Jallerat Q, Palchesko R N, Park J H, Grodzicki M S, Shue H J, Ramadan M H, Hudson A R and Feinberg A W 2015 Three-dimensional printing of complex biological structures by freeform reversible embedding of suspended hydrogels Sci. Adv. 1 e1500758

Hoff, P. (2016). Immunological characterization of the early human fracture hematoma. Immunologic Research, 64, 1195–1206, 10.1007/s12026-016-8868-9.

Hunter, R.J. (1988) Zeta Potential In Colloid Science: Principles And Applications, Academic Press, UK.

Inostroza-Brito, K. E., Collin, E. C., Majkowska, A., Elsharkawy, S., Rice, A., Del Río Hernández, A. E., Xiao, X., Rodríguez-Cabello, J., Mata, A. (2017). Cross-linking of a biopolymer-peptide co-assembling system. Acta Biomaterialia (58): 80-89. https://doi.org/10.1016/j.actbio.2017.05.043.

Inostroza-brito, K. E., Collin, E., Siton-mendelson, O., Smith, K. H., Monge-marcet, A., Ferreira, D. S., & Mata, A. (2015). Co-assembly, spatiotemporal control and morphogenesis of a hybrid protein – peptide system. Nature Chemistry, 7(11), 897–904. http://doi.org/10.1038/nchem.2349

Ippel, B. D., Dankers, P. Y. W. (2018). Introduction of Nature's Complexity in Engineered Blood-compatible Biomaterials Adv. Healthcare Mater. 2018, 7, 1700505. https://doi.org/10.1002/adhm.201700505

Jain E, Sheth S, Dunn A, Zustiak SP, Sell SA. Sustained release of multicomponent platelet-rich plasma proteins from hydrolytically degradable PEG hydrogels. J Biomed Mater Res A. 2017 Dec;105(12):3304-3314. doi: 10.1002/jbm.a.36187. Epub 2017 Sep 19. PMID: 28865187.

Jeffrey E. J., Harrison, B. (2014). Plastic and Reconstructive Surgery. 133(2):199e–207e. DOI: 10.1097/01.prs.0000437224.02985.f9

Jell G., Minelli C., Stevens M. (2009) Biomaterial-Related Approaches: Surface Structuring. In: Meyer U., Handschel J., Wiesmann H., Meyer T. (eds) Fundamentals of Tissue Engineering and Regenerative Medicine. Springer, Berlin, Heidelberg. https://doi.org/10.1007/978-3-540-77755-7_35

Jen CJ, McIntire LV. The structural properties and contractile force of a clot. Cell Motil. 1982;2(5):445-55. doi: 10.1002/cm.970020504. PMID: 6891618.

Jeyakumar V., Niculescu-Morzsa E., Bauer C., Lacza Z., Nehrer S. (2017). Platelet-Rich Plasma Supports Proliferation and Redifferentiation of Chondrocytes during In Vitro Expansion. Front. Bioeng. Biotechnol. 5:75. doi: 10.3389/fbioe.2017.00075

Jiang, H., Guler, M.O., Stupp, S. I. (2007). The internal structure of self-assembled peptide amphiphiles nanofibers. Soft Matter 3, 454-462.

Johnson WC (1996) Circular dichroism instrumentation, in circular dichroism and the conformational analysis of biomolecules. Springer, pp 635–652

Jun, H.-W., Yuwono, V., Paramonov, S. and Hartgerink, J. (2005), Enzyme-Mediated Degradation of Peptide-Amphiphile Nanofiber Networks. Adv. Mater., 17: 2612-2617. https://doi.org/10.1002/adma.200500855

Kardos, D., Simon, M., Vácz, G., Hinsenkamp, A., Holczer, T., Cseh, D., Sárközi, A., Szenthe, K., Bánáti, F., Szathmary, S., Nehrer, S., Kuten, O., Masteling, M., Lacza, Z., & Hornyák, I. (2019). The Composition of Hyperacute Serum and Platelet-Rich Plasma Is Markedly Different despite the Similar Production Method. International journal of molecular sciences, 20(3), 721. https://doi.org/10.3390/ijms20030721

Kawase, T. (2015). Platelet-rich plasma and its derivatives as promising bioactive materials for regenerative medicine: basic principles and concepts underlying recent advances. Odontology, 103(2), 126–135. doi:10.1007/s10266-015-0209-2

Khalily, M. A., Goktas, M., Guler, M. O. (2015). Tuning viscoelastic properties of supramolecular peptide gels via dynamic covalent crosslinking. Org Biomol Chem. 13(7):1983-7. doi: 10.1039/c4ob02217c.

Kim, B. S., Baez, C., Atala, A. (2000). Biomaterials for tissue engineering. A. World J Urol 18, 2. https://doi.org/10.1007/s003450050002

Kim, O. V., Litvinov, R. I., Alber, M. S., & Weisel, J. W. (2017). Quantitative structural mechanobiology of platelet-driven blood clot contraction. Nature Communications, 8(1), 1–10. https://doi.org/10.1038/s41467-017-00885-x

Kohn DB. Gene therapy for blood diseases. Curr Opin Biotechnol. 2019 Dec;60:39-45. doi: 10.1016/j.copbio.2018.11.016. Epub 2018 Dec 29. PMID: 30599357.

Koutsopoulos, S. (2016). Self-assembling peptide nanofiber hydrogels in tissue engineering and regenerative medicine: Progress, design guidelines and applications. American Chemical Society, 1002–1016. http://doi.org/10.1002/jbm.a.35638

Kretlow, J. D., Klouda, L., Mikos, A. G. (2007). Injectable matrices and scaffolds for drug delivery in tissue engineering. Advanced Drug Delivery Reviews, 59(4-5), 263–273 http://dx.doi.org/10.1016/j.addr.2007.03.013

Kumar S, Alonzo M, Allen SC, Abelseth L, Thakur V, Akimoto J, Ito Y, Willerth SM, Suggs L, Chattopadhyay M, Joddar B. A Visible Light-Cross-Linkable, Fibrin-Gelatin-Based Bioprinted Construct with Human Cardiomyocytes and Fibroblasts. ACS Biomater Sci Eng. 2019 Sep 9;5(9):4551-4563. doi: 10.1021/acsbiomaterials.9b00505. Epub 2019 Aug 1. PMID: 32258387; PMCID: PMC7117097.

Kurita J, Miyamoto M, Ishii Y, Aoyama J, Takagi G, Naito Z, Tabata Y, Ochi M, Shimizu K. Enhanced vascularization by controlled release of platelet-rich plasma impregnated in biodegradable gelatin hydrogel. Ann Thorac Surg. 2011 Sep;92(3):837-44; discussion 844. doi: 10.1016/j.athoracsur.2011.04.084. PMID: 21871267.

Lam WA, Chaudhuri O, Crow A, Webster KD, Li TD, Kita A, Huang J, Fletcher DA. Mechanics and contraction dynamics of single platelets and implications for clot stiffening. Nat Mater. 2011 Jan;10(1):61-6. doi: 10.1038/nmat2903. Epub 2010 Dec 5. PMID: 21131961; PMCID: PMC3236662.

Langer, R., Vacanti, J. P. (1993).Tissue engineering. Science 260(5110), 920-926. DOI: 10.1126/science.8493529

Lee, E. Abelseth, L. de la Vega, S.M. Willerth. (2019). Bioprinting a novel glioblastoma tumor model using a fibrin-based bioink for drug screening, Materials Today Chemistry, 12, 78-84. https://doi.org/10.1016/j.mtchem.2018.12.005.

Lee, K., Silva, E. A., Mooney, D. J., Lee, K., Silva, E. A., & Mooney, D. J. (2011). Growth factor delivery-based tissue engineering: General approaches and a review of recent developments. Journal of the Royal Society Interface, 8, 153–170. http://doi.org/10.1098/rsif.2010.0223

Lee, O.-S., Liu, Y., and Schatz, G.C. (2012). Molecular dynamics simulation of β-sheet formation in self-assembled peptide amphiphile fibers. J Nanopart Res 14, 1–7.

Li, A., Dubey, S., Varney, M. L., Dave, B. J., & Singh, R. K. (2003). IL-8 Directly Enhanced Endothelial Cell Survival, Proliferation, and Matrix Metalloproteinases Production and Regulated Angiogenesis. The Journal of Immunology, 170(6), 3369 LP – 3376. https://doi.org/10.4049/jimmunol.170.6.3369

Li, H., Tan, C., & Li, L. (2018). Review of 3D printable hydrogels and constructs. Materials and Design, 159, 20–38. https://doi.org/10.1016/j.matdes.2018.08.023

Li, J., Zhang, Y.-P. and Kirsner, R.S. (2003), Angiogenesis in wound repair: Angiogenic growth factors and the extracellular matrix. Microsc. Res. Tech., 60: 107-114. https://doi.org/10.1002/jemt.10249

Li Z, Zhang X, Yuan T, Zhang Y, Luo C, Zhang J, Liu Y, Fan W. Addition of Platelet-Rich Plasma to Silk Fibroin Hydrogel Bioprinting for Cartilage Regeneration. Tissue Eng Part A. 2020 Aug;26(15-16):886-895. doi: 10.1089/ten.TEA.2019.0304. Epub 2020 Mar 4. PMID: 32031056.

Litvinov RI and Weisel JW. Role of red blood cells in haemostasis and thrombosis. ISBT Science Series 2017, 12(1), 176-183, 10.1111/voxs.12331.

Liu X, Yang Y, Niu X, Lin Q, Zhao B, Wang Y, Zhu L. An in situ photocrosslinkable platelet rich plasma - Complexed hydrogel glue with growth factor controlled release ability to promote cartilage defect repair. Acta Biomater. 2017 Oct 15;62:179-187. doi: 10.1016/j.actbio.2017.05.023. Epub 2017 May 10. PMID: 28501713.

Loo Y. and C. A. E. Hauser. Bioprinting synthetic self-assembling peptide hydrogels for biomedical applications. Biomedical Materials, 11(1):014103, 2015.

López-Otín, C., & Bond, J. S. (2008). Proteases: multifunctional enzymes in life and disease. The Journal of biological chemistry, 283(45), 30433–30437. https://doi.org/10.1074/jbc.R800035200

Löwik, D. W. P. M., & van Hest, J. C. M. (2004). Peptide based amphiphiles. Chemical Society Reviews, 33(4), 234–245. https://doi.org/10.1039/b212638a

Madl et al. Bioengineering strategies to accelerate stem cell therapeutics. Nature 2018, 557, 335-342, 10.1038/s41586-018-0089-z.

Maldini CR, Ellis GI, Riley JL. CAR T cells for infection, autoimmunity and allotransplantation. Nat Rev Immunol. 2018 Oct;18(10):605-616. doi: 10.1038/s41577-018-0042-2. PMID: 30046149; PMCID: PMC6505691.

Man, Daniel M.D.; Plosker, Harvey M.D.; Winland-Brown, Jill E. Ed.D., M.S.N., F.N.P.-C. The Use of Autologous Platelet-Rich Plasma (Platelet Gel) and Autologous Platelet-Poor Plasma (Fibrin Glue) in Cosmetic Surgery, Plastic and Reconstructive Surgery: January 2001 - Volume 107 - Issue 1 - p 229-236

Mao AS and Mooney DJ. Regenerative medicine: Current therapies and future directions. PNAS 2015, 112(47), 14452-14459, 10.1073/pnas.1508520112.

Marsell R and Einhorn TA. The biology of fracture healing. Injury 2011, 42, 551-555, 10.1016/j.injury.2011.03.031.

Mata, A., Azevedo, H. S., Botto, L., Gavara, N., & Su, L. (2017). New Bioengineering Breakthroughs and Enabling Tools in Regenerative Medicine. Current Stem Cell Reports, http://doi.org/10.1007/s40778-017-0081-9

Mata, A., Hsu, L., Capito, R., Aparicio, C., & Stupp, S. I. (2009). Micropatterning of bioactive self-assembling gels. Soft Matter 5, 1228–1236. http://doi.org/10.1039/b819002j

Mata, A., Palmer, L., Tejeda-Montes, E., Stupp, S. I. (2012). Design of biomolecules for nanoengineered biomaterials for regenerative medicine. Methods Mol Biol. 2012;811:39-49. doi: 10.1007/978-1-61779-388-2_3.

Matson, J. B., R. Helen Zhab, H., & Stupp, S. I. (2011). Peptide self-assembly for crafting functional biological materials. Current Opinion in Solid State and Materials Science, 15(6), 225–235. http://dx.doi.org/10.1016/j.cossms.2011.08.001

Mehdizadeh, M., Yang, J. (2003). Design Strategies and Applications of Tissue Bioadhesives Macromol. Biosci. 13, 271–288.

Mehdizadeh, M., Yang, J. (2013). Design Strategies and Applications of Tissue Bioadhesives Macromol. Biosci. 13, 271–288. DOI: 10.1002/mabi.201200332

Mendes BB, Gómez-Florit M, Hamilton AG, Detamore MS, Domingues RMA, Reis RL, Gomes ME. Human platelet lysate-based nanocomposite bioink for bioprinting hierarchical fibrillar structures. Biofabrication. 2020 Nov 27;12(1):015012. doi: 10.1088/1758-5090/ab33e8. PMID: 31323659.

Mendes B. (2019). Biofabrication in press https://doi.org/10.1088/1758-5090/ab33e8

Mendes, A.C., Baran, E. T., Reis, R. L. and Azevedo, H. S. (2013). Self-assembly in nature: using the principles of nature to create complex nanobiomaterials. Wiley Interdisciplinary Reviews: Nanomedicine and Nanobiotechnology, 5(6):582-612.

Mendoza-Meinhardt, A., Lorenzo Botto, L., Mata, A. (2018). A fluidic device for the controlled formation and real-time monitoring of soft membranes self-assembled at liquid interfaces. Scientific Reports 8:2900. DOI:10.1038/s41598-018-20998-7

Mercado-Shekhar, Karla P. Effect of Clot Stiffness on Recombinant Tissue Plasminogen Activator Lytic Susceptibility in Vitro. Ultrasound in Medicine and Biology, Volume 44, Issue 12, 2710 - 2727 https://doi.org/10.1016/j.ultrasmedbio.2018.08.005

Mescher, Anthony L. (2018). "Blood". Junqueira's Basic Histology: Text and Atlas (15 ed.). McGraw-Hill Education. p. 237. ISBN 9781260026184.

Minasyan, H., & Flachsbart, F. (2019). Blood coagulation: a powerful bactericidal mechanism of human innate immunity. International reviews of immunology, 38(1), 3–17. https://doi.org/10.1080/08830185.2018.1533009

Mitchell AC et al. Engineering growth factors for regenerative medicine. Acta Biomaterialia 2016, 30, 1-12, 10.1016/j.actbio.2015.11.007.

Morgan FLC et al. Dynamic bioinks to advance bioprinting. Advanced Healthcare Materials 2020, 9(15), 1901798, 10.1002/adhm.201901798.

Mosesson, M. W., Kevin R. Siebenlist, David A. Meh, Joseph S. Wall, and James F. Hainfeld. (1998). The location of the carboxy-terminal region of γ chains in fibrinogen and fibrin D domains. PNAS 95(18), 10511-10516

Moxon S R, Cooke M E, Cox S C, Snow M, Jeys L, Jones S W, Smith A M and Grover L M 2017 Suspended manufacture of biological structures Adv. Mater. 29 1605594

Munson J, Amati V, Collard M, Macri MJ (2014) Classic Maya Bloodletting and the Cultural Evolution of Religious Rituals: Quantifying Patterns of Variation in Hieroglyphic Texts. PLOS ONE 9(9): e107982. https://doi.org/10.1371/journal.pone.0107982

Murphy S. and Atala A. 3D bioprinting of tissues and organs. Nature Biotechnology, 32(8):773{785, 2014.

Natesan S, Stone R, Coronado RE, et al. PEGylated Platelet-Free Blood Plasma-Based Hydrogels for Full-Thickness Wound Regeneration. Advances in Wound Care. 2019 Jul;8(7):323-340. DOI: 10.1089/wound.2018.0844. PMID: 31737420; PMCID: PMC6855295.

Neves, L.S., Babo, P.S., Gonçalves, A.I. *et al.* Injectable Hyaluronic Acid Hydrogels Enriched with Platelet Lysate as a Cryostable Off-the-Shelf System for Cell-Based Therapies. *Regen. Eng. Transl. Med.* **3,** 53–69 (2017). https://doi.org/10.1007/s40883-017-0029-8

Newcomb, S. Sur, J. H. Ortony, O.-S. Lee, J. B. Matson, J. Boekhoven, J. M. Yu, G. C. Schatz, and S. I. Stupp. Cell death versus cell survival instructed by supramolecular cohesion of nanostructures. Nature Communications, 5(1):3321, 2014.

Niece, K. L., Czeisler, C., Sahni, V., Tysseling-Mattiace, V., Pashuck, E. T., Kessler, J. A., Stupp, S. I. (2008). Modification of gelation kinetics in bioactive peptide amphiphiles. Biomaterials 29(34):4501-9. doi: 10.1016/j.biomaterials.2008.07.049.

Ninan, Hugo Albrecht, Anton Blencowe, Chapter 5 - Mammalian Cell-Based Assays for Studying Bio-Nano Interactions, Woodhead Publishing, 2018, Pages 129-166, ISBN 9780081019733, https://doi.org/10.1016/B978-0-08-101973-3.00005-5.

Okesola BO, Mendoza-Martinez AK, Cidonio G, Derkus B, Boccorh DK, Osuna de la Peña D, Elsharkawy S, Wu Y, Dawson JI, Wark AW, Knani D, Adams DJ, Oreffo ROC, Mata A. *De Novo* Design of Functional Coassembling Organic-Inorganic Hydrogels for Hierarchical Mineralization and Neovascularization. ACS Nano. 2021 Jun 28;15(7):11202–17. doi: 10.1021/acsnano.0c09814. Epub ahead of print. PMID: 34180656; PMCID: PMC8320236.

Okesola, B. & Mata, A. (2018). Multicomponent self-assembly as a tool to harness new properties from peptides and proteins in material design. Chem. Soc. Rev. 47, 3721-3736. DOI: 10.1039/c8cs00121a

Oliver Grundnes & Olav Reikerås (1993) The importance of the hematoma for fracture healing in rats, Acta Orthopaedica Scandinavica, 64:3, 340-342, DOI: 10.3109/17453679308993640

OpenStax College, Anatomy & Physiology. OpenStax College. 25 April 2013. <http://cnx.org/content/col11496/latest/>.

Oyane, A. , Kim, H. , Furuya, T. , Kokubo, T. , Miyazaki, T. and Nakamura, T. (2003), Preparation and assessment of revised simulated body fluids. J. Biomed. Mater. Res., 65A: 188-195. doi:10.1002/jbm.a.10482

Ozbolat I. T. and Hospodiuk M. Current advances and future perspectives in extrusion-based bioprinting. Biomaterials, 76:321{343, 2016.

Papenburg BJ, Vogelaar L, Bolhuis-Versteeg LA, Lammertink RG, Stamatialis D, Wessling M. One-step fabrication of porous micropatterned scaffolds to control cell behavior. Biomaterials. 2007 Apr;28(11):1998-2009. doi: 10.1016/j.biomaterials.2006.12.023. Epub 2007 Jan 18. PMID: 17239436.

Paramonov, S.E., Jun, H.-W., and Hartgerink, J.D. (2006). Self-assembly of peptide-amphiphile nanofibers: the roles of hydrogen bonding and amphiphilic packing. J. Am. Chem. Soc. 128, 7291–7298

Pashuck, E. T. and S. I. Stupp. (2010). "Direct observation of morphological transformation from twisted ribbons into helical ribbons." J Am Chem Soc 132(26): 8819-8821.

Pashuck, H. Cui, and S. I. Stupp. Tuning Supramolecular Rigidity of Peptide Fibers through Molecular Structure. Journal of the American Chemical Society, 132(17):6041{6046, 2010

Pate, P. Safier, Chemical metrology methods for CMP quality, Advances in Chemical Mechanical Planarization (CMP) (Second Edition), 2022, Pages 355-383, https://doi.org/10.1016/B978-0-12-821791-7.00017-4.

Patel, N. R., Gohil, P. P. (2012). A Review on Biomaterials: Scope, Applications and Human Anatomy Significance. International Journal of Emerging Technology and Advanced Engineering 2(4), 91-101.

Pavlovich et al. Biofabrication: a secret weapon to advance manufacturing, economies, and healthcare. Trends in Biotechnology 2016, 34(9), 679-680, 10.1016/j.tibtech.2016.07.002.

Pérez, C. M., Stephanopoulos, N., Sur, S., Lee, S. S., Newcomb, C., Stupp, S.I. (2015). The powerful functions of peptide-based bioactive matrices for regenerative medicine. Ann Biomed Eng. 43(3):501-14. doi: 10.1007/s10439-014-1166-6.

Peter F. Merenda (1987) Toward a Four-Factor Theory of Temperament and/or Personality, Journal of Personality Assessment, 51:3, 367-374, DOI: 10.1207/s15327752jpa5103_4

Place, E. S., Evans, N. D., Stevens, M. M. (2009). Complexity in biomaterials for tissue engineering. Nature Materials 8, 457-470. doi: 10.1038/nmat2441

Pujals, S., Feiner-Gracia, N., Delcanale, P. et al. Super-resolution microscopy as a powerful tool to study complex synthetic materials. Nat Rev Chem 3, 68–84 (2019). https://doi.org/10.1038/s41570-018-0070-2

Pyatibratov M, Alla S. Kostyukova, Chapter five - New Insights into the Role of Angiogenin in Actin Polymerization, 2012, Pages 175-198, https://doi.org/10.1016/B978-0-12-394306-4.00011-3.

Qiu, Y., Myers, D.R. & Lam, W.A. The biophysics and mechanics of blood from a materials perspective. *Nat Rev Mater* **4,** 294–311 (2019). https://doi.org/10.1038/s41578-019-0099-y

Radvar, E., & Azevedo, H. S. (2019). Supramolecular Nanofibrous Peptide/Polymer Hydrogels for the Multiplexing of Bioactive Signals. ACS Biomaterials Science and Engineering, 5(9), 4646–4656. https://doi.org/10.1021/acsbiomaterials.9b00941

Rajangam, K., Arnold, M., Rocco, M., & Stupp, S. (2008). Peptide amphiphile nanostructure-heparin interactions and their relationship to bioactivity. Biomaterials, 29(23), 3298-3305. https://doi.org/10.1016/j.biomaterials.2008.04.008

Rajangam, K., Behanna, H., Hui, M., Han, X., Hulvat, J., Lomasney, J., & Stupp, S. (2006). Heparin binding nanostructures to promote growth of blood vessels. Nano Letters, 6(9), 2086-2090. https://doi.org/10.1021/nl0613555

Rausch, M. 2021 *Prog. Biomed. Eng.* **3** 042006

Rausch, M.k., Parekh, S. H., Dortdivanlioglu, B., Rosales, A. M. (2021) Prog. Biomed. Eng. 3, 042006.

Redaelli, I., di Prisco, C., and Vescovi, D. (2016) A visco-elasto-plastic model for granular materials under simple shear conditions. *Int. J. Numer. Anal. Meth. Geomech.*, 40: 80– 104. doi: 10.1002/nag.2391.

Reviakine, I., Friedrich Jung, Steffen Braune, John L. Brash, Robert Latour, Maud Gorbet, Wim van Oeveren, (2017). Stirred, shaken, or stagnant: What goes on at the blood–biomaterial interface. Blood Reviews 31(1) 11-21. https://doi.org/10.1016/j.blre.2016.07.003.

Riddick, T. M. (1968). Control of colloid stability through zeta potential. Wynnewood, Pa., Livingston [1968]-(OCoLC)598711355

Rinieris, P. M., Christodoulou, G. N., & Stefanis, C. N. (1980). Neuroticism and ABO blood types. Acta psychiatrica Scandinavica, 61(5), 473–476. https://doi.org/10.1111/j.1600-0447.1980.tb00885.x

Saha K, Keung AJ, Irwin EF, Li Y, Little L, Schaffer DV, Healy KE. (2008). Substrate modulus directs neural stem cell behavior. Biophys J. 95(9):4426-38. doi: 10.1529/biophysj.108.132217. Epub 2008 Jul 25.

Sánchez-Cortés, J., & Mrksich, M. (2009). The platelet integrin alphaIIbbeta3 binds to the RGD and AGD motifs in fibrinogen. *Chemistry & biology*, *16*(9), 990–1000. https://doi.org/10.1016/j.chembiol.2009.08.012

Sarma R, Wong K, Lynch G. Pettitt M.(2018). Peptide Solubility Limits: Backbone and Side-Chain Interactions*J. Phys. Chem. B* 2018, 122, 13, 3528–3539 https://doi.org/10.1021/acs.jpcb.7b10734

Schell H, Duda GN, Peters A, Tsitsilonis S, Johnson KA, Schmidt-Bleek K. The haematoma and its role in bone healing. J Exp Orthop. 2017 Dec;4(1):5. doi: 10.1186/s40634-017-0079-3. Epub 2017 Feb 7. PMID: 28176273; PMCID: PMC5296258.

Schmidt 1981. Gelation and Coagulation. Protein Functionality in Foods. Chapter 7pp 131-147

Schmidt-Bleek K et al. Inflammatory phase of bone healing initiates the regenerative healing cascade. Cell Tissue Research 2012, 347, 567-573, 10.1007/s00441-011-1205-7.

Shi, Y., Lin, R., Cui, H., Azevedo, H.S. (2018). Multifunctional Self-Assembling Peptide-Based Nanostructures for Targeted Intracellular Delivery: Design, Physicochemical Characterization, and Biological Assessment. In: Chawla, K. (eds) Biomaterials for Tissue Engineering. Methods in Molecular Biology, vol 1758. Humana Press, New York, NY. https://doi.org/10.1007/978-1-4939-7741-3_2

Schwertz, H., Zimmerman, G. A., & Weyrich, A. S. (2009). Fibrinogen selects selectins. Blood, 114(2), 234. https://doi.org/10.1182/blood-2009-04-216135

Seelbach, R. J., Fransen, P., Pulido, D., D'Este, M., Duttenhoefer, F., Sauerbier, S., Freiman, T. M., Niemeyer, P., Albericio, F., Alini, M., Royo, M., Mata, A., Eglin, D. (2015). Injectable Hyaluronan Hydrogels with Peptide-Binding Dendrimers Modulate the Controlled Release of BMP-2 and TGF-β1. Macromolecular Bioscience, 15(8), 1035–1044. doi: 10.1002/mabi.201500082

Sharma S, Sharma P, Tyler LN. Transfusion of blood and blood products: indications and complications. Am Fam Physician. 2011 Mar 15;83(6):719-24. PMID: 21404983.

Shiu HT et al. The roles of cellular and molecular components of a hematoma at early stage of bone healing. Journal of Tissue Engineering and Regenerative Medicine 2018, 12(4), e1911-e1925, 10.1002/term.2622.

Simon, M., Major, B., Vácz, G., Kuten, O., Hornyák, I., Hinsenkamp, A., … Lacza, Z. (2018). The Effects of Hyperacute Serum on the Elements of the Human Subchondral Bone Marrow Niche, 2018.

Sperling, C., Fischer, M., Maitz, M. F., Werner, C. (2009). Blood coagulation on biomaterials requires the combination of distinct activation processes. Biomaterials 30: 4447–4456. doi: 10.1016/j.biomaterials.2009.05.044.

Spotnitz WD, Burks S. Hemostats, sealants, and adhesives III: a new update as well as cost and regulatory considerations for components of the surgical toolbox. Transfusion. 2012 Oct;52(10):2243-55. doi: 10.1111/j.1537-2995.2012.03707.x. Epub 2012 May 21. PMID: 22612730.

Stendahl

J C, Rao MS, Guler MO, Stup SI. (2006). Intermolecular Forces in the Self-Assembly of Peptide Amphiphile Nanofibers. Adv. Funct. Mater 16 (4): 499–508. doi: 10.1002/adfm.200500161

Stupp 2010 S. I. Stupp. Self-Assembly and Biomaterials. Nano Letters, 10(12):4783{4786,
2010.

Sur S, Newcomb CJ, Webber MJ, Stupp SI. (2013). Tuning supramolecular mechanics to guide neuron development. Biomaterials 34(20):4749-57. doi: 10.1016/j.biomaterials.2013.03.025

Taboada, G.M., Yang, K., Pereira, M.J.N. et al. Overcoming the translational barriers of tissue adhesives. Nat Rev Mater 5, 310–329 (2020). https://doi.org/10.1038/s41578-019-0171-7

Tahergorabi Z, Khazaei M. A review on angiogenesis and its assays. Iran J Basic Med Sci. 2012 Nov;15(6):1110-26. PMID: 23653839; PMCID: PMC3646220.

Tejeda-montes, E., Klymov, A., Nejadnik, M. R., Alonso, M., Rodriguez-cabello, J. C., Walboomers, X. F., & Mata, A. (2014). Biomaterials Mineralization and bone regeneration using a bioactive elastin-like recombinamer membrane. Biomaterials, 35(29), 8339–8347. http://doi.org/10.1016/j.biomaterials.2014.05.095

Tekin, E.D. (2015). Molecular dynamics simulations of self-assembled peptide amphiphile based cylindrical nanofibers. RSC Adv. 5, 66582–66590.

Terzic A et al. Regenerative medicine build-out. Stem Cells Translational Medicine 2015, 4, 1373- 1379, 10.5966/sctm.2015-0275.

Toksoz S, Mammadov R, Tekinay AB, Guler MO. (2011). Electrostatic effects on nanofiber formation of self-assembling peptide amphiphiles. J Colloid Interface Sci. 1;356(1):131-7. doi: 10.1016/j.jcis.2010.12.076.

Tutwiler, V., Litvinov, R. I., Lozhkin, A. P., Peshkova A. D., Lebedeva, T., Ataullakhanov, F. I., Spiller, K. L., Cines, D. B., Weisel, J. W. (2016). Kinetics and mechanics of clot contraction are governed by the molecular and cellular composition of the blood. Blood 127(1):149-59. doi: 10.1182/blood-2015-05-647560.

Uhlen M. (2019). A genome-wide transcriptomic analysis of protein-coding genes in human blood cells. *Science.* (2019). DOI: 10.1126/science.aax9198

Uskoković V, Ghosh S. Carriers for the tunable release of therapeutics: etymological classification and examples. Expert Opin Drug Deliv. 2016 Dec;13(12):1729-1741. doi: 10.1080/17425247.2016.1200558. Epub 2016 Jun 27. PMID: 27322661; PMCID: PMC5161035.

Vats, A., Tolley, N. S., Polak, J. M., Gough, J. E. (2003). Scaffolds and biomaterials for tissue engineering: a review of clinical applications Clinical Otolaryngology 28(3), 165-172.

Veiga A, Silva IV, Duarte MM, Oliveira AL. Current Trends on Protein Driven Bioinks for 3D Printing. Pharmaceutics. 2021 Sep 10;13(9):1444. doi: 10.3390/pharmaceutics13091444. PMID: 34575521; PMCID: PMC8471984.

Veiga, A., Silva, I. V., Duarte, M. M., & Oliveira, A. L. (2021). Current Trends on Protein Driven Bioinks for 3D Printing. Pharmaceutics, 13(9), 1444. doi:10.3390/pharmaceutics13091444

Velichko YS, Stupp SI, de la Cruz MO. (2008). Molecular simulation study of peptide amphiphile self-assembly. J Phys Chem B. 112(8):2326-34. doi: 10.1021/jp074420n.

Vincent LG, Choi YS, Alonso-Latorre B, del Alamo JC, Engler AJ. 2013. Mesenchymal stem cell durotaxis depends on substrate stiffness gradient strength. *Biotechnol. J.* **8**, 472–484. (10.1002/biot.201200205)

Vinik, A. I., Erbas, T., Sun Park, T., Nolan, R., & Pittenger, G. L. (2001). Platelet dysfunction in type 2 diabetes. Diabetes Care, 24(8), 1476–1485. https://doi.org/10.2337/diacare.24.8.1476

Vu TD, Pal SN, Ti LK, Martinez EC, Rufaihah AJ, Ling LH, Lee CN, Richards AM, Kofidis T. An autologous platelet-rich plasma hydrogel compound restores left ventricular structure, function and ameliorates adverse remodeling in a minimally invasive large animal myocardial restoration model: a translational approach: Vu and Pal "Myocardial Repair: PRP, Hydrogel and Supplements". Biomaterials. 2015 Mar;45:27-35. doi: 10.1016/j.biomaterials.2014.12.013. Epub 2015 Jan 13. PMID: 25662492.

Wang H., Paul A., Nguyen D., Enejder A.(2018)ACS Appl. Mater. Interfaces 2018, 10, 21808−21815

Wang Z, Quan Qing, Xi Chen, Cheng-Jun Liu, Jing-Cong Luo, Jin-Lian Hu, Ting-Wu Qin. (2016). Effects of scaffold surface morphology on cell adhesion and survival rate in vitreous cryopreservation of tenocyte-scaffold constructs, Applied Surface Science, Volume 388, Part A,Pages 223-227. https://doi.org/10.1016/j.apsusc.2016.01.187.

Weisel, J. W., & Litvinov, R. I. (2013). Mechanisms of fibrin polymerization and clinical implications. Blood, 121(10), 1712–1719. http://doi.org/10.1182/blood-2012-09-306639

Wenzhen Zhu, Yon Jin Chuah, Dong-An Wang, Bioadhesives for internal medical applications: A review, Acta Biomaterialia, Available online 22 April 2018, ISSN 1742-7061, https://doi.org/10.1016/j.actbio.2018.04.034.

William J. Wedemeyer, Ervin Welker, Mahesh Narayan, and Harold A. Scheraga. (2000). Disulfide Bonds and Protein Folding. Biochemistry 39 (15), 4207-4216. https://doi.org/10.1021/bi992922o

Wilson, M. (2020). Development of new methods for detecting bloodstream pathogens, Clinical Microbiology and Infection, 26 3, 319-324, https://doi.org/10.1016/j.cmi.2019.08.002.

World Health Organisation, 2017. https://www.who.int/groups/expert-committee-on-selection-and-use-of-essential-medicines/essential-medicines-lists

Wu RX et al. Biomaterials for endogenous regenerative medicine: Coaxing stem cell homing and beyond. Applied Materials Today 2018, 11, 144-165, 10.1016/j.apmt.2018.02.004.

Wu Y, Okesola BO, Xu J, Korotkin I, Berardo A, Corridori I, di Brocchetti FLP, Kanczler J, Feng J, Li W, Shi Y, Farafonov V, Wang Y, Thompson RF, Titirici MM, Nerukh D, Karabasov S, Oreffo ROC, Carlos Rodriguez-Cabello J, Vozzi G, Azevedo HS, Pugno NM, Wang W, Mata A. Disordered protein-graphene oxide co-assembly and supramolecular biofabrication of functional fluidic devices. Nat Commun. 2020 Mar 4;11(1):1182. doi: 10.1038/s41467-020-14716-z. PMID: 32132534; PMCID: PMC7055247.

Xu, L. C., James W. Bauer, Christopher A. Siedlecki. (2014). Proteins, platelets, and blood coagulation at biomaterial interfaces. Colloids and Surfaces B: Biointerfaces 124, 49-68. ISSN 0927-7765. https://doi.org/10.1016/j.colsurfb.2014.09.040.

Yu, Z., Erbas, A., Tantakitti, F., Palmer, L. C., Jackman, J. A., Olvera de la Cruz, M., Cho, N., and Stupp, S.I. (2017). Co-assembly of Peptide Amphiphiles and Lipids into Supramolecular Nanostructures Driven by Anion−π Interactions. Journal of the American Chemical Society 2017 139 (23), 7823-7830. DOI: 10.1021/jacs.7b02058

Zhang C et al. Nano/micro-manufacturing of bioinspired materials: A review of methods to mimic natural structures. Advanced Materials 2016, 28, 6292–6321, 10.1002/adma.201505555.

Zhang, M. a. Greenfield, A. Mata, L. C. Palmer, R. Bitton, J. R. Mantei, C. Aparicio, M. O. de la Cruz, and S. I. Stupp. A self-assembly pathway to aligned monodomain gels. Nature Materials, 9(7):594{601, 2010.

Zhang, S., Greenfield, M. A., Mata, A., Palmer, L. C., Bitton, R., Mantei, J. R., & Stupp, S. I. (2010). A self-assembly pathway to aligned monodomain gels. Nature Materials, 9(7), 594–601. http://doi.org/10.1038/nmat2778

Zudaire E, Gambardella L, Kurcz C, Vermeren S (2011) A Computational Tool for Quantitative Analysis of Vascular Networks. PLOS ONE 6(11): e27385. https://doi.org/10.1371/journal.pone.0027385